UNIVERSITÀ
DEGLI STUDI
DI PADOVA

Sede Amministrativa: Università degli Studi di Padova

Dipartimento di Scienze Biomediche Sperimentali

SCUOLA DI DOTTORATO DI RICERCA IN BIOSCIENZE
INDIRIZZO NEUROBIOLOGIA
CICLO XXII

PRESENILINS AND Ca^{2+} HOMEOSTASIS: ROLE IN ALZHEIMER'S DISEASE AND CELL PHYSIOLOGY

Direttore della Scuola : Ch.mo Prof. Tullio Pozzan
Coordinatore d'indirizzo: Ch.mo Prof. Daniela Pietrobon
Supervisore :Ch.mo Prof. Cristina Fasolato

Dottorando : Lucia Brunello

Index

Abbreviations

Ab	antibody
Aβ	amyloid β
AD	Alzheimer's Disease
ADAM	a disintegrin and metalloproteinase
Aeq	aequorin
AICD	APP intracellular domain
AM	acetoxymethyl
AMPA	α-amino-3-hydroxy-5-methyl-4-isoxazolepropionic
APH-1	anterior pharynx-defective-1
ApoE	apolipoprotein E
APP	Amyloid Precursor Protein
BACE	β-site APP cleaving enzyme
BSA	bovine serum albumine
CALHM1	calcium homeostasis modulator 1
CaM	calmodulin
Casp	caspase
Cdk5	cyclin-dependent kinase-5
cDNA	complementary DNA
CFP	cyan fluorescent protein
CPA	cyclopiazonic acid
CTF	C-terminal fragment
CRAC	Ca^{2+} release-activated channel
CWP	cotton wool plaques
DKO	double knock-out
DMEM	Dulbecco's modified Eagle medium
DREAM	downstream regulatory-element antagonist modulator
ER	endoplasmic reticulum
FAD	Familial Alzheimer's Disease
FCS	foetal calf serum
FRET	fluorescence resonance energy transfer
FTDP-17	Fronto-Temporal Dementia with Parkinsonism
GFP	green fluorescent protein
GRB2	growth factor receptor-bound protein 2
GSK-3β	glycogen synthase kinase-3β
ICD	intracellular domain
i-Clip	intramembrane cleaving protease
IP_3	inositol-1,4,5-triphosphate
IP_3R	inositol-1,4,5-triphosphate receptors
KChIP3	potassium channel α-subunit interacting protein
LDLR	low-density lipoprotein receptor
LTD	long-term depression

LTP	long-term potentiation
MEF	murine embryonic fibroblast
mKRB	modified Krebs–Ringer buffer
MTP	mitochondrial permeability transition pore
MW	molecular weight
NCX	Na^{+}/Ca^{2+} exchanger
NFT	neurofibrillary tangles
NICD	Notch intracellular domain
NMDA	N-methyl-D-aspartate
NTF	N-terminal fragment
PEN-2	presenilin enhancer-2
PHF	paired helical filaments
PLB	phospholamban
PLC	phospholipase C
PM	plasma membrane
PMCA	plasma membrane Ca^{2+} ATPase
PrPC	cellular prion protein
PS	presenilin
PS1	presenilin-1
PS2	presenilin-2
R	ratio
RACC	receptor-activated Ca^{2+} channel
RIP	regulated intramembrane proteolysis
RyR	ryanodine receptor
SERCA	sarco-endoplasmic reticulum Ca^{2+}-ATPase
siRNA	small interfering RNA
SLN	sarcolipin
SOCC	store-operated Ca^{2+} channel
SOCE	store-operated Ca^{2+} entry
SORL1	sortilin-related receptor
SPCA	secretory-pathway Ca^{2+} ATPase
SR	sarcoplasmic reticulum
STIM	stromal interaction molecule
TGN	trans-Golgi network
TMD	transmembrane domain
TRPC	Transient receptor potential channel
UV	ultraviolet
V_{max}	maximal uptake rate
VOCC	voltage-operated Ca^{2+} channel
wt	wild-type
YFP	yellow fluorescent protein

Summary

Alzheimer's Disease (AD) is a progressive neurodegenerative disorder and the most common form of senile dementia. The characteristic histopathological hallmarks of AD are the intracellular neurofibrillary tangles and the amyloid plaques, made of aggregated amyloid peptides (Aβ), that deposit in the extracellular matrix of the brain. Aβ peptides are the result of two sequential cleavages of the amyloid precursor protein (APP); Aβ is eventually released by the γ-secretase enzyme. The most abundant Aβ peptide species, both physiologically produced throughout life, are $A\beta_{40}$ and $A\beta_{42}$, which is more insoluble and aggregation-prone.

Although most AD cases are sporadic, a small percentage of patients is affected by the hereditary form of AD (Familial Alzheimer's Disease, FAD), caused by dominant mutations in one of three genes. These genes code for the APP, presenilin-1 (PS1) and presenilin-2 (PS2); PSs are the catalytic subunits of the γ-secretase enzyme complex. FAD-linked mutations in PSs lead to an increased $A\beta_{42}/A\beta_{40}$ ratio, that promotes Aβ plaques deposition. Beside this effect on Aβ production, many mutations in PS1 and PS2 have been extensively demonstrated to cause alterations in the intracellular Ca^{2+} homeostasis, thus making neurons more sensitive to excitotoxic stimuli and apoptosis. Nevertheless, the effects and the mechanisms of this interference in the Ca^{2+} balance are still unclear and under intense investigation. For a long time, the most popular hypothesis has been the "Ca^{2+} overload" hypothesis, which claims that mutated PSs give rise to exaggerated Ca^{2+} responses upon stimulation, sustained by intracellular stores, and the endoplasmic reticulum (ER) in particular, overloaded with Ca^{2+}. However, an increasing number of studies has recently began to critically question this hypothesis and different possible targets of PSs action have been proposed.

Previous works from our laboratory showed that a number of FAD-linked PS1 and PS2 mutants reduce the ER Ca^{2+} content; starting from this evidence, we investigated the mechanism(s) leading to this effect.

The SERCA-2 pump was identified as the most likely target of FAD-linked PS2-T122R action and indeed the two protein interact, as co-immunoprecipitation assays demonstrated. PS2-T122R was shown to impair the pump activity by decreasing its maximal Ca^{2+} uptake rate, while leaving its protein level unaltered. Interestingly, similar results were obtained with wild-type (wt) PS2: transient expression of wt PS2 in a PSs null background led to a lower steady-state ER Ca^{2+} concentration and a slower ER Ca^{2+} uptake rate. Consistently with this observation, knocking down the endogenous PS2 level by small interefering RNAs increased both parameters. These results suggest a physiological role for PS2 in regulating intracellular Ca^{2+} handling, acting as a brake for the SERCA pumps. Finally, over-expression of SERCA-2B together with PS2-T122R

rescued the ER Ca^{2+} content and the pump uptake rate at the respective values observed in control cells.

A long-term goal of the project is studying intracellular Ca^{2+} dynamics, both *in vitro* and *in vivo*, in the brain of AD mouse models based on APP and FAD-linked PS mutants, through single cell live Ca^{2+} imaging experiments with FRET-based *cameleon* Ca^{2+} probes. Thus, the second part of this work has been dedicated to a preliminary set up of the suitable experimental conditions to be employed with two *cameleon* sensors genetically targeted to the lumen of the ER and the Golgi apparatus. While the results obtained with the ER-targeted *cameleon* probe matched those previously obtained with an ER-targeted aequorin probe, an unexpected result was obtained with a novel *cameleon* localized to a specific sub-compartment of the Golgi apparatus. This new sensor helped us to better define the mechanism of action of PS2-T122R, showing that it selectively acts on SERCA-2 but not on SPCA-1 pumps.

Riassunto

La malattia di Alzheimer (*Alzheimer's Disease*, AD) è una patologia neurodegenerativa progressia e rappresenta la forma più comune di demenza senile. Le caratteristiche istopatologiche dell'AD sono le fibrille intraneuronali e le placche amiloidi, formate da aggregati di peptidi amiloidi (Aβ), che si depositano nella matrice extracellulare del cervello. I peptidi Aβ sono il prodotto di due tagli sequenziali della proteina precursore dell'amiloide (*amyloid precursor protein*, APP). L'ultimo taglio proteolitico di APP, che porta al rilascio degli Aβ nella matrice extracellulare, è opera dell'enzima γ-secretasi. Le forme più abbondanti di peptidi Aβ, entrambe fisiologicamente prodotte nel corso della vita, sono $A\beta_{40}$ e $A\beta_{42}$, che è più insolubile e incline ad aggregare.
Sebbene la maggioranza dei casi di AD sia di origine sporadica, una piccola percentuale di pazienti è affetta dalla forma ereditaria di AD (*Familial Alzheimer's Disease*, FAD), causata da mutazioni dominanti in uno dei tre geni che codificano per l'APP, per la presenilina-1 (PS1) e la presenilina-2 PS2). Le preseniline (PSs) sono le subunità catalitiche del complesso enzimatico della γ-secretasi. Mutazioni associate a FAD nelle PSs portano ad un aumento del rapporto $A\beta_{40}/A\beta_{42}$, che favorisce il depositarsi delle placche amiloidi. Oltre a questo effetto sulla produzione di Ab, è stato ampiamente dimostrato che molte mutazioni nelle PS1 e PS2 causano alterazioni nell'omeostasi intracellulare del Ca^{2+}, rendendo così i neuroni più sensibili a stimoli eccitotossici e all'apoptosi. Ciò nonostante, gli effetti e i meccanismi di questa interferenza nel normale equilibrio intracellulare del Ca^{2+} sono ancora poco chiari e oggetto di intensa indagine. A lungo, l'ipotesi più popolare è stata l'ipotesi del "sovraccarico di Ca^{2+}", la quale afferma che le PSs mutate danno origine a esagerate risposte Ca^{2+} in seguito a stimolazione, sostenute da depositi intracellulari (in particolare, il reticolo endoplasmatico, ER) sovraccarichi di Ca^{2+}. Tuttavia, un crescente numero di studi ha di recente iniziato a mettere in discussione questa ipotesi e diversi possibili bersagli dell'azione delle PSs sono stati proposti.
Studi precedenti condotti nel nostro laboratorio hanno mostrato che un certo numero di PS1 e PS2 mutate associate a FAD riducono il contenuto di Ca^{2+} dell'ER; partendo da queste osservazioni, abbiamo indagato il/i meccanismo/i alla base di questo effetto.
La pompa SERCA-2 è stata identificata come il bersaglio più probabile dell'azione della mutazione associata a FAD T122R nella PS2 (PS2-T122R) e infatti le due proteine, SERCA-2 e PS2-T122R, interagiscono, come dimostrato da esperimenti di co-immunoprecipitazione. E' stato dimostrato che la PS2-T122R danneggia l'attività della pompa riducendo la sua velocità massima di trasporto, mentre il livello della proteina rimane inalterato. E' interessante notare, inoltre, che risultati simili sono stati ottenuti con la PS2 non mutata (*wild-type*, wt): l'espressione transiente della PS2 wt in un modello cellulare privo di PSs ha avuto come conseguenze un abbassamento della concentrazione

di Ca^{2+} nell'ER all'equilibrio e un rallentamento della velocità di importo del Ca^{2+} nell'ER. Coerentemente con questa osservazione, l'abbattimento dell'espressione della PS2 endogena mediante la tecnica di RNA *interference* ha portato ad un incremento di entrambi questi parametri. Questi risultati suggeriscono un ruolo fisiologico della PS2 nella regolazione intracellulare del Ca^{2+}; la PS2 agirebbe come un freno per le pompe SERCA. Infine, la sovra-espressione della SERCA-2B assieme alla PS2-T122R ha permesso di riportare i valori del contenuto di Ca^{2+} nell'ER e della velocità della pompa ai valori di controllo.

Uno degli obiettivi a lungo termine di questo progetto è studiare le dinamiche intracellulari del Ca^{2+}, sia *in vivo* che *in vitro*, nel cervello di topi transgenici usati come modello di AD, in quanto basati su mutazioni nell'APP e in PS associate a FAD. L'approccio scelto è monitorare le variazioni di Ca^{2+} in singola cellula attraverso sonde per il Ca^{2+} basate su FRET, i *cameleons*. Pertanto, la seconda parte di questo lavoro è stata dedicata alla messa a punto preliminare delle condizioni sperimentali più adatte da adottare con due sonde *cameleons*, geneticamente indirizzate nel lume dell'ER e dell'apparato di Golgi. Mentre i risultati ottenuti con il *cameleon* indirizzato all'ER corrispondono a quelli ottenuti in precedenza con un'equorina indirizzata all'ER, un risultato inaspettato è emerso utilizzando un nuovo *cameleon* localizzato in uno specifico compartimento del Golgi. Questa nuova sonda ci ha aiutato a definire meglio il meccanismo di azione della PS2-T122R, mostrando che agisce selettivamente sulle pompe SERCA-2 ma non sulle pompe SPCA1.

Introduction

1. Alzheimer's Disease

Alzheimer's Disease (AD) is a slow, progressive neurodegenerative disorder and accounts for about 60-70% of all cases of senile dementia. Most of the AD cases are 'sporadic', with a disease onset after the age of 65 years (late-onset AD). AD phenotype is the result of the degeneration and shrinkage of brain regions involved in learning and memory, in particular the frontal cortex, the temporal lobes and the hippocampus; memory loss, agitation, wandering and sleeping disorders are the most frequent symptoms. As the disease gets worse, locomotion, speech and the ability to recognize people and everyday objects are completely lost.
The characteristic histopathological hallmarks of AD are extracellular senile plaques, made up mainly of Aβ peptides, and intracellular neurofibrillary tangles (NFT), made up of hyperphosphorylated tau proteins.

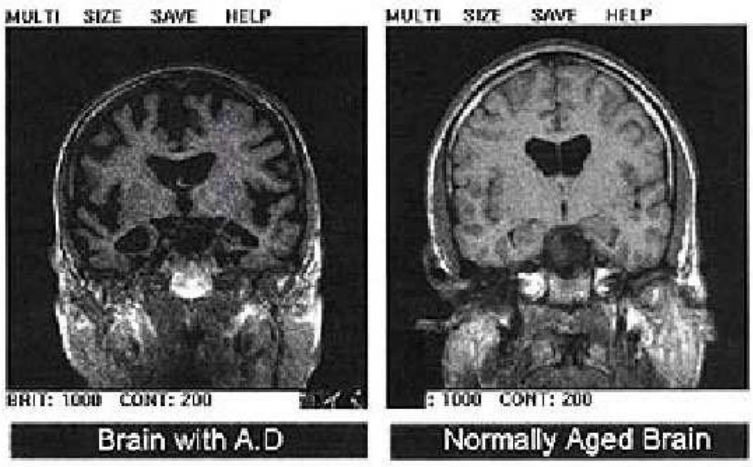

Figure 1.1. Magnetic Resonance Imaging of an AD brain (left) and of an age-matched healthy brain (right).

Tau

Tau is a microtubule-associated protein of about 55 kDa that stabilizes the cytoskeleton, constantly undergoing phosphorylation and dephosphorylation. Tau is highly expressed in adult human brain, where six different isoforms are produced from a single gene by alternative splicing. These isoforms present a tandem of either three or four tubulin-binding domains in the C-terminal region. All six isoforms can be phosphorylated through the action of several kinases, including glycogen synthase kinase-3β (GSK-3β), cyclin-dependent kinase-5 (Cdk5) and other tau kinases (Alvarez et al., 1999; Lucas et al., 2001). In normal ageing, AD and other neurodegenerative diseases, natively unfolded tau

becomes hyperphosphorylated and folds into a β conformation, forming abnormal filaments which become the paired helical filaments of NFT and neuritic infiltrates in plaques (Mandelkow et al, 2007).
In AD, tau neurotoxicity is, at least in part, due to an increase in the phosphorylation of all six isoforms; hyperphosphorylation leads to reduced microtubule binding, destabilization of the cytoskeleton, reduced axonal transport (Stoothoff and Johnson, 2005) and insoluble intracellular fibril formation (Augustinack et al., 2002), thus impairing synaptic functions and eventually causing neuronal death. Once a neuron dies NFT can persist in an extracellular (or ghost) form due to their intense hyperphosphorylation and insolubility (Iqbal et al., 2008). Recently, it has been pointed out that soluble tau is more toxic to neurons than aggregated, paired helical filament forms (Gomez-Ramos et al., 2006). Hyperphosphorylated tau can exist as soluble oligomeric aggregates that are considered as the toxic species (Iqbal et al., 2008). In AD, neuronal loss occurs in brain regions depositing tau fibrils (Wyss-Coray, 2006).
NFT formation can be divided in six stages, with four of these stages occurring prior to the development of dementia. NFT stages I/II occur in the entorhinal region, stages III/IV infiltrate into limbic regions and stages V/VI include the neocortex. These three groups correspond respectively to normal cognition, some cognitive impairment and frank dementia (Braak and Braak, 1991).
Neurofibrillary tangles are not an exclusive marker of AD: they also feature in other neurodegenerative diseases named tauopathies. Among these pathologies, Fronto-Temporal Dementia with Parkinsonism (FTDP-17), an hereditary disease associated to numerous tau mutations, is characterized, at cellular level, by deposition of paired helical filaments (PHF, Kidd, 1963) of hyperphosphorylated tau (Hutton et al., 1998).

Senile plaques

Senile plaques are proteic aggregates that deposit in the extracellular space of the brain of AD patients. The main component of these plaques are the amyloid β peptides (Aβ). These peptides are protein fragments of around 40 amino acids and the most common forms are $A\beta_{40}$ and $A\beta_{42}$. They are all released in the extracellular space from the Amyloid Precursor Protein (APP) after two sequential cleavages (see paragraph “APP and Aβ”, p. 12).
$A\beta_{40}$ and $A\beta_{42}$ exist in different conformational states anywhere from monomers to dodecamers or even higher molecular weight complexes. Anything larger than a monomer can be referred to as an oligomer. Oligomers may then grow in size and the $A\beta_{42}$ peptide is more inclined to create insoluble fibrils than the $A\beta_{40}$ form (Bitan et al., 2003). Due to their greater aggregation capabilities, longer forms of the Aβ peptides, particularly $A\beta_{42}$, are considered more neurotoxic, although it is the oligomeric rather than the fibrillar insoluble amyloid forms which appear most damaging (Walsh et al., 1997 and 2002). There is a strong correlation between soluble oligomeric Aβ levels and the extent of

synaptic loss and severity of cognitive dysfunction in AD (McLean et al., 1999; Shankar et al., 2008).

Aβ can be toxic in several different ways: it can cause oxidative stress, mitochondrial damage, inflammation and it can form pores in the plasma membrane thus causing Ca^{2+} overload (Lin et al., 2001). The suggested Aβ targets are numerous, however it appears clear that both intraneuronal and secreted Aβ are responsible of synaptic dysfunction (Moreno et al., 2009; Wei et al., 2009). Aβ can also alter tau phosphorylation, cleavage and aggregation (De Felice et al., 2008), thus providing a link between the two major pathological hallmarks of AD.

A sub-type of plaques that can also be found in AD brains are neuritic plaques. Neuritic plaques are associated with fibrillar Aβ and dystrophic tau-positive neuritis (Benzing et al., 1993). These plaques are smaller in size but, in contrast to diffuse plaques (which predominantly contain $Aβ_{42}$), they contain both $Aβ_{40}$ and $Aβ_{42}$ peptides. Regions where neuritic and cored plaques are commonly found in AD include the middle frontal, superior and middle temporal, inferior parietal and entorhinal cortices and the hippocampus.

Aβ cotton wool plaques

Aβ cotton wool plaques (CWP) are a different type of aggregate deposition that has been observed in patients affected by the hereditary form of AD (see chapter 3, p. 23). Aβ CWP are most often observed in presenilin-1 (PS1) mutation (Dumanchin et al., 2006). They occur in addition to the diffuse, neuritic and cored AD plaque types, and have been noted infrequently in sporadic AD (Le et al., 2001). Cotton wool plaques have several characteristic features: they are larger than most diffuse or neuritic plaques (up to 150 μm in diameter), have eosinophilic properties, clearly defined margins and little neuritic or inflammatory infiltrate. When immunostained, CWP display strong positivity for $Aβ_{42}$ and weak or little $Aβ_{40}$ (Uchihara et al., 2003). The typical distribution pattern of CWP follows that of neuritic and diffuse plaques in AD (Takao et al., 2002).

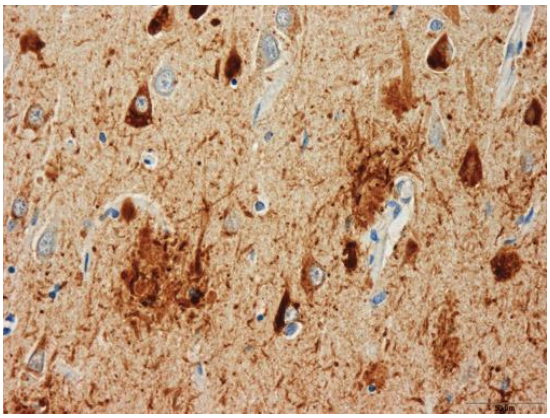

Figure 1.2. Tissue from the hippocampal region of an AD brain, stained for tau. The triangular shapes are neurofibrillary tangles. Amyloid plaques are the round, less dense structures (Washington University School of Medicine).

AD molecular mechanisms

Although some atrophy of white matter (less than 0,25% per year) is a normal consequence of age, once clinical AD starts, progressive atrophy and neuronal loss speed up to ten times faster: mean brain atrophy rates for well-established, clinically diagnosed AD are 2,4% per year (Fox et al., 2000).

Beside the deposition of fibrillary forms of hyperphosphorylated tau, there are other possible molecular mechanisms leading to neuronal loss: there is substantial evidence demonstrating that at least some cells in sporadic AD die via apoptosis (Stadelmann et al., 1999), as demonstrated by the observation of typical signs of apoptosis in AD brains, such as mitochondrial dysfunction, caspase activity, nuclear abnormalities, DNA damage and altered activity of apoptosis-related genes, such as p53 and Bax (Su et al., 1997).

Also Aβ peptides can trigger apoptosis by inducing oxidative stress and lipid peroxidation, which are common features in AD brains (Butterfield et al., 2002). Oligomeric Aβ can induced synaptic changes that result in synaptic degradation and remodeling of dendritic spines (Lacor et al., 2007; Wei et al., 2009). Such changes are thought to occur prior to the complete loss of neurons in AD.

Alzheimer's disease is also characterized by a chronic inflammatory response. An increased number of activated microglia has been reported associated particularly with neuritic plaques (Sheng et al., 1997), even though they inefficiently clear Aβ and degrade it extremely slowly (Paresce et al., 1997). Microglial activation recruits astrocytes to clear the Aβ deposits and astrocytes in the entorhinal cortex of AD cases have been shown to contain $A\beta_{42}$ in amounts proportionate to the severity of regional AD pathology (Nagele et al., 2003). Besides, activated microglia directly produce toxic oxygen species that damage neurons (Gahtan and Overnier, 1999). Nonetheless, in transgenic APP mouse strains in which nearly complete ablation of microglia was achieved, amyloid plaque formation and amyloid-associated neuritic dystrophy was maintained (Grathwohl et al., 2009).

APP and Aβ

According to the "amyloid cascade" hypothesis, the key event initiating AD is the abnormal processing of APP by the γ-secretase complex (Selkoe, 2002), leading to the abnormal accumulation of Aβ peptides.

The APP molecule is a type I transmembrane glycoprotein that is proteolytically processed by two competing pathways, the non-amyloidogenic and amyloidogenic (Aβ forming) pathways. Three major secretases are assumed to be involved in the proteolytic cleavage of APP. These include α-secretase, β-site APP cleaving enzyme (BACE, formally known as β-secretase) and γ-secretase.

Two members of the ADAM family (a disintegrin and metalloproteinase), ADAM-10 and ADAM-17 (or TACE), have been shown to display α-secretase activity (Buxbaum et al., 1998; Lammich et al., 1999). BACE was identified as an aspartyl protease and a type I membrane protein (Hussain et al., 1999; Sinha et al., 1999; Vassar et al., 1999).

The α-secretase cleaves within the Aβ domain of APP thus preventing the formation of Aβ and generating non-amyloidogenic fragments: an N-terminally truncated Aβ fragment, called p3, and a secreted form of APP (α-APPs). In the amyloidogenic pathway, BACE removes the bulk of the ectodomain of APP, cleaving near the N-terminus of the Aβ domain on the APP molecule, releasing another soluble form of APP, β-APPs, and leaves behind a small membrane-retained C-terminal fragment (C99) containing the whole Aβ domain (Cole and Vassar, 2008). The final step in the amyloidogenic pathway is the intramembranous cleavage of the C99 fragment by γ-secretase, releasing the Aβ peptide (Verdile et al., 2007).

Aβ fragments longer than 42 amino acids have been detected; γ-secretase inhibitors prevent the production of these fragments, suggesting that the γ-secretase complex itself can form them and therefore has multiple, topologically distinct cleavage sites (ε, γ and ζ sites) (Weidemann et al., 2002; Zhao et al., 2004; Haass and Selkoe, 2007). The cleavages at the individual sites are heterogeneous and give rise to roughly two different product lines, $A\beta_{49}$ (ε) - $A\beta_{46}$ (ζ) - $A\beta_{43}$ (γ) - $A\beta_{40}$ (γ) and $A\beta_{37}$ (γ), whereas the other product line generates $A\beta_{48}$ (ε) - $A\beta_{45}$ (ζ) - $A\beta_{42}$ (γ) - $A\beta_{39}$ (γ). The current model suggests that the cleavage occurs in a stepwise manner, with γ-secretase cutting the APP CTF first at the ε-site, which is close to the cytoplasmic border of the membrane. This cleavage releases the APP intracellular domain (AICD) from the membrane and leaves a long Aβ species in the membrane. Further cleavages then occur roughly every third amino acid down the α-helical transmembrane domain via the ζ- to the γ-site, progressively removing C-terminal residues until the peptide is short enough to be released from the membrane (Kakuda et al, 2006). It is likely that the hydrophobicity of the remaining peptide is then sufficiently reduced to facilitate its release into the extracellular medium.

The consecutive cleavage of APP could provide an explanation for how loss-of-function mutations in PS might result in decreased Aβ generation and simultaneous increased production of longer Aβ (see paragraph “Presenilin mutations”, p. 26).

Since the original amyloid-cascade hypothesis for AD was put forward (Hardy & Higgins, 1992), many modifications and refinements have been proposed. For example, no absolute relationship exists between Aβ load in the brain and the clinical manifestation of AD symptoms in humans or mice (Price & Morris, 1999). This has led to the concept of ‘soluble toxic oligomers’ (Lambert et al, 1998). These Aβ oligomers are intermediary forms between free soluble Aβs and insoluble amyloid fibers, and seem to be toxic both *in vitro* and *in vivo*.

Different Aβ-peptide species contribute to the generation, stability and toxic properties of the oligomers. The relative combination of these peptides could be much more important than the total load of Aβ in the brain.

During normal APP processing, the more common α-secretase cleavage occurs. Aβ is normally secreted by healthy cells throughout life, but its normal physiological function remains largely unknown. Of the two major Aβ species that are being formed, the 40-amino-acid form ($A\beta_{40}$) and the 42-amino-acid-long peptide ($A\beta_{42}$), the latter is the more

aggregation-prone form. Under physiological conditions, $A\beta_{40}$ constitutes about 90% of the total amount of Aβ (Van Broeck et al., 2007).
The physiological role of APP remains unclear. APP binds to the kinesin light chain subunit, kinesin-I, thus it is postulated to be involved in the axonal transport in neurons (Kamal et al., 2000; Stokin and Goldstein, 2006). It is also likely that APP functions as a modulator of intracellular signal transduction.

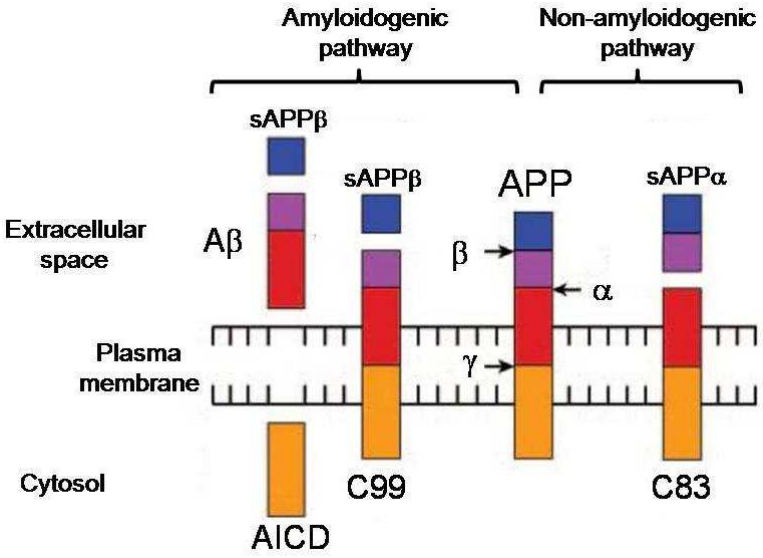

Figure 1.3. Schematic representation of APP processing. APP is processed by two competing pathways. In the non-amyloidogenic, α-secretase pathway, the sAPPα and C83 fragments are generated, while in the amyloidogenic, β-secretase pathway, APP is cleaved into the sAPPβ and C99 fragments. C99 is further cleaved by γ-secretase into Aβ and AICD (adapted from Wippold et al., 2008).

2. γ-secretase

Three laboratories independently discovered that Aβ is physiologically produced throughout life by a cellular pathway that involves intramembrane proteolysis (Busciglio et al., 1993; Shoji et al., 1992; Haass et al., 1992). Thus, APP processing turned out to be the first example not only for intramembrane cleavage but also for a cellular pathway now termed regulated intramembrane proteolysis (RIP). In 1999, the concept of intramembrane cleaving proteases (i-Clips) and of regulated intramembrane proteolysis became established (Brown et al, 2000), demonstrating that intramembrane cleavage of proteins is a general and biologically widespread mechanism. Although these proteases have widely divergent structures and functions, they all bury their catalytic site deeply in their large hydrophobic cores. Most recently, crystal structures of some i-Clips have been published, providing a first glimpse on how these proteins are capable of catching water and performing hydrolysis in the lipid environment of the membrane (Feng et al., 2007).

γ-secretase is the founding member of the intramembrane cleaving aspartyl proteases; regulated intramembrane proteolysis by γ-secretase describes the sequential processing of an increasing number of single-pass transmembrane proteins. The only requirements are apparently a type I conformation of the transmembrane domain (amino terminus oriented to the extracellular side of the membrane) and a short (<50 aa) ectodomain (Struhl and Adachi, 2000). In the first step, the substrate's bulky ectodomain of 200 and more amino acid residues that prevents γ-secretase cleavage is usually removed by membrane bound (metallo)-proteases or "sheddases" at the cell surface. In most cases, these enzymes belong to the family of the ADAM proteases. After the sheddase's cleavage, the remaining stub is cleaved within its transmembrane domain by intramembrane-cleaving proteases (Wolfe and Kopan, 2004). In several cases, the intramembrane cleavage results in the release of an intracellular domain (ICD). The polypeptides released at the intracellular side are by many authors considered the business ends of the process.

γ-secretase turned out to be a complicated complex composed of four essential subunits (Edbauer et al., 2003): anterior pharynx-defective-1 (APH-1), nicastrin, presenilin enhancer-2 (PEN-2) and presenilin (PS), which is the catalytic core. The γ-secretase enzyme is a barrel-like integral protein of the lipid bi-layer (Lazarov et al, 2006); despite its characteristic intramembrane cleavage, a transient hydrophilic environment for catalysis within the lipid membrane must be created.

Structural studies using electron microscopy recently showed a large spherical structure of γ-secretase with the interesting feature of two small central openings, one oriented to the extracellular space and the other to the cytosol (Lazarov et al., 2006). These small openings might represent exit sites of an internal water-containing cavity for the cleavage products. Consistent with a water-containing cavity are two recent studies showing that the active-site region in transmembrane domains (TMD) 6 and 7 of presenilins is water-accessible (Tolia et al, 2006).

Estimates of the molecular weight (MW) of this complex have been highly divergent (250 to >2,000 kDa). The different methodologies used might explain these discrepancies, but likely this heterogeneity also reflects weak or transient interactions of proteins with the complex, since such interactions probably regulate its trafficking and activity. The minimum MW estimate of this complex is 250 kDa and equals more or less the sum of the MWs of the four components of γ-secretase. However, the interaction between the components of the γ-secretase complex is not sufficient to create a macromolecular enzyme complex such as γ-secretase (Verdile et al, 2007). Thus, dimer or trimer formation must occur within the complex. To date, the only member of the complex that is known to undergo this process is PS1.

γ-secretase activity requires the coexpression of all four components and was not observed when either one of the four components was lacking. Moreover, reconstitution of γ-secretase activity is associated with PS endoproteolysis and is dependent on biologically active PS (Kaether et al., 2006). Presenilin contains the two catalytically active aspartate residues (Wolfe et al., 1999), which are located within TMD 6 and TMD7. However, this

transmembrane protein is not a conventional aspartyl protease, with the typical D(T/S)G aspartyl protease active site. The critical PS aspartates were functionally conserved during evolution (Leimer et al., 1999). The N-terminal catalytically active site of PS is embedded in a conserved YD motif, whereas the C-terminal active-site domain contains the equally conserved GxGD motif, which now serves as the family-characterizing name of the GxGD-type aspartyl proteases (Haass and Steiner, 2002).

APH-1

The anterior pharynx-defective-1 (APH-1) protein is a ~20 kDa, 308 amino acid long 7-transmembrane protein existing in two homologous forms, coded by genes located on chromosome 1 and chromosome 15 (aph-1a & aph-1b respectively; (Goutte et al., 2002). In addition, as the result of alternate splicing, a long and short isoform of APH-1a, which differ in their C-terminus (Lee SF et al., 2002), have also been reported, with the short isoform more abundantly expressed in most tissues. Indeed, multiple γ-secretase complexes containing APH-1 isoforms are thought to exist (Shirotani et al., 2004). Because neither the catalytic subunits PS1 and PS2 nor APH-1a (including splice variants) and APH-1b occur in the same complexes, a minimal set of at least six (not taking PS splice variants into account) distinct γ-secretase complexes exist in human cells. The γ-secretase enzyme therefore consists of several distinct complexes depending on the respective tissue expression of its core components.

The APH-1 protein forms a stable and intermediate ~140 kDa complex with nicastrin, before binding presenilin. The APH-1-nicastrin sub-complex appears to play a scaffolding function in the initial stabilization and assembly of presenilin in the γ-secretase complex (LaVoie et al., 2003). APH-1 is also critical for the activity of the fully constructed γ-secretase complex. It interacts with the other components on the cell surface where it also binds the γ-secretase substrate Notch and facilitates its cleavage (Hansson et al., 2005).

Nicastrin

Nicastrin is a type I transmembrane protein with a 670 amino acid long hydrophilic N-terminal domain, a transmembrane domain, and a relatively short cytoplasmic C-terminus of 20 amino acid residues (Yu et al., 2000). The protein undergoes glycosylation and sialylation within the secretory pathway to yield a mature ~150 kDa protein, the largest component of the γ-secretase complex (Yang et al., 2002). Nicastrin acts as a scaffold for the building of the active complex, and as a possible substrate docking site. In fact, nicastrin appears to be involved in the formation of the first sub-complex between itself and APH-1. Nicastrin is critical for the correct assembly of the γ-secretase complex within the endoplasmic reticulum and the intracellular trafficking of the complex to the cell surface (Zhang et al., 2005). Furthermore, nicastrin is essential for the interaction between the complex and APP-C99 and thus acts as a receptor for γ-secretase substrates (Shah et al., 2005). Nicastrin is believed to identify the free N-terminus of a γ-secretase substrate, probably by measuring the length of the ectodomains of type I transmembrane proteins

(Shah et al., 2005). The initial recognition of substrates by nicastrin requires the bulk of the substrate ectodomain to be removed by shedding.

PEN-2

The presenilin enhancer-2 (PEN-2) protein is a ~12 kDa, 101 amino acid long hairpin protein, with two transmembrane domains and its N- and C-terminals facing the lumen of the endoplasmic reticulum (De Strooper, 2003). PEN-2 has been shown to interact with all the three other components of the γ-secretase; without this interaction, PEN-2 undergoes degradation, possibly by the proteasome (Bergman et al., 2004). PEN-2 is thought to be the last protein incorporated into the γ-secretase complex, through an interaction with PS; in fact, trimeric sub-complexes made of the other components have been detected in PEN-2-lacking cells (Takasugi et al., 2003). Association of PEN-2 to this trimeric assembly intermediate triggers the endoproteolytic cleavage of the PS holoprotein. Moreover, PEN-2 C-terminus has been suggested to act as a ‘‘molecular clamp’’ holding together the PS fragments and the whole γ-secretase complex (Prokop et al., 2005).

Presenilins

Presenilin 1 (PS1) and presenilin 2 (PS2) encode two homologous ~50-kDa polytopic membrane proteins, that consist of 9 transmembrane domains (Henricson et al., 2005). Both are rapidly endoproteolytically cleaved within the large cytoplasmic loop between TMDs 6 and 7, within a short hydrophobic domain that is believed to dive into the membrane and it is very likely an autoproteolytic event. An N-terminal and a C-terminal fragment (NTF, CTF) are the result of this cleavage. (Thinakaran et al., 1996; Podlisny et al., 1997). These fragments are thought to interact with each other. The stoichiometry and the nature of the interaction between these fragments remain unclear. It has been shown by many studies that they form a heterodimer in mammalian cells (Capell et al., 1998). However, there is also evidence that the PS1 fragments can form a tetramer (Cervantes et al., 2001). It has yet to be established whether the hypothetical ‘‘core’’ is formed between fragments from one PS1 molecule or multiple molecules within the complex. Endoproteolysis is required to maximize stable conformation of the two active site aspartates in TMD6 and TMD7 of PS and thus allow enzymatic γ-secretase activity (Wolfe et al., 1999).

PS expression is regulated by the presence of the other γ-secretase components, that act as limiting factors (Thinakaran et al., 1997). Consistent with this observation, excess PS holoprotein that fails to become processed into its stable fragments is rapidly degraded by the proteasome (Steiner et al., 1998).

The PS proteins share an overall homology of 67%, with the highest similarities in the predicted transmembrane domains. Nevertheless, several lines of evidence suggest that these proteins may have distinct functions. Compared to neuronal cultures isolated from PS1 ablated mice, those isolated from PS2 knockout mice exhibit higher Aβ production. Evidence to date suggests that PS2 containing complexes have different functions, less γ-secretase processing power than PS1 containing complexes and are less sensitive to γ-

secretase inhibitors (Lai et al., 2003). Taken together these findings suggest that PS1 containing complexes predominate in generating $A\beta_{40}$ and $A\beta_{42}$.

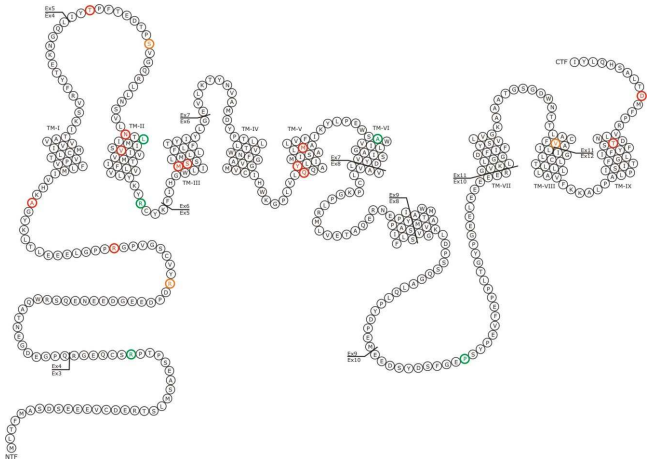

Figure 2.1. Graphic representation of PS2 structure (from http://www.molgen.ua.ac.be/Admutations/).

Assembly

The four subunits of γ-secretase assemble into a functional complex in the early compartments of the secretory pathway (Kim et al., 2004; Kaether et al., 2006a).

Nicastrin and APH-1 form an initial assembly intermediate, which stabilizes the PS holoprotein. Finally, PEN-2 assembles into this ternary complex and triggers endoproteolysis of PS. When assembly is completed, the complex travels to its functional sites at the plasma membrane and the late compartments of the secretory pathway. Complex formation is tightly regulated and depends on the availability of the individual subunits, which is apparently maintained by a balanced expression of the subunits. The subunits which are in excess over the others and thus lack their stabilizing partners are rapidly degraded. Once assembled into the full complex or into an assembly intermediate, the subunits become highly stable. Apart from degradation, it is known that complex formation is also regulated by control mechanisms that ensure that only fully assembled complexes leave the endoplasmic reticulum (ER), while unassembled subunits are retained/retrieved by specific retention/retrieval signals. ER retention/retrieval signals lie in two γ-secretase subunits, PS1 and PEN-2. The molecular machinery recognizing these signals in mammals is unknown. In yeast, a protein called Rer1p was shown to retrieve unassembled subunits of several complexes to the ER. The human orthologue, Rer1, is a 23-kDa protein with four TMDs; human Rer1 is involved in the retention/retrieval of unassembled PEN-2 or nicastrin within the endoplasmic reticulum (Spasic et al., 2007) and is a possible auxiliary factor for γ-secretase complex assembly (Kaether et al., 2006b).

Although quantitation of the four subunits in an active γ-secretase complex suggests a 1:1:1:1 stoichiometry (Sato et al., 2007), evidence for PS dimerization has also been provided (Schroeter et al., 2003). In addition, the complex may contain additive non-essential regulatory subunits such as TMP21 and CD147 (see paragraph “Accessory proteins”, p. 20).

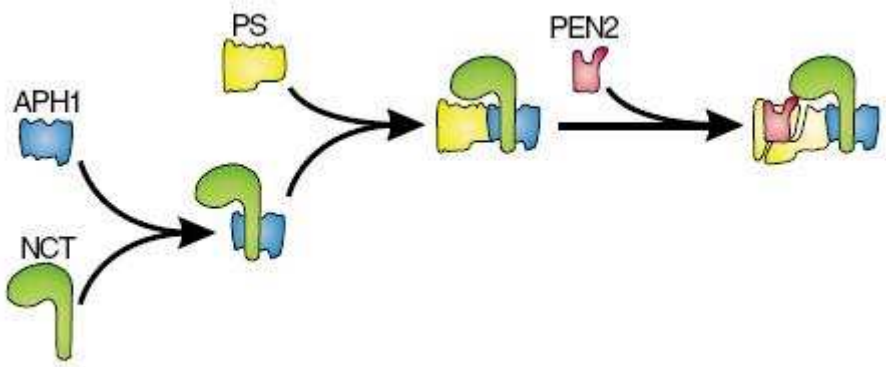

Figure 2.2. Temporal sequence of steps leading to γ-secretase complex formation. The earliest interaction probably occurs between NCT (green) and APH-1 (blue) in the ER. Then, full-length PS (yellow) bind to NCT-APH-1; this event is followed by recruitment of PEN-2 (red), which promotes endoproteolysis and stabilisation of the full complex (adapted from Spasic and Annaert, 2008).

Localization

Soon after the initial identification of PS1, its intracellular localization was determined to be mostly in the ER (Kovacs et al., 1996). In contrast, presumed sites of γ-secretase activity ranged from the ER to the Golgi, the trans-Golgi network (TGN), secretory vesicles, plasma membrane (PM) and endosomes/lysosomes. These observations led to the proposal of the 'spatial paradox' (Annaert and De Strooper, 1999), that referred to the apparent discrepancy in the localization of PS in the ER and the sites of γ-secretase activity proposed to be in later compartments of the secretory pathway.

Only fully assembled complexes leave the ER and reach later compartments of the secretory pathway. It has been demonstrated that all four γ-secretase complex components are localized in an active form at the PM (Chyung et al., 2005) and in lysosomes, while there is no substantial γ-secretase activity in the ER, the Golgi and the TGN. Therefore, γ-secretase activity is localized to the PM and/or endosomes (Kaether et al., 2006).

Function

PSs have been implicated in the Notch signalling pathway, which is required for cell differentiation during development and adulthood. Notch is a cell surface receptor with type I membrane topology, which is processed in a very similar manner like APP. Following cleavage of the Notch ectodomain at the cell surface, γ-secretase cleaves the resultant C-terminal Notch membrane fragment to release Nβ, an Aβ-like peptide, into the extracellular space and the Notch intracellular domain (NICD) into the cytosol (Okochi et al., 2002). The NICD translocates to the nucleus, where it functions as a transcriptional regulator of target genes required for cell differentiation. Thus, enabling Notch signalling is a major function of γ-secretase.

Notch is apparently the most important physiological substrate of γ-secretase, as genetic ablations of PSs and other γ-secretase subunits are associated with severe Notch phenotypes (Selkoe and Kopan, 2003). Based on the canonical Notch model for this type of signalling, it is usually proposed that the intracellular fragments released by γ-secretase

cleavage are involved in nuclear signalling and transcriptional regulation (Haass, 2004). Indeed, the fact that intracellular domains become released during this degradation process does not necessarily imply that they have also a signalling function. Moreover, most of these fragments are degraded very rapidly in the cytoplasm. The i-Clip γ-secretase may also fulfill a second and probably more important function: it seems to be required for the efficient destruction of membrane-retained protein fragments. This activity has been called the "membrane-proteasome" function of γ-secretase.

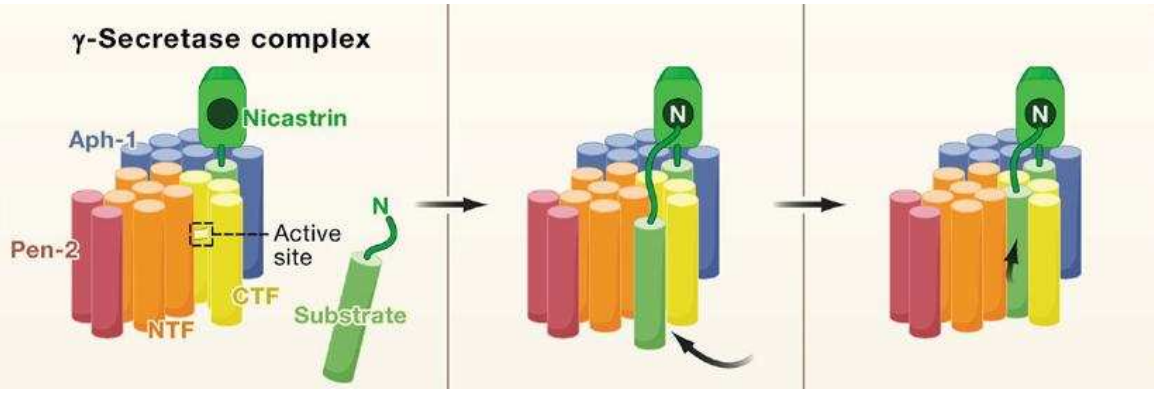

Figure 2.3. Schematic drawing of the interactions between the γ-secretase complex components: presenilin (as NTF and CTF subunits; orange and yellow, respectively), nicastrin (bright green), Aph-1 (blue), and PEN-2 (red), with the active site inside presenilin at the NTF-CTF interface. Membrane protein stubs serving as substrates (pale green) dock both on the outer surface of presenilin at the NTF-CTF interface and with the nicastrin ectodomain before entering into the internal active site (from Selkoe and Wolfe, 2007).

Accessory proteins

TMP21

The type 1 transmembrane protein termed TMP21 is a member of the p24 cargo-family which may have a signalling role in the sorting and transport of proteins from the ER to the Golgi. It was shown that TMP21 is a member of the γ-secretase complex as it was isolated in a high molecular weight PS complex, interacts with all of the known components of the γ-secretase complex and co-localised with the complex components in the ER, Golgi and cell surface (Chen et al., 2006). A role has been proposed for TMP21 in modulating γ-secretase activity to generate Aβ. This role for TMP21 appears to be independent of its role in protein transport. It appears that TMP21 may function to regulate intramembrane proteolysis controlling γ-secretase activity and thus preventing the over-production of Aβ.

CD147

CD147, a transmembrane glycoprotein and a member of the immunoglobulin (IgG) superfamily of receptors, is involved in many physiological and pathological conditions (Muramatsu and Miyauchi, 2003). CD147 was suggested to be an additional, regulatory subunit associated to the γ-secretase complex (Zhou et al., 2005). CD147 decreases Aβ production without any significant effect on AICD production or Notch cleavage.

Immunohistochemistry of brain tissues from AD and control revealed specific up-regulation of CD147 in neurons, axons and capillaries of AD frontal cortex and thalamus (Nahalkova et al., 2009).

Presenilin interacting proteins

In addition to Aβ generation and Notch signalling, PSs have been implicated in a variety of intracellular processes including membrane trafficking, neuronal plasticity, cell adhesion, regulation of Ca^{2+} homeostasis, the unfolded protein response, and apoptosis. PS1 has been identified as an element of intercellular junctions together with E-cadherin and β-catenin (Georgakopoulos et al., 1999). PS1 was also shown to mediate intercellular contacts, act as a scaffold protein for kinases and their substrates.
Therefore it is not surprising that PSs have a growing list of binding partners, beside those in the γ-secretase complex; here are a few examples.

Calsenilin

Calsenilin is a calcium binding protein, that was first identified through yeast two hybrid screening using the PS2 C-terminus as the bait protein (Buxbaum et al., 1998). Calsenilin is also called downstream regulatory-element antagonist modulator (DREAM) or potassium channel α-subunit interacting protein (KChIP3). The three proteins are the products of a single gene, their function being specified by their cellular location. Calsenilin may facilitate PS mediated apoptosis, since calsenilin was shown to preferentially interact with the C-terminal fragment of PS2 that results from caspase cleavage of the PS holoprotein (Choi et al., 2001). The interaction between PS and calsenilin may also be involved in ER Ca^{2+} release (Leissring et al., 2000; Lilliehook et al., 2002; Fedrizzi et al., 2008). Calsenilin may also be implicated in APP processing and Aβ generation, suggesting that calsenilin has another function, to facilitate γ-secretase activity.
In fact, calsenilin expression was reported to be increased in brain tissues of AD patients and over-expression of calsenilin enhanced γ-secretase activity in cells (Jo et al., 2005). The histochemical localization of calsenilin and its expression levels in the brains of sporadic AD have been investigated. Both messenger RNA and protein expression of calsenilin were observed in neurons and reactive astrocytes of the cerebral cortex and hippocampus of control brains; a more intense staining was detected in AD brains; this increased expression is consistent with the regions that are affected by pathological changes caused by AD (Jin et al, 2005). Calsenilin may thus play an important role in apoptosis and in AD pathology.

Sorcin

It has been observed a molecular interaction of the large hydrophilic loop region of PS2 with sorcin, a cytosolic penta-EF-hand Ca^{2+}-binding protein that serves as a modulator of the ryanodine receptor intracellular Ca^{2+} channel (RyR) (Pack-Chung et al., 2000). The

association of endogenous sorcin and PS2 was demonstrated in cultured cells and human brain tissues. Sorcin was found to interact with the stable C-terminal endoproteolytic fragment of PS2 but not with the immature full-length form, and the sorcin/PS2 interaction was greatly enhanced by treatment with the Ca^{2+} ionophore A23187, indicating that the recruitment of sorcin into a membrane-bound molecular complex harboring PS2 is modulated by intracellular Ca^{2+} levels.

This interaction between sorcin and PS2-CTF has important implications at cardiac level. In the heart, sorcin is localized at or near the T tubules and binds to the cardiac ryanodine receptor RyR2. Studies of RyRs incorporated into lipid bilayers have revealed that sorcin reduces the open probability of RyR2. PS2 interacts with both RyR2 and sorcin and plays an important role in excitation-contraction coupling by interacting with RyR2 in hearts (Takeda et al., 2005). Elevated Ca^{2+} attenuated the association of RyR2 with PS2, whereas the association of sorcin with PS2 was enhanced (Pack-Chung et al., 2000). With low Ca^{2+} concentrations, PS2 binds to RyR2 to inhibit RyR2 activity. The inhibition of RyR2 activity by PS2 and sorcin raises the possibility that PS2 and sorcin together may help prevent an excessive release of Ca^{2+} by inhibiting RyR2 activity. PS2 dysfunction may thus lead to the abnormality of Ca^{2+} homeostasis and disturb the cardiac function and be involved in the pathogenesis of heart failure.

Caspase-6

Caspases (Casps), a group of cysteinyl endoproteases that cleave proteins after aspartic acid residues, are activated in inflammatory and apoptotic conditions. Caspase has been demonstrated to increase Aβ production in various cell types (Gervais et al., 1999; Tesco et al., 2003). In primary cultures of human neurons, the caspase responsible for increasing Aβ is Casp-6. Activated Casp-6 has been detected in NFT, and neuritic plaques in the hippocampus and temporal cortex in sporadic AD (Guo et al., 2004). Casp-6 activation is an early event in AD and it may precede the development of frank lesions. Casp-6 may play a key role in the development of AD because, being early activated (Albrecht et al., 2007), it can cleave important synaptic and cytoskeleton proteins and generate high levels of Aβ (LeBlanc, 1995). Casp-6 is also activated in familial AD, as previously observed in sporadic forms (Albrecht et al., 2009).

GRB2

GRB2 (growth factor receptor-bound protein 2) adaptor protein provides a critical link between cell surface growth factor receptors, Ras signalling and cell proliferation. Both APP and PS1 interact with GRB2 in vesicular structures at the centrosome of the cell, a crucial region for microtubule nucleation, cell cycle progression, migration, cytokinesis, and cell division. The final target for these interactions is ERK1,2, which is activated in mitotic centrosomes in a PS1- and APP-dependent manner. Therefore, both APP and PS1 could be part of a common signalling pathway that regulates ERK1,2 and the cell cycle (Nizzari et al, 2007). In AD brain, APP interaction with GRB2 is enhanced (Russo et al., 2002).

Ubiquilin

Ubiquilin was originally identified in a yeast 2-hybrid screen as an interactor of PSs (Mah et al., 2000). Ubiquilin interacts with the their cytosolic loop (Mah et al., 2000). Ubiquilin has been shown to affect PS accumulation and biogenesis, as over-expression of ubiquilin results in increased accumulation of full-length proteins and a parallel decrease in the production of PS N- and C-terminus fragments (Massey et at., 2004 and 2005).

3. Familial Alzheimer's Disease

Although the great majority of AD cases are sporadic, of unknown aetiology, a low percentage of patients are affected by the familial form of the disease (Familial Alzheimer's Disease, FAD), whose prevalence is estimated below 5%. Genetic abnormalities that cause FAD are largely due to fully penetrant, autosomal dominant mutations in 3 genes: the APP gene on chromosome 21, PS1 on chromosome 14 (Sherrington et al., 1995) and PS2 on chromosome 1 (Levy-Lahad et al., 1995; Rogaev et al., 1995). Mutations in PS1 account for the majority of autosomal dominant cases with 178 mutations described to date, compared to 32 and 14 mutations in APP and PS2, respectively (from http://www.molgen.ua.ac.be/ADMutations, last update January 2010). In the majority of cases, these mutations occur before the age of 65 years (early-onset AD).

Beside the dominant mutations in APP, PS1 and PS2 genes that cause FAD, polymorphisms increasing risk of sporadic AD have also been identified, in the genes for apolipoprotein E4, sortilin-1, Ca^{2+} homeostasis modulator 1 (CALHM1) and ubiquilin-1 (Cedazo-Minguez and Cowburn, 2001; Rogaeva et al., 2007; Dreses-Werringloer et al., 2008; Bertram et al., 2005).

CALHM1

Recently, a novel Ca^{2+} -conducting channel has been discovered, with polymorphisms associated with increased risk for the development of sporadic AD (Dreses-Werringloer et al., 2008). This Ca^{2+} channel was found to be a conserved three-transmembrane domain containing glycoprotein and it has been called Ca^{2+} homeostasis modulator 1 (CALHM1). Expression of CALHM1 was found in all brain regions and cells of neuronal lineage. CALHM1 localized predominantly to the ER but also exists at the plasma membrane, where it forms a novel Ca^{2+} influx route to the cytosol.

CALHM1 appears to exist as multimeric complexes, forming a functional ion channel, and has structural similarities with the N-methyl-D-aspartate (NMDA) receptor within the ion selectivity region. Critically, Ca^{2+} influx through CALHM1 decreases Aβ production and is accompanied by increases in α-APPs.

A polymorphism in the CALHM1 gene, the P86L variant, has been linked to sporadic AD: it decreases Ca^{2+} permeability and also increases Aβ production. This finding provides

direct genetic evidence of a Ca^{2+} -conducting channel impacting the development of AD and shows that Ca^{2+} influx pathways can affect APP processing to modulate the production of Aβ.
An increase in Ca^{2+} can stimulate the metabolism of APP (Pierrot et al., 2004). Ca^{2+} entry through CALHM1 may represent a tightly controlled influx pathway with novel spatial links to APP processing, which other cytosolic Ca^{2+} influx pathways do not seem to mimic. One possibility is that the entry through the CALHM1 channel normally activates the non-amyloidogenic pathway and thus prevents the conversion of APP to amyloids. The other unexplored possibility is that the effects of CALHM1 and the P86L variant exert their effects on Aβ processing via their spatial location in the ER rather than the smaller pool found on the plasma membrane, given that the vast majority of CALHM1 was localized to the ER.
The channels responsible for the passive Ca^{2+} leak from the ER remain to be properly characterized (see also paragraph "Ribosome - Translocon Complex", p. 30). One possibility is that the CALHM1 channel may function as a leak channel. The P86L CALHM1 polymorphism would then increase the level of stored Ca^{2+} by reducing this putative leak pathway.

ApoE

Apolipoproteins are responsible for transporting cholesterol from the blood into cells. Apolipoprotein E (ApoE) has a major role in influencing how Aβ is formed and hydrolysed (Jiang et al., 2008). It can increase Aβ peptides degradation by functioning as a chaperone to shepherd them to the insulin-degrading enzyme.
Aβ peptides can be removed by different mechanisms. First, the Aβ formed in the late endosomes can be transferred to lysosomes where they are degraded. Autophagy is also an efficient mechanism for removing amyloids (Nixon, 2007). During the onset of AD, autophagy is increased but the transfer of autophagic vesicles to the lysosomes is impaired and this may contribute to the accumulation of Aβ peptides, likely due to reduced levels of beclin-1 (Pickford et al. 2008). Finally, the Aβ monomers that are released to the outside of the neuron can be removed by the microglia.
ApoE can also bind to various members of the low-density lipoprotein receptor (LDLR) family that control the endocytosis of lipoproteins. Some of these LDLRs, such as SORL1, interact with APP directing it to the recycling endosome and thus redirect it back to the surface and prevent it from being hydrolysed by the β-secretase pathway (Offe et al., 2006). In this way, ApoE protects neurons by reducing both the formation of the Aβ monomers and by enhancing their degradation. Polymorphisms of the ApoE gene markedly increase the susceptibility of developing AD. The ApoE gene encodes three isoforms: ApoE2, ApoE3, and ApoE4. Of the three isoforms, E3 is the most common and E2 the least common. The risk of developing AD is markedly increased in individuals that inherit the ApoE4 isoform (Cedazo-Minguez and Cowburn, 2001), whereas the E2 isoform reduces the risk (Huang, 2006). It would seem that ApoE4 enhances the onset of

AD by increasing the conversion of APP into the amyloids and by reducing their clearance by the degradation pathway. On the other hand, ApoE2, but not ApoE4, can inhibit Aβ association with phosphatidylserine in the membrane, providing a potential explanation for protective effects of ApoE2 in AD.
Several studies indicate a potential link between ApoE and synaptic Ca^{2+} signalling. It has been demonstrated a neurotoxic effect of the ApoE fragment, mediated by Ca^{2+} influx through NMDA receptor channels (Tolar et al., 1999). Moreover, it was reported that the receptor-binding domain of ApoE is capable of stimulating ER Ca^{2+} release and extracellular Ca^{2+} influx (Wang and Gruenstein, 1997).

SORL1

Recent reports have implicated the neuronal sortilin-related receptor gene (SORL1, also known as SORLA and LR11) as a susceptibility gene for late-onset AD.
The first study that reported the allelic and haplotypic associations between AD and variants in SORL1 was in 2007 by Rogaeva and co-workers (Rogaeva et al., 2007). This finding corroborates a previous study which showed a decreased expression of Sorl1 protein in the brain of AD patients that correlates with an increased Aβ production (Andersen et al., 2005). Subsequently, several studies supported the initial finding by showing that genetic variants in SORL1 contribute toward AD (Lee JH et al., 2008a and 2008b). SORL1 is a member of the low density lipoprotein receptor family of ApoE receptors. It is located on chromosome 11 and encodes a 250-kD membrane protein expressed in neurons of the central and peripheral nervous system. It is known to be involved in intracellular trafficking between the membrane and intracellular organelles, interacting with APP in endosomes and the trans-Golgi network (TGN) in both *in vitro* and *in vivo* experiments (De Strooper and Annaert, 2000).
Under-expression of SORL1 leads to over-expression of Aβ; furthermore, SORL1 levels are reduced in AD patients (Scherzer et al., 2004).
The TGN and the endosomes were identified as the key organelles organizing the complex movements of the transmembrane proteins via secretory and endocytic pathways. Important coat complexes initiating the transport of APP and BACE through this sorting itinerary are the clathrin coat and the retromer (Small et al., 2005). Clathrin coats are involved in the endocytic pathway connecting the cell surface to the endosome and the pathway connecting the TGN to the endosome. The retromer is involved in the trafficking from the endosome to the TGN. Through the retromer complex, SORL1 directly binds APP and differentially regulates its sorting into endocytic or recycling pathways. In the absence of SORL1, APP is released into late endosomal pathways, where it is subjected to both β- and γ-secretase cleavages, which eventually lead to Aβ production. Therefore, genetic variants in SORL might influence Aβ processing.

Presenilin mutations

PS mutations are scattered throughout the PS polypeptide. Most PS mutations are simple missense mutations that result in single amino-acid substitutions. Some are more complex, for example, small deletions, insertions or splice mutations. The most severe mutation in PS1 is a donor–acceptor splice mutation that causes two amino acid substitutions and an in-frame deletion of exon 9. Of note, this deletion causes the loss of endoproteolysis but not of γ-secretase activity (Verdile et al., 2004; Garcia-Alloza et al., 2006; Ruan et al., 2009). A truncation or absence of the protein has never been observed, indicating that haploinsufficiency does not cause AD.

All these PS1 and PS2 mutations influence APP metabolism to alter Aβ production, leading to a shift of the preferred cleavage site from position 40 to 42 (Suzuki et al., 1994). Not all FAD-linked PS mutations cause an increase in $A\beta_{42}$ production, while importantly they more consistently result in a decrease in absolute $A\beta_{40}$ generation, leading to an increased $A\beta_{42}/A\beta_{40}$ ratio (Kumar-Singh et al., 2006) $A\beta_{42}$ has a much higher propensity to aggregate and be neurotoxic; it has been described as a 'nucleation' factor, which notably accelerates the aggregation of Aβ into amyloid *in vitro* (Jarrett & Lansbury, 1993). $A\beta_{42}$, although generated by neurons at a tenfold lower rate than $A\beta_{40}$, is the first and predominant species accumulating in amyloid plaques in the brains of AD patients (Iwatsubo et al, 1994). Given that inactivation of PS1 and PS2 completely prevents Aβ generation (Herreman et al, 2000), an absolute or a relative increase in $A\beta_{42}$ production can represent a gain of toxic function.

Several studies describe a reduced function of PS mutations towards the cleavage of APP, Notch and other γ-secretase substrates (Song et al., 1999; Bentahir et al., 2006); therefore, PS mutations result in a loss of function of the γ-secretase. This apparently translates into an 'incomplete digestion' of the APP substrate, generating fewer but longer Aβs (Qi et al., 2005), causing an increase in the $A\beta_{42}/A\beta_{40}$ ratio. There is still the possibility that partial dysfunction of PS1—for example, in the Notch signalling pathway that modulates neurite outgrowth and brain repair—makes the brain more prone to Aβ toxicity. This would fit with the previously proposed 'two-hit' model for AD (Marjaux et al, 2004), and would also explain why familial AD generally strikes earlier and is more aggressive than sporadic AD. Thus FAD mutations might cause AD by the combined effect of a partial loss of function in Notch signalling, AICD production and signalling, as well as a toxic gain of misfunction.

A proposed model for γ-secretase, is that the substrate-binding site is distinct from the catalytic active site and that, once the substrate is 'docked', it is subsequently displaced to the catalytic site of the enzyme (Berezovska et al., 2003; Tian et al., 2003). Thus the clinical mutations could cause loss of function not only by interfering with the catalytic efficiency of the protease, but also by subtly modifying the docking of substrates and/or by interfering with the mechanism that moves the substrate towards the catalytic site. This would also explain the diverse effects on APP and other substrates of the PS mutants.

The next aspect to consider is how this change in amyloid processing remodels neuronal Ca^{2+} signalling pathways to disrupt the mechanisms of learning and memory.

4. Calcium

A role for Ca^{2+} dysregulation in Alzheimer's disease was first proposed 20 years ago by Khachaturian, who postulated that sustained intracellular Ca^{2+} disturbances are the proximal causes of neurodegenerative disorders, including AD (Khachaturian, 1987 and 1994). This theory was supported by experimental studies which showed alterations in Ca^{2+} signalling both in sporadic and in familial cases of AD (Etcheberrigaray et al., 1998; Ito et al., 1994). Moreover, Ca^{2+} disturbances long precede the onset of other AD symptoms, as shown in cells obtained from presymptomatic family members of examined FAD patients who subsequently developed AD (Etcheberrigaray et al., 1998; Giacomello et al., 2005).

Ca^{2+} ions are indispensable for a number of functions of the nervous system, including regulation of gene expression, proliferation, excitability, release of neurotransmitters, and cell death. The ''Ca^{2+} hypothesis of ageing'' proposed that brain ageing might be a result of a subtle, but long-lasting, dysregulation of Ca^{2+} homeostasis in neurons. During physiological ageing, such changes lead to a slight neuronal dysfunction, but, usually, not to neuronal death. What is likely to be altered in aged neurons is their capacity to maintain a steady level of Ca^{2+}; therefore, upon stress, Ca^{2+} in the cytoplasm might go up. Some parameters of Ca^{2+} homeostasis, such as the duration of cytoplasmic Ca^{2+} signals and the restoration of the Ca^{2+} concentration to basal levels are consistently shown to be longer in aged neurons than in young ones (Thibault et al., 2007).

Even though dysregulation of Ca^{2+} handling and signalling seems not to be an initializing factor of ageing, it is a crucial component of this process. Ca^{2+} homeostasis seems to be most altered in energy consuming cells, like neurons and the striated and smooth musculature of the cardiovascular system of aged humans, which are the sites of most common age-related diseases, dementia and cardiovascular disease.

As regard AD, altered neuronal Ca^{2+} homeostasis may affect the metabolism and production of the pathological proteins associated with the disease: elevated basal Ca^{2+} concentration results in excessive tau phosphorylation (Mattson et al., 1991) and in amyloid precursor protein processing leading to an excessive Aβ production (Buxbaum et al., 1994). Conversely, events downstream from the accumulation of these pathological proteins may further exacerbate Ca^{2+} dysregulation, causing synaptic dysfunction and neurodegeneration, the neurobiological substrates underlying the cognitive decline.

Several studies describe that pathogenesis of AD is frequently accompanied by changes in the expression levels of Ca^{2+}-buffer and Ca^{2+}-sensor proteins (Braunewell and Gundelfinger, 1999). It still remains elusive whether these alterations are secondary to neurodegeneration or whether they underlay the pathogenesis of the disease.

The involvement of Ca^{2+} in AD was further substantiated with the recognition that clinical mutations in both PS1 and PS2 genes associated with familial AD profoundly disrupt intracellular Ca^{2+} signaling.

Ca^{2+} through the plasma membrane

Various Ca^{2+}-permeable channels are present in the plasma membrane (PM). In excitable cells, depending on the cell type, voltage-operated Ca^{2+} channels (VOCCs) (Felix, 2005) or receptor-activated Ca^{2+} channels (RACCs) (Trebak et al., 2003) predominate. Transient receptor potential channels (TRPCs) are RACCs that are activated by different stimuli, such as intra- and extracellular messengers, chemical, mechanical, and osmotic stress, and by the Ca^{2+} content of intracellular stores (Clapham, 2003). However, both VOCCs and RACCs are also present in non-excitable cells.

Receptor-induced Ca^{2+} signals lead to the release of Ca^{2+} from the endoplasmic reticulum (ER) stores, triggering Ca^{2+} entry through the different store-operated Ca^{2+} channels (SOCCs) that are present in the PM. Ca^{2+} release-activated channels (CRACs) are activated by depletion of Ca^{2+} from the ER (see paragraph on p. 31).

Since Ca^{2+} regulates numerous and distinct cellular processes, stimulus-evoked Ca^{2+} responses need to be spatially and temporally restricted: Ca^{2+} influx across the PM or its release from the ER creates microdomains with high local concentrations of Ca^{2+} (estimated to be in the range of 50–100 μM) (Targos et al., 2005).

Clearance of Ca^{2+} from the cytoplasm is attributed mainly to Ca^{2+} pumps and exchangers such as the plasma membrane Ca^{2+} ATPase (PMCA) and the Na^{+}/Ca^{2+} exchanger (NCX) present in the PM, the sarco-endoplasmic reticulum Ca^{2+}-ATPase (SERCA) pump located in the ER membrane, and the mitochondrial uniporter.

Endoplasmic Reticulum

ER is continuous with the outer nuclear membrane and is often associated intimately with plasma membrane and mitochondria, which suggests functional coupling between these structures (Rizzuto et al., 1998). It is classically divided into two subtypes: ‘rough’ ER, which contains ribosomes and is responsible for protein synthesis, and ‘smooth’ ER, which can serve a particularly important role in Ca^{2+} signalling. The specialized endings of neurites (growth cones, axon terminals and dendritic spines) contain mainly smooth ER.

The ER is the most important intracellular Ca^{2+} store that can accumulate Ca^{2+} to micromolar concentrations of up to a few hundred μM, while the concentration of the ion in the cytoplasm of the resting cell remains within the range of 100–300 nM (Rossi et al., 2008). This Ca^{2+} gradient is maintained by an ATP-dependent pump called sarco-endoplasmic reticulum Ca^{2+}-ATPase (SERCA) in the ER membrane. Upon stimulation of PM receptors or upon electrical excitation of the PM, the ER releases Ca^{2+}, thus participating in the generation of rapid Ca^{2+} signals. Since the ER storage capacity is

limited, Ca^{2+} release must be followed by Ca^{2+} replenishment. Ca^{2+} movements across the ER membrane are facilitated by three classes of proteins: Ca^{2+} release channels – inositol-1,4,5-triphosphate (IP_3) receptors (IP_3Rs) (Mikoshiba, 2007) and ryanodine receptors (RyRs) (Hamilton, 2005), Ca^{2+} re-uptake pumps –SERCAs (Periasamy and Kalyanasundaram, 2007), and luminal Ca^{2+}-binding proteins, such as calsequestrin, sarcalumenin, histidine-rich Ca^{2+}-binding protein, calreticulin, etc. Different 'pools' of ER Ca^{2+} might exist that contain either IP_3Rs, RyRs, or both.

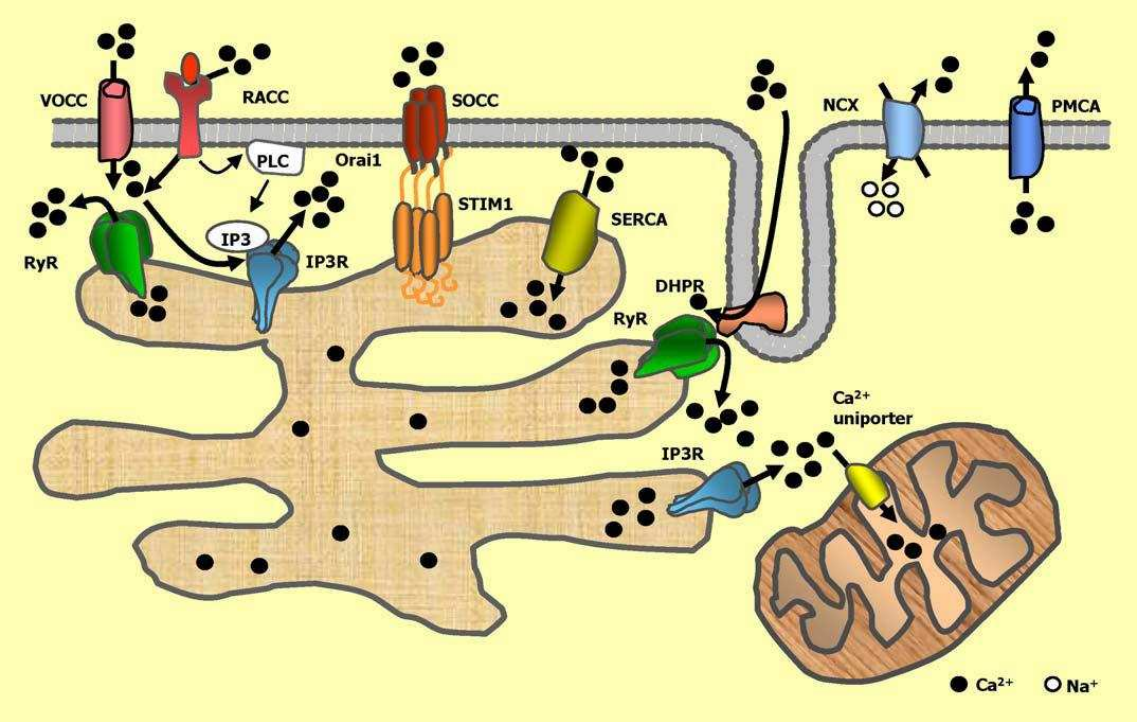

Figure 4.1. A simplified model of ER Ca^{2+} homeostasis and signalling (from Puzianowska-Kuznicka and Kuznicki, 2009).

IP_3 Receptor

IP_3Rs, protein components of Ca^{2+} release channels present in the ER membrane, are expressed in all mammalian cells. IP_3R contains the IP_3-binding domain, and two putative Ca^{2+}-binding sites in its N-terminal part and in its C-terminal channel-forming domain. There are three isoforms of IP_3R (IP_3R1–3). The channel is composed of four IP_3R subunits (Bezprozvanny, 2005). It releases Ca^{2+} into the cytoplasm in response to IP_3 produced by diverse stimuli; however, it is also regulated by other ligands, such as cytoplasmic Ca^{2+} (Foskett et al., 2007).

Ca^{2+} is released from IP_3R-containing pools in response to agonists that activate receptors coupled to phospholipase C (PLC). Activation of PLC results in cleavage of PtdIns(4,5)P2, which results in the liberation of diacylglycerol and IP_3. IP_3 binds to the IP_3Rs in the ER, which results in channel opening (Mattson et al., 2000).

Ryanodine Receptor

RyRs are large proteins positioned in the ER membrane with a major part of their molecules facing the cytoplasm. Transmembrane and luminal domains constitute only approximately 20% of the RyR mass. RyR tetramers form massive Ca^{2+} release channels that interact with many accessory proteins. Ca^{2+}-sensing domains (putative EF-hands) are present on both the luminal and the cytoplasmic sides of RyRs. There are three isoforms of RyR known (RyR1–3). RyR1 and RyR2 are mostly expressed in the skeletal and cardiac muscles, respectively, while RyR3 is expressed ubiquitously. The release of Ca^{2+} from the ER, mediated by RyR channels, is essential for striated muscle contraction and for diverse neuronal functions (Hamilton, 2005).

IP_3Rs and RyRs are found in overlapping populations of neurons throughout the nervous system, but also exhibit clear differences in relative levels and in subcellular localization. The presence of caffeine-sensitive Ca^{2+} stores (presumed ryanodine sensitive) in presynaptic nerve terminals, together with the possibility that neurotransmitter release might be triggered by Ca^{2+} released through intraterminal RyRs, suggests that ER has a central role in the control of neurotransmitter release (Etcheberrigaray et al., 1991; Avidor et al., 1994)

Ribosome – Translocon Complex

Under resting conditions, the ER Ca^{2+} concentration results from the active Ca^{2+} influx of SERCA pumps that balances the efflux due to passive Ca^{2+} leak. It has been shown that the permeability of the ER is dynamically coupled to protein synthesis and that polarized molecules could cross the ER membrane through the translocon, which is the complex implicated in protein translocation during translation (Roy and Wonderlin, 2003). Nascent proteins cross the membrane of the rough ER by passing through a protein-conducting channel in the translocon complex. The pore of this protein-conducting channel must be large enough to be permeated by a nascent protein chain. This pathway is therefore large enough to be permeated by many other small molecules (like sugars), when a ribosome-bound translocon is translationally inactive and empty, *i.e.* the pore is not occupied by a nascent protein (Heritage and Wonderlin, 2001). Indeed, other studies have demonstrated that the open translocon complex is permeable to Ca^{2+} and, therefore, it has been suggested that the ribosome-translocon complex could potentially play a role in Ca^{2+} leakage (Lomax et al., 2002; Van Coppenolle et al., 2004; Flourakis et al., 2006).

SERCA

The Sarco-Endoplasmic Reticulum Ca^{2+} ATPase belongs to the family of P-type ATPases that includes plasma membrane Ca^{2+} ATPase (PMCA), Na^+/K^+ ATPase, and H^+, K^+ ATPase. The SERCA pump is a single polypeptide of molecular mass of 110 kDa and is localized both in the ER and Sarcoplasmic Reticulum (SR) membrane. A notable feature of P-type ATPases is the transfer of terminal phosphate from ATP to an aspartate residue in the catalytic domain, resulting in a reversible conformational change. P-type ATPases couple the hydrolysis of ATP to the movement of ions across a biological membrane. The

SERCA pump utilizes the energy derived from ATP hydrolysis to transport Ca^{2+} across the membrane. The mechanism of the coupling process is such that two Ca^{2+} ions are transported for each molecule of ATP hydrolyzed. In vertebrates there are three distinct genes encoding SERCA 1, 2, and 3 that are known to produce more than 10 isoforms, mainly through alternative splicing (Brandl et al., 1986; Lytton et al., 1988, Periasamy and Kalyanasundaram, 2007). These isoforms exhibit both tissue and temporal specificity. Their activity is regulated by N-glycosylation, glutathionylation, Ca^{2+}/calmodulin kinase II-dependent phosphorylation, and interaction with other small-molecular-weight proteins such as phospholamban (PLB) and sarcolipin (SLN) expressed in cardiac and skeletal muscles (Traaseth et al., 2008). SERCA-2 is evolutionary the oldest and the most widely expressed isoform. SERCA-1 is expressed in fast-twitch skeletal muscle and is alternatively spliced to encode SERCA-1A (994 aa, adult) and 1b (1011 aa, fetal). SERCA-2 encodes SERCA-2A (997 aa), which is expressed predominantly in cardiac and slow-twitch skeletal muscle, and SERCA-2B (1042 aa), which is expressed in all tissues at low levels including muscle and non muscle cells (Guntenski-Hamblin et al., 1988). Recently, a third isoform, SERCA-2C (999 aa), has been reported in cardiac muscle. SERCA-3 isoforms are expressed in several non muscle tissues but appear to be a minor form in muscle (Wuytack et al., 1994). A notable feature of SERCA isoforms is that their primary structure is highly conserved; therefore, all of the SERCA isoforms are predicted to have essentially identical transmembrane topologies and tertiary structures. Another interesting feature is that all of the SERCA isoforms are inhibited by thapsigargin. The crystal structure of SERCA confirmed the presence of 10 transmembrane helices, three cytoplasmic domains, an A domain (actuator or anchor domain), a P domain (phosphorylation domain), and an N domain where ATP binds (Moller et al., 2005). The crystal structure further showed that the two Ca^{2+} binding sites lie side by side, near the cytoplasmic surface of the lipid layer. Ca^{2+} binding sites are accessible only from the cytoplasm and not from the ER lumen. SERCA-2A and the ubiquitous SERCA-2B isoforms are structurally similar for the first 993 amino acids, whereas SERCA-2B has an extension of 49 amino acids and SERCA-2A has only four C-terminal unique amino acids. The two isoforms showed functional differences: SERCA-2B has a higher affinity for Ca^{2+} compared to SERCA-2A, whereas SERCA-2A has a higher turnover rate than SERCA-2B. The structural differences in the C-terminal amino acids have been shown to contribute to the functional differences between SERCA-2A and 2B (Verboomen et al., 1992).

Ca^{2+} release-activated channels (CRACs)

In the majority of excitable cells, a major route of Ca^{2+} entry into the cytoplasm are channels located in the PM. However, intracellular Ca^{2+} stores, including the ER, also play an important role in signal propagation. A major Ca^{2+} entry pathway in non-excitable cells is initiated by depletion of Ca^{2+} from the ER.

Concentration of Ca^{2+} in the lumen of the ER is ‘sensed’ by stromal interaction molecule 1 (STIM1), a protein residing in the ER membrane and containing a single transmembrane

domain. Its N-terminus positioned in the lumen of the ER contains the Ca^{2+}-sensing region (Stathopulos et al., 2008). When the ER Ca^{2+} content is high, STIM1 molecules are distributed throughout the ER membrane, bind a single Ca^{2+} ion, and their N-termini are folded. Upon Ca^{2+} depletion, the Ca^{2+} ion detaches from the EF-hand of STIM1; this results in partial unfolding of the N-terminus and in the aggregation of STIM1 molecules (Luik et al., 2008; Stathopulos et al., 2008). STIM1 oligomers translocate to the proximity of the PM (Liou et al., 2007) and form so-called ‘‘punctae’’. The C-terminal regions of STIM1 molecules activate Ca^{2+} release-activated Ca^{2+} modulator 1 (Orai1) proteins that reside in the PM. Each Orai1 molecule possesses four transmembrane domains and both its N- and C-termini are positioned inside the cell (Huang et al., 2006). Four Orai1 molecules create the pore-forming subunit of CRAC that opens upon stimulation by STIM1, with the C-terminus of STIM1 and N-terminus of Orai1 participating in this process (Lewis, 2007). This facilitates Ca^{2+} influx into the cytoplasm, a mechanism called store-operated Ca^{2+} entry (SOCE). Ca^{2+} inflow through the PM refills the ER store, enabling it to release Ca^{2+} in response to a subsequent stimulus.

Some authors suggest that STIM2 has a function distinct from that of STIM1; namely, STIM2 is a feedback regulator that stabilizes basal cytosolic and ER Ca^{2+} levels (Brandman et al., 2007).

Golgi Apparatus

The Golgi complex may store up to 5% of the total cellular Ca^{2+} at significantly higher concentrations (1–2 mM) than any other region of the cell (Chandra et al., 1991). The Ca^{2+} pools represented by the ER and the secretory pathway (Golgi complex and different types of secretory vesicles) participate in the regulation of a variety of cell functions. For instance, a sufficiently high luminal Ca^{2+} concentration in these organelles is absolutely required for the normal synthesis, chaperone-dependent processing, glycosylation, sorting and eventual breakdown of newly formed proteins. Moreover, the Golgi apparatus, as well as the ER, is a potential provider for Ca^{2+} ions in the cytosol, where Ca^{2+} controls a whole range of physiological processes depending on the amplitude, the frequency and the subcellular localization of the cytosolic Ca^{2+} signal. The Golgi apparatus also typically contains several different luminal Ca^{2+}-binding proteins and is equipped with Ca^{2+}-release channels such as the IP_3 receptor. Hence the Golgi compartments and perhaps secretory vesicles can potentially act as dynamic Ca^{2+} stores (Pinton et al., 1998; Mitchell et al., 2001).

Ca^{2+} uptake mechanisms in the Golgi complex consist of the well-known SERCAs and the much less characterized secretory-pathway Ca^{2+} ATPases (SPCA) It is now generally accepted that SPCA1 is present in the Golgi membranes, but it is not the only pump in this compartment. A significant part of the Ca^{2+} uptake into the Golgi compartment depends on SERCA pumps, since it has been shown that Ca^{2+} uptake by the Golgi apparatus is reduced in the presence of thapsigargin (Vanoevelen et al., 2004). Whereas the SERCA pumps are expressed in both the ER and the Golgi complex, SPCA1 appears to be more specifically confined to the latter compartments of the secretory pathway, i.e. the Golgi

stacks, the TGN and the secretory vesicles. SPCA1 is highly expressed in human epidermal keratinocytes and at variable levels in all other human tissues tested, suggesting that it is a housekeeping gene.

Mitochondria

Mitochondria play a role in Ca^{2+} homeostasis too. These organelles can store Ca^{2+} in their matrix by action of a uniporter that uptakes Ca^{2+} exploiting the high electrochemical H^+ gradient across the mitochondrial membrane that is created by the respiratory chain. However, this influx never reaches a steady-state; in fact, in the mitochondrial inner membrane there is also an antiport system that extrudes Ca^{2+} from the organelle exchanging it with H^+ or Na^+. This antiport is necessary to avoid the dissipation of the H^+ gradient. Mitochondrial Ca^{2+} concentration has been measured, showing that when there is an agonist-evoked transient cytosolic Ca^{2+} increase, even mitochondria respond with a transient Ca^{2+} increase, that can reach values up to 100-fold higher than the cytosolic increase (Rizzuto et al., 1992). This finding led to the hypothesis that mitochondria localize in microdomains where Ca^{2+} can reach very high levels.
There are functional relationships between Ca^{2+} release from IP_3-sensitive ER stores and mitochondrial Ca^{2+} uptake. Mitochondria in close physical proximity to ER rapidly take up Ca^{2+} released from ER such that local cytoplasmic Ca^{2+} levels in the ER–mitochondria cleft are markedly higher than global increases in cytoplasmic Ca^{2+} concentration (Rizzuto et al., 1998; Csordas et al., 1999). These data, and other morphological findings, suggest that mitochondrial uptake sites might be concentrated in regions of the membrane opposed to IP_3R-containing ER.
Periodic oscillations of cytosolic Ca^{2+} levels are believed to have important roles in various metabolic and signalling processes in many cell types, including neurons. Reciprocal interactions between ER Ca^{2+} stores, mitochondria and plasma membrane Ca^{2+} channels appear to be required for Ca^{2+} oscillations (Li et al., 1995).
The impaired Ca^{2+} signalling that occurs during AD might increase the amount of Ca^{2+} being taken up by the mitochondria. Such an excessive uptake of mitochondrial Ca^{2+} results in opening of the mitochondrial permeability transition pore (MTP), collapse of the mitochondrial membrane potential and the release of factors such as cytochrome c that activate the caspase cascade responsible for apoptosis.

5. Presenilins and calcium

The effects of PS mutations on Ca^{2+} are striking and have been hotly debated. According to the most followed scheme of the "Ca^{2+} hypothesis" of AD, mutated PSs cause neuronal degeneration through an exaggerated or supranormal ER Ca^{2+} release, that in turn leads to abnormal mitochondrial Ca^{2+} uptake and apoptosis (LaFerla, 2002; Thinakaran and Sisodia, 2006). Indeed, it was reported that different FAD-linked mutations in PS1 (PS1-L286V, PS1-A246E and PS1-M146V) caused larger Ca^{2+} release from intracellular stores

in PC12 cells (Guo et al., 1996 and 1997; Keller et al., 1998) as well as in neurons from transgenic mice expressing the mutant protein (Chan et al, 2000; Pak et al., 2003; Stutzmann et al., 2004 and 2006); these neurons also showed an increased sensitivity to excitotoxicity. Further support to this "Ca^{2+} overload" hypothesis came from two recent studies where in membrane bilayers, microsomes and living cells, PSs have been shown to form Ca^{2+} leak channels that are defective in the presence of FAD mutations (Tu et al., 2006; Nelson et al., 2007). Consequently, in cells carrying these mutant PSs, the reduced ER Ca^{2+} conductance of leak channels is thus responsible of the ER Ca^{2+} overload.
All these observations in favour of the "Ca^{2+} overload hypothesis" made it for a long time the only "Ca^{2+} hypothesis" for AD, stating that FAD-linked PS mutations, by increasing the ER Ca^{2+} content, cause excessive Ca^{2+} release from the intracellular store, increasing sensitization to Aβ and excitotoxic stimuli and eventually leading to cell death via Ca^{2+}-dependent mechanisms (Bezprozvanny and Mattson, 2008).

Nevertheless, different works reported either no alteration or a reduced store Ca^{2+} content in cells expressing wt or FAD-mutant PSs (Moerman and Barger, 1999; Lessard et al., 2005; Fedrizzi et al., 2008; Cheung et al., 2008). In particular, it was demonstrated that the FAD-linked PS2 mutations M239I and T122R reduce rather than increase Ca^{2+} release in fibroblasts from FAD patients and in cell lines stably or transiently expressing the PS2 mutants (Zatti et al., 2004; Giacomello et al., 2005). In addition, an extended investigation of other FAD-linked PS mutants (PS2-N141I, PS1-A246E, PS1-L286V, PS1-M146L, PS1-P117L), by directly monitoring the ER and the Golgi Ca^{2+} content in different cell lines, confirmed that the FAD-linked PS2 mutations cause a reduction in the Ca^{2+} level of these organelles and none of the PS1 mutations cause an increase (Zatti et al., 2006). Moreover, PS1 and PS2 mutants were also tested in rat cortical neurons upon transient co-expression with green fluorescent protein (GFP): among GFP-positive cells, only those expressing PS2-T122R, but not PS1-A246E or PS1-M146L, showed a marked reduction of Ca^{2+} release induced by an IP_3 generating agonist.
The absence of elevated $[Ca^{2+}]_{ER}$ in these models suggests that the enhanced Ca^{2+} release observed by other studies, upon expression of various FAD-linked PS mutants, might depend on different mechanisms, rather than be necessarily due to an increased amount of Ca^{2+} within the stores. Consequently, the "Ca^{2+} overload" hypothesis should be rethought, as it often takes the form of an "exaggerated Ca^{2+} release", not necessarily reflecting the store Ca^{2+} content (Green and LaFerla, 2008).
Interestingly, at variance with the effects of different FAD mutations in PS1, the partial ER Ca2+ depletion induced by mutations in PS2 can be regarded as a protective event against the possible damage caused by Aβ oligomers or oxidative stress, given the anti-apoptotic effect of low ER Ca^{2+} levels (Giacomello et al., 2007). Accordingly, mutations in PS2 appear to be endowed of a lower toxicity (with respect to those in PS1), considering also the later onsets and milder AD phenotypes usually associated to those mutations. The Ca^{2+} dysregulation so often described in different AD models could thus

be considered as either a positive or a negative modulator, rather than a causative factor involved in the neurodegeneration which is typical of the disease.

The hypothetical mechanisms through which PS mutants exert their effect on Ca^{2+} homeostasis are numerous. Over-expression of mutant PS1 or PS2 directly increased IP_3 channel activity by prolonging the channel open time. Increased IP_3R gating accounted for the enhanced IP_3R-mediated Ca^{2+} release observed in the presence of FAD-linked PS mutants. In fact, an indirect measurement of $[Ca^{2+}]_{ER}$ showed either no change or a modest reduction in the cells expressing the mutant PSs, compared to control cells. These results show a novel interaction between FAD-PS mutants and IP_3Rs, where PSs are able to modulate the IP_3Rs gating activity and affect global Ca^{2+} dynamics (Cheung et al 2008). Noteworthy, in this work, no current was measured by patch clamp through ER membrane, despite over-expression of wild-type or FAD-linked PS mutants, arguing against PS forming Ca^{2+} leak channels (Tu et al., 2006; Nelson et al., 2007).
PS have been shown to interact also with the RyR, via its N-terminus, and to increase the open channel probability and mean current (Rybalchenko et al., 2008; Hayrapetyan et al., 2008).
Increased Ca^{2+} release via the RyR has been described in a number of systems, including slice recordings from FAD-PS mutant knockin mice (Stutzmann et al., 2007) and primary neuronal cultures and may be due to increased RyR expression and activity (Smith et al., 2005; Lee et al., 2006).
Finally, endogenous PS seems to interact with SERCA and modulate SERCA function; SERCA pumping is impaired in the absence of both PSs (Green et al., 2008).

Taken together, PSs appear to interact and modulate Ca^{2+} influx into the ER via SERCA, and Ca^{2+} extrusion from the ER via interactions with the ryanodine and IP_3 receptors. Further experiments will be required to show which interactions are mediated in an endogenous role versus those influenced by FAD mutant PSs.
It needs also to be elucidated whether the effects of wt and mutant PSs on Ca^{2+} homeostasis are dependent on γ-secretase activity or whether these effects are independent and perhaps rely on uncleaved PS prior to its recruitment into the γ-secretase complex.

The PS mutants may also contribute to Ca^{2+} signalling remodeling by altering the expression levels of various components of the Ca^{2+} signalling toolkit. In fact, γ-secretase releases the APP intracellular domain (AICD), which is a transcription factor that may result in a significant remodeling of the Ca^{2+} signalling system (Leissring et al., 2002). It has been known for some time that during normal ageing there are gradual changes in certain Ca^{2+} signalling components that increase neuronal vulnerability to cell death stimuli. For example, there is a decline in the level of the Ca^{2+} buffer calbindin D-28 k that normally functions to restrict the amplitude of Ca^{2+} signals and protects neurons from excitotoxicity (Geula et al., 2003). The number and size of calbindin immunoreactive neurons in the cerebral cortex areas were significantly reduced in AD patients when

compared with age-matched controls (Ichimiya et al., 1988). Mice expressing mutant APP also display a decline in the level of calbindin D-28 k, especially in the dentate gyrus region of the hippocampus, which functions in learning and memory (Palop et al., 2003), while calbindin knockout mice have increased dendritic spine basal Ca^{2+} and develop abnormal spine morphologies (Vecellio et al., 2000).

Aβ and calcium

Evidence suggests that Ca^{2+} might be the upstream factor that, during ageing and AD, results in increased production and aggregation of Aβ.

Exposure of cultured neurons to Ca^{2+} ionophores increases their production of Aβ, as do conditions such as ischemia that cause sustained elevations of intracellular Ca^{2+} (Querfurth and Selkoe, 1994). By contrast, physiological Ca^{2+} transients increase α-secretase cleavage of APP and might thereby decrease Aβ production (Buxbaum et al., 1994).

Aβ peptides may impair Ca^{2+} signalling by enhancing Ca^{2+} entry. The cellular prion protein (PrPC), which is tethered to the outside of the membrane through a glycosylphosphatidylinositol anchor, functions as an Aβ receptor (Laurén et al., 2009) and may thus carry out some of the pathological actions of $Aβ_{42}$. Aβ oligomers also bind to the N-methyl-D-aspartate (NMDA) receptor and induce Ca^{2+} influx (De Felice et al., 2007). Influx through the NMDA receptor also leads to further Ca^{2+} release into the cytosol from internal stores within the spine, which forms the major component of spine Ca^{2+} transients. Aβ peptides thus increase the vulnerability of neurons to excitotoxicity mediated by the NMDA receptor (Mattson et al., 1992).

Another mechanism by which Aβ can cause Ca^{2+} influx is by inserting into the plasma membrane and forming ion conducting pores (Arispe et al., 1993; Demuro et al., 2005). Neurotoxic forms of Aβ are oligomers that share structural and functional homology with pore-forming bacterial toxins and the cytotoxic lymphocyte protein perforin (Yoshiike et al., 2007). Interestingly, the ability of Aβ to associate with membranes and form channels is enhanced by exposure of phosphatidylserine on the cell surface (Lee G et al., 2002). Because cell-surface exposure of phosphatidylserine is usually indicative of apoptotic or energy-deprived cells, it is possible that age-related mitochondrial impairments might increase surface phosphatidylserine levels in affected neurons and thereby facilitate Aβ-mediated pore formation, Ca^{2+} influx and cell death.

A different mechanism by which Aβ perturbs neuronal Ca^{2+} homeostasis in synaptic terminals is by inducing membrane lipid peroxidation, resulting in Ca^{2+} overload, synaptic dysfunction, neuronal degeneration and cognitive impairment (Mark et al., 1997; Mattson, 2004).

Finally, in addition to increasing the production of Aβ, amyloidogenic processing of APP can perturb neuronal Ca^{2+} homeostasis through the AICD, that affects ER Ca^{2+} release by regulating the expression of genes involved in Ca^{2+} homeostasis (Leissring et al., 2002).

Ca^{2+} signalling, learning and memory in AD

There are clear indications that AD is a progressive disease where changes in synaptic physiology and decline in cognitive function become apparent before any significant neuronal loss (Jacobsen et al., 2006; Hsieh et al., 2006). Synaptic terminals are particularly vulnerable to Ca^{2+}-mediated degeneration because they experience repeated bouts of Ca^{2+} influx and have unusually high energy requirements to support their ion-homeostatic and signalling systems. Activation of the amyloidogenic pathway results in a remodeling of the neuronal Ca^{2+} signalling pathway. This remodeling then functions to distort the normal Ca^{2+}-dependent mechanisms responsible for learning and memory. Remodeling of Ca^{2+} signalling affects both entry of external Ca^{2+} and release from internal stores.

Long-lasting changes in synaptic efficacy that result from prior activity in neuronal circuits are believed to have important roles in learning and memory. The appearance of amyloid oligomers has been linked to a decline in both neural activity and the mechanisms responsible for learning and memory (Walsh et al., 2002). These learning mechanisms are carefully orchestrated by neuronal Ca^{2+} signalling systems through a bimodal action that is revealed physiologically as either long-term potentiation (LTP) or long-term depression (LTD) of the α-amino-3-hydroxy-5-methyl-4-isoxazolepropionic (AMPA) receptors responsible for fast excitatory neurotransmission. High levels of Ca^{2+} cause LTP, activating processes such as AMPA receptor phosphorylation, remodeling of the cytoskeleton and the trafficking and insertion of AMPA receptors. These are dynamic processes that are readily reversible by lower Ca^{2+} rises to cause LTD. This LTD mechanism, which erases putative memories, appears to depend on activation of the Ca^{2+}-dependent protein phosphatase calcineurin. In aged rats and in APP transgenic mice, which show defects in cognition, there is an up-regulation of calcineurin (Dineley et al., 2007).

Aβ oligomers can inhibit the induction of LTP (Walsh et al., 2002). LTP was however reduced also in the PS double knock out mouse where there appeared to be a selective decrease in presynaptic transmitter release (Zhang, et al., 2009). The remodeling of the Ca^{2+} signalling system may have a major impact on the process of LTD (Hsieh et al., 2006; Kuchibhotla et al., 2008). Since LTD is driven by small elevations in Ca^{2+}, any up-regulation of Ca^{2+} signalling will selectively enhance LTD to continuously erase any memories initiated by LTP.

The ER plays a central role in the regulation of neurotransmitter release (Neher and Sakaba, 2008) and has important functions in both presynaptic and postsynaptic processes associated with synaptic transmission and plasticity. In fact, one of the mechanisms for inducing LTD is the activation of metabotropic glutamatergic receptors that generate IP_3 to release Ca^{2+} from internal stores. Treatment of hippocampal slices with agents that deplete ER Ca^{2+} (thapsigargin and cyclopiazonic acid) blocks the induction of LTD (but not its maintenance) without affecting basal synaptic transmission (Reyes and Stanton, 1996).

Beside considering global Ca^{2+} dynamics within neurons in pathologically affected areas, it is also informative to take a closer look at discrete areas of neurons, such as the dendritic spines, which contain many of the postsynaptic synapses. An elegant approach to cast some light on this aspect was stereotactically injecting an adeno-associated virus expressing the YC3.6 ratiometric Ca^{2+} indicator into APP mouse models of AD (Kuchibhotla et al., 2008). Neurons were predominantly infected, thereby allowing the visualization of dendritic spines and other fine structures. The study identified that plaque-containing transgenic mice had significantly elevated numbers of neuritis (ten times more) with overloaded cytosolic Ca^{2+} compared to age-matched non-transgenic controls, although these overloaded neuritis represented only a small fraction of the total. The resting Ca^{2+} concentration in these overloaded spines affected neurite morphology, with higher basal levels being associated with abnormal beaded morphology. These results highlight that proximity to Aβ plaques induces Ca^{2+} dysregulation, and, in discrete subcellular compartments relevant to learning, also memory (LTP) and synaptic loss.

6. Calcium probes

The study of the dynamics of intracellular Ca^{2+} concentration $[Ca^{2+}]_i$ in cell physiopathology requires the ability to monitor the changes in $[Ca^{2+}]_i$ in living cells with both spatial and temporal precision. Ca^{2+} probes are molecules that can form selective and reversible complexes with Ca^{2+} ions and, most importantly, the physicochemical characteristics of the free and bound form are sufficiently different to enable their relative concentrations to be measured. So, the Ca^{2+} indicator monitors the amounts of free and complexed probe and thus the concentration of free Ca^{2+} is indirectly measured. All Ca^{2+} sensors are Ca^{2+} buffers too; therefore, unavoidably, the measurement of the Ca^{2+} concentration ($[Ca^{2+}]$) with indicators leads to an increase in the Ca^{2+} buffering capacity.
Ca^{2+} sensors can be divided in two main families: synthetic dyes and protein-based indicators.

Synthetic dyes

The first, rationally designed, fluorescent Ca^{2+} probes were created back in early 1980s (Tsien, 1980). These fluorescent polycarboxylate dyes are derivatives of the selective Ca^{2+}-chelator EGTA. In BAPTA, the prototype fluorescent polycarboxylate dye, the two methylene groups of EGTA have been replaced by two benzene rings to enable it to function as a chromophore. The conformational change caused by Ca^{2+} binding to the carboxyl groups is transmitted to the chromophore and results in changes in the excitation and/or emission properties of the dye. BAPTA itself could not be used as an intracellular indicator because it absorbs light in the far ultraviolet (UV) spectrum, but its derivative quin2 became immediately popular.
The modification that really improved and made these dyes extremely easy to use was the synthesis of their hydrophobic acetoxymethyl (AM) esters (Tsien, 1981), which allowed

the trapping of these indicators in living cells. The ester-loading technique is simple; the dyes need just to be added to the medium: thanks to their hydrophobicity, the AM esters can diffuse across the plasma membrane of the cell. Once in the cytoplasm, they are hydrolized by the endogenous esterases. The original, hydrophilic dye is thus released and at the same time trapped in the cytoplasm.

There are two different types of synthetic dye: ratiometric dyes and non-ratiometric dyes.
In ratiometric dyes, such as fura-2 and indo-1, the excitation (or emission) spectrum changes according to the free [Ca^{2+}]. The [Ca^{2+}] is measured as the ratio between two fluorescence intensity values that are taken at two wavelengths, λ1 and λ2, corresponding to the fluorescence peak in high or low free [Ca^{2+}] condition respectively. The advantage of ratiometric dyes is the intrinsic correction for unequal dye loading, bleaching and focal-plane shift, as the ratio does not depend on the absolute intensity of the two signals.
In non-ratiometric dyes, such as fluo dyes and rhod dyes, [Ca^{2+}] is determined solely by a relative increase in the fluorescence intensity on elevation of the free [Ca^{2+}]. The single excitation or acquisition allows for simpler instrumentation or simultaneous observation of other parameters, but a complex calibration is needed to translate the fluorescence intensity into actual [Ca^{2+}] values.

Protein-based sensors

Back in the 1960s, the phenomenon of bioluminescence was investigated in the jellyfish *Aequorea victoria*. These studies identified two proteins - aequorin (Aeq) (Shimomura et al., 1962) and green fluorescent protein (GFP) (Morise et al., 1974), both of which have impacted greatly on the life science. Proof of this is the 2008 Nobel Prize in Chemistry awarded to Osamu Shimomura, Martin Chalfie and Roger Y. Tsien “for the discovery and development of the green fluorescent protein”.

Aequorin

Apoaequorin is a 21-kDa photoprotein that is linked covalently to a hydrophobic prosthetic group, coelenterazine. Upon Ca^{2+} binding, aequorin undergoes a conformational change that leads to the irreversible peroxidation of the coenzyme to the oxidized form, coelenteramide, with production of blue light. The fractional rate of Aeq consumption is proportional, in the physiological pCa range, to [Ca^{2+}]. The cloning of the Aeq complementary DNA (cDNA) (Prasher et al., 1985) allowed the recombinant expression of the Aeq protein; this, in turn, eliminated the need for traumatic loading procedures, since the protein could be endogenously produced by cells (Button and Brownstein, 1993; Sheu et al., 1993). Moreover, the aequorin cDNA can be engineered to include specific targeting signals, thus leading to selectively localize the Ca^{2+} probe in subcellular compartments (Rizzuto et al., 1992, 1993, 1994b and 1995; Brini et al., 1993 and 1994; Kendall et al., 1992 and 1994). Recombinant apoaequorin can be reconstituted into active photoprotein by simply adding the coenzyme to the incubation medium; aequorin light emission then allows the monitoring of the [Ca^{2+}] in the compartment to which the

photoprotein is confined. However, aequorin probes present one important flaw: although the amount of photons that are emitted from a cell population is more than adequate for the measurement of the [Ca^{2+}], the amount of photons that are emitted by a single cell is very low. Better tools to this purpose are GFP-based Ca^{2+} sensors.

GFP-based probes

Heterologously expressed GFP maintains its strong fluorescence (Chalfie et al., 1994) and recombinant Ca^{2+} probes based on GFP were developed (Romoser et al., 1997). At present, there are three main types of this sensor that are commonly used; the so-called *camgaroos* (Baird et al., 1999), the *pericams* (Nagai et al., 2001) and the *cameleons* (Miyawaki et al., 1997). *Camgaroos* and *pericams* are single GFP-based probes, while *cameleons* are made up of two GFP variants. All of these probes use calmodulin (CaM) as a molecular switch, which changes its conformation upon the binding of Ca^{2+}. In turn, this conformational change alters the fluorescence properties of the GFP-based sensor, and this is then used to calculate the [Ca^{2+}].

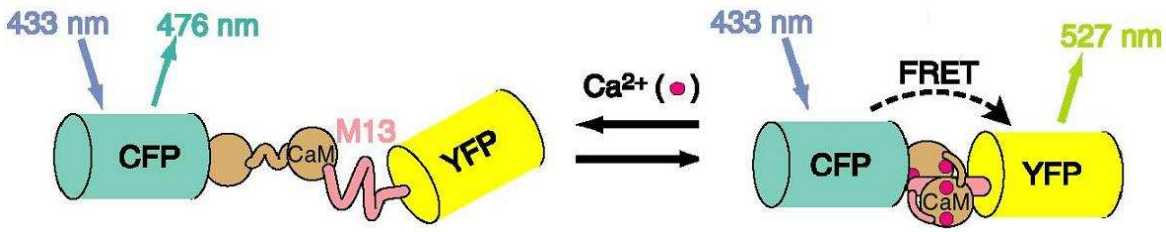

Figure 6.1. Schematic representation of how a classic *cameleon* Ca^{2+} sensor works. Upon binding Ca^{2+}, calmodulin and the M13 peptide fold, bringing the two GFP variants close enough to enable FRET (adapted from Zhang et al., 2002).

Cameleons are based on a strategy - the change of fluorescence resonance energy transfer (FRET). FRET is the physicochemical phenomenon that is characterized by the transfer of energy from an excited donor chromophore to an acceptor chromophore, without associated radiation release. FRET occurs when the donor emission and acceptor excitation spectra overlap considerably and the two dipoles are very close to each other (2–7 nm). FRET is proportional to the 6th power of the distance between the chromophores and, therefore, even minor conformational changes can induce considerable FRET changes. The occurrence of FRET results in the change of several fluorescence parameters; the most used in the measurement of Ca^{2+} concentration is the changes in the emission spectrum at constant excitation. It has been used the most because of the simplicity of its use, the relatively limited cost and the high velocity of image acquisition, which mainly depends on the speed of the imaging system and the dissociation time constant of Ca^{2+} from the probe. In the *cameleons*, FRET occurs between two differently coloured mutants of GFP (usually the cyan fluorescent protein - CFP - and the yellow fluorescent protein - YFP -) and it is caused by the interaction between Ca^{2+}-activated CaM and the target peptide (Miyawaki et al., 1997; Romoser et al., 1997). In the *cameleon* probe designed by Tsien and co-workers, the target peptide (the CaM-binding peptide

M13) and CaM are fused together. A Ca^{2+}-induced interaction between calmodulin (CaM) and M13 increases FRET, leading to a decrease in the fluorescence of CFP and an increase in the fluorescence of YFP. Several variations of these probes have been produced by replacing the GFP variants, by introducing mutations in the CaM domain and by replacing M13 with a different CaM-binding peptide (Miyawaki et al., 1999; Truong et al., 2001; Persechini et al., 1997). Many of the recombinant expression strategies initially used for Aeq have also been used with the *cameleons*, and several variants with targeting sequences and Ca^{2+} sensitivity that are suitable for many subcellular compartments are now available (Emmanouilidou et al., 1999; Jaconi et al., 2000; Isshiki et al., 2002). The success of the *cameleons*, however, is limited by two principal experimental problems. The first is the relatively small change in signal on Ca^{2+} binding, and the second is the large size and molecular complexity that might, in some cases, significantly impair its targeting efficiency, for example to the mitochondrial matrix. However, the low diffusion rate due to its high molecular mass might turn into an advantage when high spatial accuracy is needed, for example, to measure and localize Ca^{2+} 'puffs' or 'sparks'.
Sensitivity to pH is another serious problem with GFP-based indicators. With the synthetic dyes, pH has an effect on fluorescence and Ca^{2+} affinity only below about pH 6,5, whereas with most GFP-based probes, even pH changes around neutral can lead to marked changes in fluorescence. Finally, it is worth pointing out that the loss of signal (owing to photobleaching and/or photoisomerization) with protein dyes is more significant than with synthetic dyes, and that some GFPs have absorption spectra that are not suitable for standard confocal microscope laser lines.

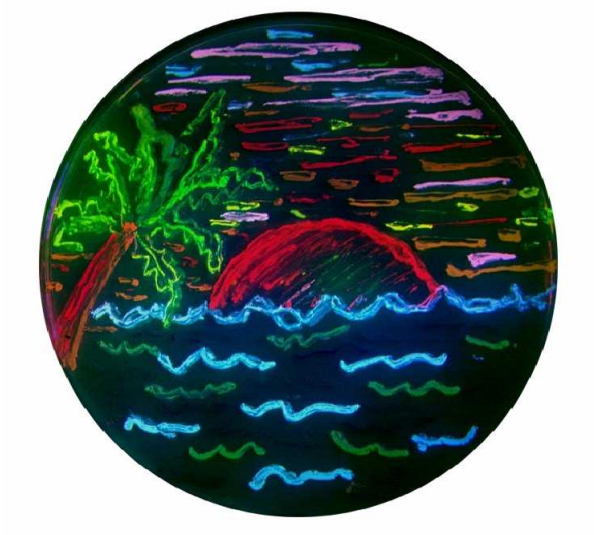

Figure 6.2. Bacteria expressing differently coloured GFP variants on a Petri dish (from R.Y. Tsien's lab).

Aim

It has previously been demonstrated that different FAD-linked mutations in PS2, and to a lesser extent also in PS1, reduce the steady-state ER and Golgi apparatus Ca^{2+} level ($[Ca^{2+}]_{ER}$ and $[Ca^{2+}]_{Go}$ respectively) (Zatti et al., 2004; Giacomello et al., 2005; Zatti et al., 2006). Yet the molecular mechanism(s) underlying the effect of PS mutants on store Ca^{2+} handling is still an open question. Looking for answers, we started studying the PS2-induced Ca^{2+} imbalance at the ER level. We picked as cellular models of choice SH-SY5Y cells and murine embryonic fibroblasts (MEFs). The first model was preferred because it is an immortalized cell line derived from a human neuroblastoma: it is therefore more similar to neurons, the cellular target of FAD. MEFs were equally useful because, a clone, double knock-out (DKO) for both PS1 and PS2, was available and well described in the literature. This cell line could allow us to investigate the effect of different PSs in a null background, while avoiding possible misleading contribution of the endogenous proteins. The FAD-linked mutant PS2 that was used for most of the experiments was PS2-T122R. In fact, among the various PS constructs that were tested,this particular mutation was the one exerting the most striking effect on intracellular Ca^{2+} handling.
The ER Ca^{2+} content can be reduced by either increasing the passive leak or by impairing the active uptake of the ion (or both). So, potential targets of PS2-T122R could be the physiological Ca^{2+} release channels, like IP_3Rs or RyRs, and/or the SERCA pumps. Hints from the very first experiments performed suggested that the latter could be mainly affected by PS2, so we focused on the interaction between these two proteins. Ca^{2+} measurements were carried out with aequorin-based probes; cell biology techniques (Western blotting and co-immunoprecipitation assays) were also used to address the issue. Moreover, opposite strategies, as over-expression and down-regulation experiments, were also designed to further confirm the results obtained.

The second part of this work was dedicated to a more technical issue. A long-term goal of the project is studying Ca^{2+} dynamics, both *in vitro* and *in vivo*, in the brain of AD mouse models based on APP and FAD-linked PS mutants through single cell live Ca^{2+} imaging with FRET-based *cameleon* probes. To this purpose, a preliminary set up of the suitable experimental conditions to be employed with these Ca^{2+} sensors was thus necessary. SH-SY5Y cells, as the cell model closest to neurons, were used to test whether the ER-D1 and the novel Go-D1cpV *cameleons* could properly be used to reproduce the Ca^{2+} defect induced by PS2-T122R, previously observed with the aequorin-based probes.

Results I

The main part of this work was dedicated to unraveling the molecular mechanism(s) underlying the PS2-induced reduction in the ER Ca^{2+} level. To this purpose, FAD-linked PS2-T122R was selected as the reference mutation, although the role of wt PS2 has also been investigated. Ca^{2+} measurements were performed with aequorin-based probes in different cell models. In the second part of this section, the results obtained from the tests carried out with the ER-D1 and the Go-D1cpV *cameleons* in SH-SY5Y cells are reported.

FAD-linked PS2-T122R reduces steady-state $[Ca^{2+}]_{ER}$ in permeabilized cells

Previous experiments carried out in intact cells demonstrated that FAD-linked mutations in PS2 decrease the ER Ca^{2+} content (Zatti et al., 2004; Giacomello et al., 2005; Zatti et al., 2006). However, in intact cells, ER Ca^{2+} uptake can be influenced by a number of factors, such as, for instance, the activity of the Ca^{2+} ATPase pump PMCA and the Na^{+}/Ca^{2+} exchanger in the plasma membrane. Therefore, we performed similar experiments in permeabilized cells to avoid the interference of these mechanisms. The cells were transiently transfected with ER-Aeq and PS2-T122R or the void vector (pcDNA3) as control and 24 h after transfection, ER-Aeq reconstitution was carried out with emptied stores as described (see Materials and Methods, p. 61). Cells were then permeabilized with digitonin (20 - 100 μM for 1 – 2 minutes, according to the cell model) in an EGTA-buffered intracellular solution. After permeabilization, cells were extensively (2 - 5 minutes) washed with the same solution and perfused with a Ca^{2+}-EGTA buffered solution with a known free Ca^{2+} concentration; the ER refilling process was then continuously monitored. These experiments were performed in different cell models (SH-SY5Y, wild-type MEFs and DKO MEFs) (fig. 1.1 and table 1): under these conditions, the reduction in the steady-state $[Ca^{2+}]_{ER}$ in PS2-T122R transfected cells was not only consistently observed but also of entity similar to the one previously measured in intact cells: for instance, 47% reduction in permeabilized SH-SY5Y cells with respect to 53% measured in intact cells (Zatti et al., 2006).

Noteworthy, as it can be seen from the average refilling traces in fig. 1.1, also the rate of the ER Ca^{2+} uptake was sensibly reduced in PS2-T122R over-expressing cells, if compared to control cells. This difference was clear since the very beginning of ER refilling, when the store is still almost completely empty. Therefore, it seemed unlikely that the main effect of the mutant PS2 was to increase the Ca^{2+} leakage out of the ER. We thus decided to focus our efforts on unraveling the possible interaction between mutant PS and SERCA pump.

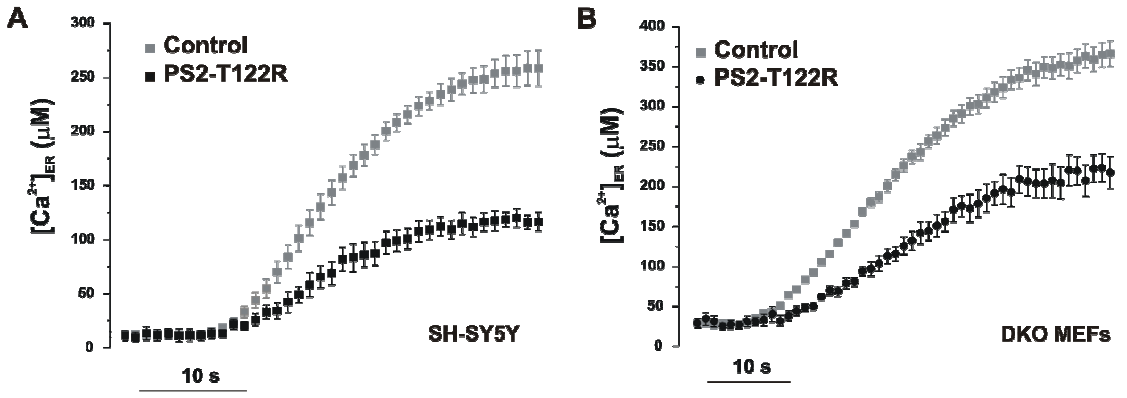

Figure 1.1. SH-SY5Y cells (panel A) and DKO MEFs (panel B) were transiently co-transfected with the cDNAs coding for ER-Aeq and PS2-T122R (black) or the void vector as control (grey). Upon Aeq reconstitution, the cells were washed and bathed in a Ca^{2+}-free, EGTA (0.6 mM) containing medium. After digitonin permeabilization and washing in an EGTA-based intracellular buffer, ER Ca^{2+} uptake was followed, perfusing the cells in an EGTA-based intracellular buffer with ATP (0.2 mM) and free [Ca^{2+}] = 0.3 mM (see Materials and Methods). Traces were aligned to Ca^{2+} addition, black and grey symbols for PS2-T122R expressing and control cells respectively (mean ± s.e.m., n = 12 for SH-SY5Y and n = 16 for DKO MEFs).

Cell type	Control	n	PS2-T122R	n	% Change
SH-SY5Y	298,2 ± 9,6	28	140,5 ±8,0 ***	29	-53
wt MEFs	310,7 ± 27,0	27	180,0 ± 21,8 ***	9	-42
DKO MEFs	306,5 ±27,4	11	211,6 ± 16,1 ***	10	-31

Table 1. ER steady-state Ca^{2+} levels (μM). Steady-state $[Ca^{2+}]_{ER}$ was measured in digitonin permeabilized cells transfected with ER-Aeq in experiments performed as described in fig. 1.1 (*** = $p < 0.001$).

PS2-T122R does not alter SERCA-2 protein levels

Upon the observation that PS2-T122R seems to somehow impair the SERCA pump, by slowing down the Ca^{2+} uptake rate, we first checked the SERCA-2 protein level in cells over-expressing the mutant PS2, to rule out the possibility that PS2-T122R might act by reducing SERCA pump expression.

From an evolutionary point of view, SERCA-2 is the the oldest isoform among SERCA pumps and its alternative splicing variant SERCA-2B is ubiquitously expressed and present also in non muscle cells.

In none of the cell models tested, over-expression of PS2-T122R led to a reduction in the SERCA-2 protein level, as shown by Western blots in fig. 1.2.

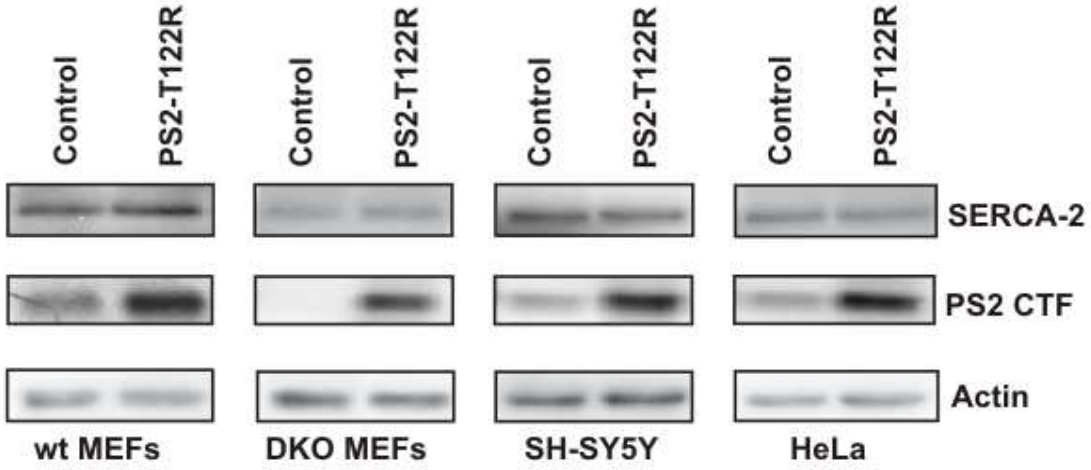

Figure 1.2. Western blots showing SERCA-2 and PS2 levels in control and PS2-T122R expressing cell lines.

PS2-T122R impairs the maximal uptake rate (V_{max}) of the SERCA-2 pump

The effect of PS2-T122R on SERCA-2 seems then to be a functional impairment; to test this hypothesis, we performed a series of experiments in permeabilized cells in different cell lines (SH-SH5Y and DKO MEFs). The cells, transiently co-transfected with ER-Aeq and PS2-T122R or the void vector; were permeabilized and the ER refilling process was achieved by perfusing cells with an EGTA-based intracellular buffer containing free Ca^{2+} at different, known concentrations. For each experimental trace showing how $[Ca^{2+}]_{ER}$ changes during time (in particular during ER Ca^{2+} uptake, see fig. 1.1), the first derivative was calculated. The maximal value of the first derivative corresponds to the maximal uptake rate (V_{max}) value of the SERCA-2 pump. These values were plotted as a function of the corresponding free external $[Ca^{2+}]_o$ used. Fig. 1.3 shows that, at each $[Ca^{2+}]_o$ tested, the cells expressing PS2-T122R have a lower V_{max} value if compared to their control cells. In the DKO MEFs model we also checked the effect of wild-type (wt) PS2 on the uptake rate of SERCA-2. Interestingly, wt PS2 has a similar effect to PS2-T122R, although slightly weaker: V_{max} was 9.4 ± 0.9 μM/s (n = 7) and 14.4 ± 0.8 μM/s (n = 8), respectively at 0.3 and 1.5 μM $[Ca^{2+}]_o$.

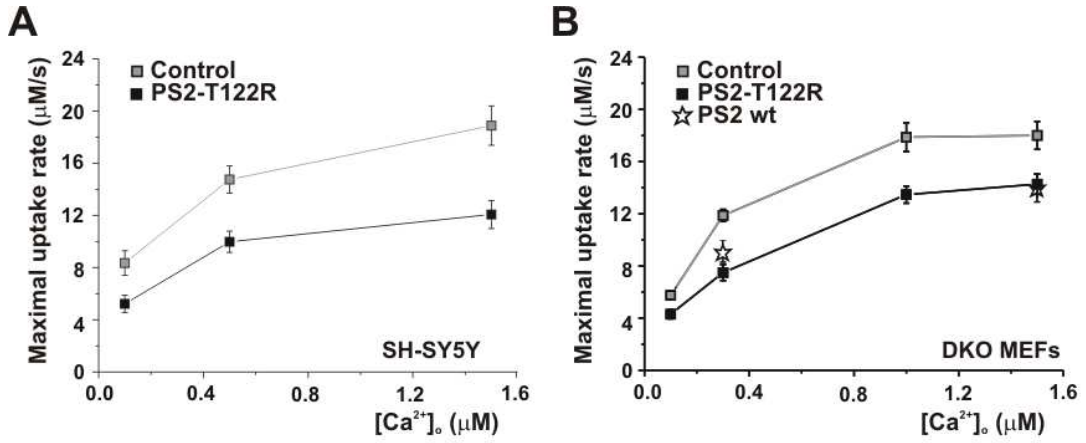

Figure 1.3. ER Ca^{2+} uptake was followed in permeabilized SH-SY5Y cells (panel A) and DKO MEFs (panel B) at different free $[Ca^{2+}]_o$. The maximal values of the first derivative of the instantaneous $[Ca^{2+}]_{ER}$ ($d[Ca^{2+}]_{ER}/dt$) were plotted as a function of the free external $[Ca^{2+}]_o$ (mean ± s.e.m, n ranging from 6 to 20). Panel B also shows the values obtained with wt PS2 (empty stars).

A double reciprocal fitting curve of these plots allowed us to infer the Ca^{2+} binding affinity (K_m) and V_{max} values of the SERCA-2 pump in both PS2-T122R expressing and control cells, as reported in table 2. The V_{max} was the SERCA-2 pump kinetic parameter mostly impaired by PS2-T122R while the K_m was almost unaffected.

Cell type	K_m (nM)		% Change	V_{max} (μM/s)		% Change
	Control	*PS2-T122R*		*Control*	*PS2-T122R*	
SH-SY5Y	150	167	11	19,3	12,8	-34
wt MEFs	164	175	7	14,5	10,1	-30
DKO MEFs	277	321	16	21	16,4	-22

Table 2. Kinetic parameters of ER Ca^{2+} uptake.

Ca^{2+} release from intracellular stores is unaltered in cells co-expressing SERCA-2B and PS2-T122R

With these results in mind, we wondered whether co-expression of the SERCA-2B pump together with PS2-T122R was enough to compensate for the Ca^{2+} handling defects induced by the latter. SH-SY5Y cells were thus transiently co-transfected with the cDNAs codying for Cyt-Aeq and PS2-T122R plus void vector in the presence or absence of SERCA-2B. After aequorin reconstitution, cells were bathed in an EGTA-containing solution, to prevent any interference from the external Ca^{2+}, and challenged with bradykinin (Bk), an IP_3-generating stimulus, and cyclopiazonic acid (CPA), a reversible inhibitor of the SERCA pump, to obtain a rapid, complete release of Ca^{2+} from the intracellular stores. In these experiments the Ca^{2+} content of intracellular stores was estimated by integrating the area of Ca^{2+} peaks induced by Ca^{2+} release. Fig. 1.4A shows the trace of a typical experiment with Cyt-Aeq, following changes in cytosolic Ca^{2+}

concentration ($[Ca^{2+}]_{cyt}$) with time. Histograms in fig. 1.4B represent, for each cell group, the average of the areas above baseline, measured between the addition of the stimuli and the moment the $[Ca^{2+}]_{cyt}$ returned to the resting level. Area values were also normalized to the average area of control cells. While cells over-expressing only PS2-T122R over-expressing cells released a significantly smaller amount of Ca^{2+} when compared to control cells, cells expressing SERCA-2B together with PS2-T122R had Ca^{2+} contents comparable or even higher than that of control, void vector transfected, cells. Upon cell stimulation, not only the areas but also the peak in $[Ca^{2+}]_{cyt}$ reached by PS2-T122R and SERCA-2B co-expressing cells was as high as that reached by control cells, indicating full recovery of the IP_3-sensitive stores.

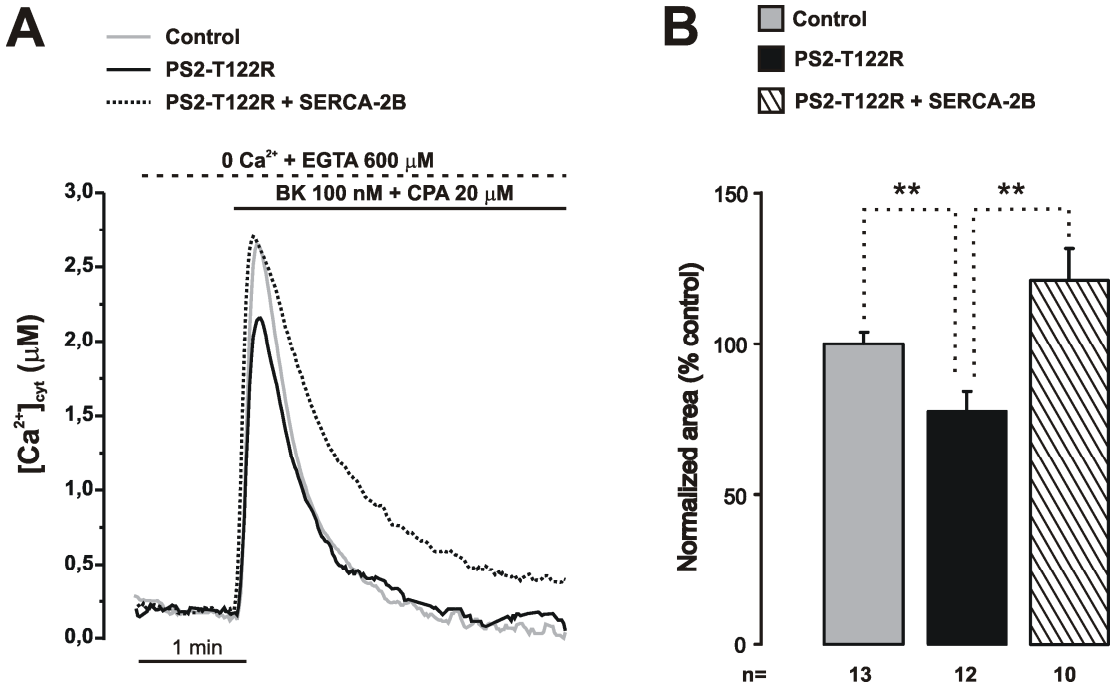

Figure 1.4. A: representative traces from a typical experiment of cytosolic Ca^{2+} measurement using Cyt-Aeq in SH-SY5Y cells: traces from void vector-transfected, control cells (grey line), PS2-T122R expressing cells (black line) and PS2-T122R plus SERCA-2B expressing cells (dotted black line) are shown. B. Histograms representing the different average areas normalized to the average control area (mean ± s.e.m). The area measured for the cells co-expressing PS2-T122R and SERCA-2B (hatched bar) was comparable to that of control cells (grey bar), while the area resulting from PS2-T122R over-expressing cells (black bar) was significantly reduced (** = $p < 0.01$).

Co-expression of SERCA-2B in PS2-T122R transfected cells rescues both the steady-state $[Ca^{2+}]_{ER}$ and SERCA-2 V_{max}

Unlike the cells expressing PS2-T122R only, which had partially depleted stores and therefore gave rise to lower peaks and smaller areas, the cells transfected with SERCA-2B together with PS2-T122R released as much Ca^{2+} as control cells. We then checked

whether this recovery could be detected at the ER level too. We transfected SH-SY5Y cells as described for fig. 1.4, but with ER-Aeq instead of Cyt-Aeq. Experiments were performed in permeabilized cells, treated as in fig. 1.1. The results obtained confirmed that co-expression of SERCA-2B together with PS2-T122R could restore the steady-state ER Ca^{2+} content to control levels. Moreover, this treatment also allowed a complete recovery of the SERCA-2 pump maximal uptake rate, as shown in fig. 1.5B.

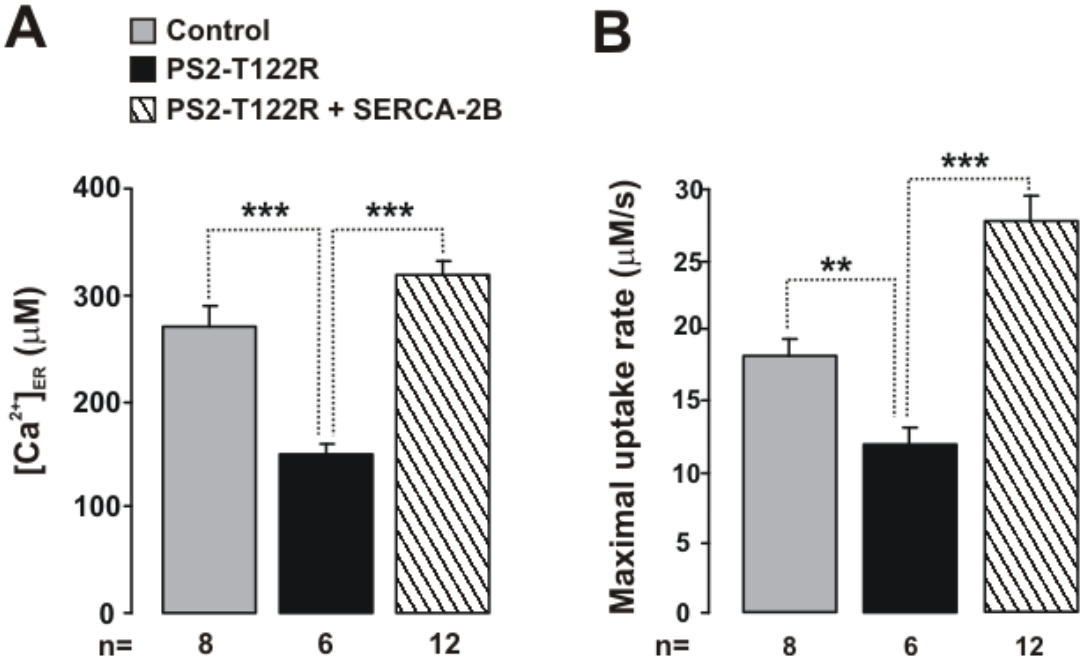

Figure 1.5. SH-SY5Y cells were transiently co-transfected with the cDNAs coding for ER-Aeq and PS2-T122R, in the absence (black bars) or presence (hatched bars) of SERCA-2B cDNA; control cells were co-transfected with ER-Aeq cDNA and with the void vector (grey bars). Bars represent the average steady-state $[Ca^{2+}]_{ER}$ (μM) (panel A) and maximal uptake rates (μM/s) (panel B) (mean ± s.e.m) (** = $p < 0.01$; *** = $p < 0.001$).

Down-regulation of endogenous PS2 enhances both the steady-state $[Ca^{2+}]_{ER}$ and SERCA-2 V_{max}

Since the expression of wt PS2 in a PS-free environment such as DKO MEF cells induced a partial depletion of ER Ca^{2+} content mainly by slowing down the SERCA-2 maximal Ca^{2+} uptake (fig. 1.3B), we decided to test whether an approach aimed at down-regulating the endogenous level of PS2 could end up with the opposite effect on SERCA pump's activity. Therefore, we down-regulated the expression of the PS2 protein in wt MEFs by an RNA interference treatment. The cells were transfected with ER-Aeq cDNA and small interfering RNAs (siRNAs) against mouse PS2 (or control siRNAs). 48 h after transfection, experiments were carried out as previously described to monitor ER Ca^{2+} uptake in permeabilized cells. Under these conditions, down-regulation of PS2 reached 50-80% as checked by Western blot (fig. 1.6C) As shown in fig. 1.6, siRNA against

endogenous mouse PS2 significantly increased both the steady-state $[Ca^{2+}]_{ER}$ and SERCA-2 V_{max}. These results are consistent with the opposite effect on SERCA-2 due to over-expression of wt PS2 in DKO MEFs and also strongly argue for a physiological role of endogenous PS2 in cellular Ca^{2+} handling.

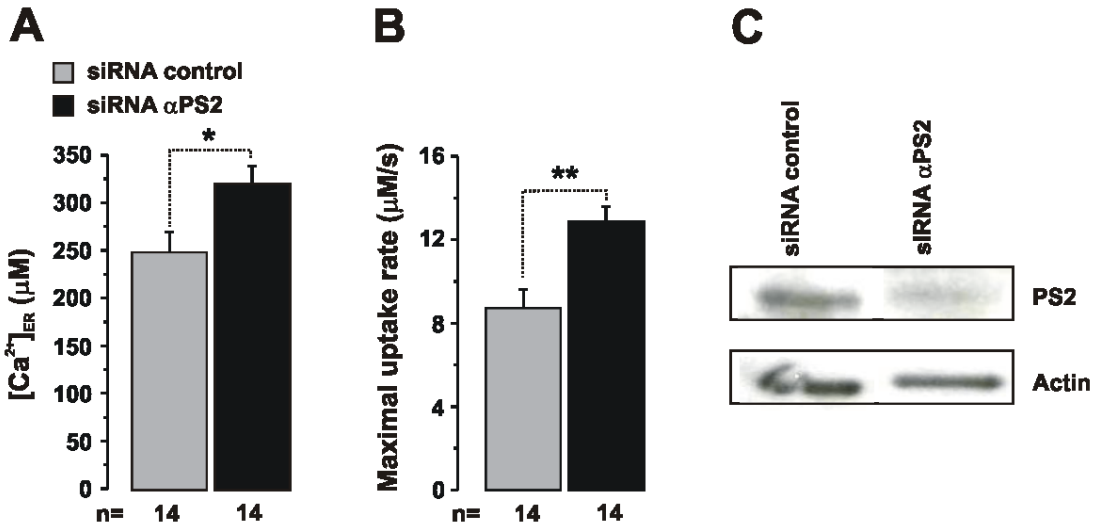

Figure 1.6. Wt MEFs, seeded on both coverslips and 6-well plates, were transfected with the cDNA coding for ER-Aeq and siRNA specific for mouse PS2 or control siRNA (20 nM). After 48 hours, the cells seeded on coverslips were used to estimate ER Ca^{2+} uptake upon cell permeabilization with the protocol described in fig. 1.1. Bars (grey bars for control cells, black bars for interfered cells) represent the average $[Ca^{2+}]_{ER}$ (μM) (panel A) and maximal uptake rates (μM/s) (panel B) (mean ± s.e.m). The remaining cells were harvested to check the expression level of PS2 by Western blotting (panel C) (* = $p < 0.05$; ** = $p < 0.01$).

Co-immunoprecipitation: a physical interaction between PS2 and SERCA-2B

Evidence so far is that PS2 and SERCA-2 somehow interact; thus, we decided to perform co-immunoprecipitation (IP) assays to check whether there is a physical association between these two proteins. SH-SY5Y cells were transfected with PS2-T122R or the void vector (as control) cDNAs. After 24h, cells were harvested: protein extracts were split in two to perform IP of both SERCA-2 and PS2. Each protein sample was tested in two separate Western blots. In the first one, the antibody used was the same employed to immunoprecipitate the proteins: this was a control experiment required to ensure that the IP protocol worked *per se* (fig. 1.7A, upper panel and fig. 1.7B, lower panel). In the second Western blot, it was used an antibody against the hypothetical interacting protein: a signal should be found where the other partner was immunoprecipitated. As fig. 1.7 shows, a physical link between PS2 and SERCA-2 could be demonstrated: when SERCA-2 was immunoprecipitated, PS2 was also detectable in Western blot (fig. 1.7A, lower panel) and vice versa (fig. 1.7B, upper panel). The interaction between the two proteins is reasonably strong: in fact, a preliminary cross-linking treatment to fix endogenous weak

bonds between proteins was not necessary to see co-immunoprecipitation of PS2 and SERCA-2.

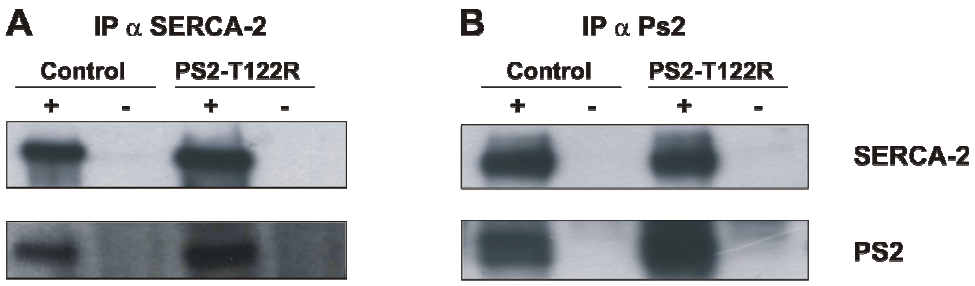

Figure 1.7. Co-immunoprecipitation of SERCA-2 and PS2 in SH-SY5Y cells. PS2-T122R expressing and control cells were harvested 24 h after transfection and IPs of SERCA-2 (panel A) and PS2 (panel B) were performed. Each protein extract was split in two: a half was treated with an antibody against SERCA-2, or PS2, to immunoprecipitate the protein (+), while the other half was used as a negative control, having the same treatment but without the addition of the antibody (-). Western blots show the protein samples detected with an antibody against SERCA-2 (upper boxes in panels A and B) or PS2 (lower boxes).

Results II

The PS2-T122R-induced reduction of steady-state $[Ca^{2+}]_{ER}$ measured with ER-Aeq is detected also with an ER-D1 *cameleon* Ca^{2+} probe

Cameleons are FRET-based ratiometric Ca^{2+} sensors that can be genetically targeted to intracellular organelles or sub-compartments (see Introduction, p. 40). *Cameleons* are excellent tools to perform single cell live imaging experiments to monitor Ca^{2+} oscillations under different conditions. Our future aim is to take advantage of these probes to investigate Ca^{2+} dynamics in primary cultures of cortical neurons or brain slices from mice carrying a FAD-linked PS2 mutation alone or in combination with mutant APP, this latter strain also employed as a mouse model of amyloidosis. However, first of all we need to set the proper experimental conditions and to make sure that *cameleons* are suitable probes for our purposes.

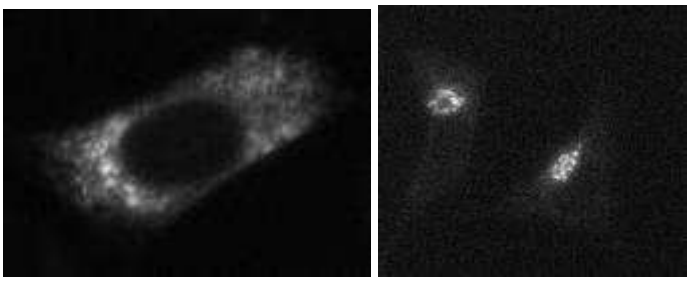

Figure 2.1. SH-SY5Y cells expressing the ER-D1 (left) and the Go-D1cpV (right) *cameleons*.

We tested the ER-D1 *cameleon* in SH-SY5Y cells. The cells were transiently transfected with ER-D1 and PS2-T122R or the void vector as control. The experimental protocol used was exactly the same designed for ER-Aeq experiments in intact cells (see Materials and Methods, p. 62, for details). Similarly to ER-Aeq reconstitution, before starting the experiment the ER was depleted of Ca^{2+} by exposing the cells to ionomycin (1 μM) in an EGTA-containing (0.6 mM) solution. After extensive washing with BSA, the cells were bathed in an EGTA-containing (50 μM) solution; Ca^{2+} was added (2 mM) and the refilling of the store was monitored. Fig. 2.2A shows a representative experimental trace: the arbitrary fluorescence values of yellow and cyan fluorescent proteins (YFP and CFP respectively) were normalized to the respective initial value; the same normalization was done for the YFP/CFP ratio. Upon Ca^{2+} entry within the ER, the typical antiparallel behaviour of YFP and CFP fluorescence traces was observed, and their ratio mirrored the $[Ca^{2+}]$ changes occurring in the ER compartment. Histograms in fig. 2.2B show the

steady-state ER-D1 ratio value (R) reached in PS2-T122R expressing and control cells: the difference with the starting value (R_0), normalized to the latter ($\Delta R/R_0$), reflects changes in the $[Ca^{2+}]_{ER}$. As expected, the cells transfected with PS2-T122R reached a significantly lower plateau level, compared to control cells. This result allowed us to draw two important conclusions. First, the ER-D1 *cameleon* is a reliable $[Ca^{2+}]_{ER}$ sensor in our cell model; secondly, the PS2-T122R-induced reduction in the steady-state $[Ca^{2+}]_{ER}$ was confirmed once again with a different Ca^{2+} probe.

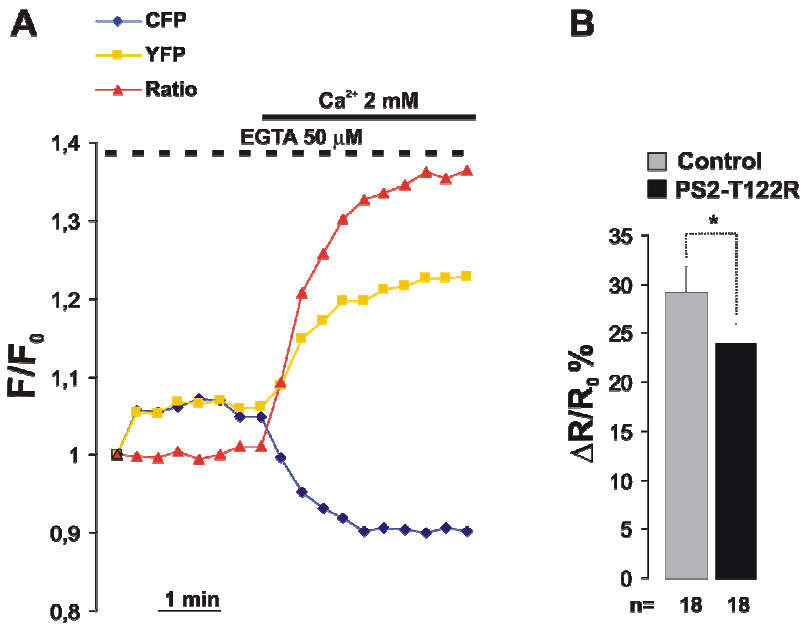

Figure 2.2. Panel A shows a typical experimental trace following the changes in the $[Ca^{2+}]_{ER}$ in a SH-SY5Y cell that was transfected with the ER-D1 *cameleon*. The fluorescence values of YFP, CFP and the YFP/CFP ratio were normalized to each respective initial value (F_0). Panel B: bars representing the ER Ca^{2+} refilling plateaus reached by control (grey bar) and PS2-T122R over-expressing (black bar) SH-SY5Y cells (mean ± s.e.m). Plateaus are expressed as percentage of normalized ΔR (* = $p < 0.05$).

The PS2-T122R-induced reduction of steady-state $[Ca^{2+}]_{Go}$ measured with Go-Aeq is NOT detected with Go-D1cpV, a novel *cameleon* Ca^{2+} probe

It has been demonstrated that, in HeLa and SH-SY5Y cells, PS2-T122R not only dramatically reduces the steady-state $[Ca^{2+}]$ in the ER, but has also a similar effect on Golgi apparatus Ca^{2+} level (Zatti et al., 2006; fig. 2.3A). In these cells, $[Ca^{2+}]_{Go}$ was directly measured using a recombinant aequorin probe, Go-Aeq. A new *cameleon* probe has been recently developed in our laboratory, the Go-D1cpV probe, targeted to the lumen of the Golgi apparatus (Lissandron et al., submitted). We therefore took advantage of this new tool and tested it in SH-SY5Y cells. Again, the cells were transfected with PS2-T122R or the void vector together with the probe. The experimental protocol followed was

the same used for ER-D1 experiments. Histograms in fig. 2.3B show the Golgi steady-state ratio reached by PS2-T122R transfected and control cells, expressed as the percentage change in the normalized YFP/CFP ratio, as described for fig. 2.2. Surprisingly, no statistically significant difference between PS2-T122R expressing and control cells was detected.

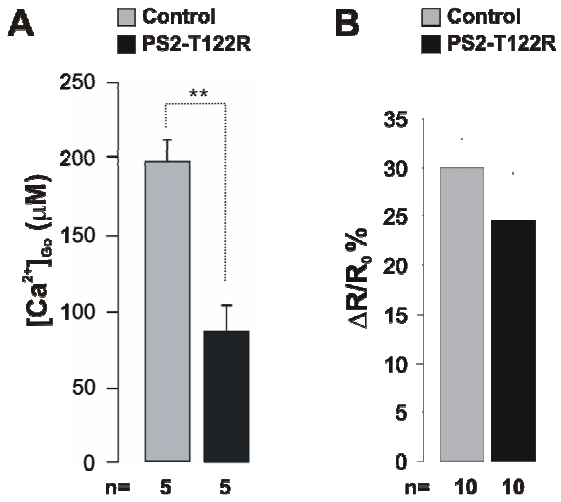

Figure 2.3. The Golgi apparatus Ca^{2+} content in SH-SY5Y cells, measured with Go-Aeq (panel A) and the novel *cameleon* probe Go-D1cpV (panel B). Bars represent the steady-state $[Ca^{2+}]_{Go}$ reached after store refilling by PS2-T122R transfected (black bars) and control cells (grey bars) (mean ± s.e.m). In Go-D1cpV experiments, refilling plateaus are expressed as percentage of normalized ΔR (panel B) (** = $p < 0.01$).

Discussion

It has been previously reported that different FAD-linked PS2 mutants (and PS1 mutants as well, although to a minor extent) significantly reduce the ER Ca^{2+} content in different model cells, including fibroblasts from FAD patients and rat primary neurons. This effect is also mimicked by over-expression of wt PS2 (Zatti et al., 2004; Giacomello et al., 2005; Zatti et al., 2006). Both fura-2 and aequorin approach were applied to measure $[Ca^{2+}]_{ER}$ in the different cell types and the results obtained with these techniques were consistently reproduced. Similar conclusions were also reached in neuroblastoma cells by over-expression of the wt form of PS2 or PS1 (Fedrizzi et al., 2008).

It has recently been shown that FAD-linked PS1 and PS2 mutants interact with the IP_3R, stimulating its gating activity. This led to an enhanced Ca^{2+} signalling, but exaggerated ER Ca^{2+} release was not supported by ER Ca^{2+} overload. Indeed, the ER Ca^{2+} content was unchanged or even decreased (Cheung et al., 2008). Altogether these data strongly undermine the "Ca^{2+} overload" hypothesis (LaFerla, 2002; Cowburn et al., 2007) and suggest a key role for PSs in setting the ER Ca^{2+} level.

The next step in the overall project an the main target of this work was unraveling the molecular mechanism(s) by which wt and mutant PS2 reduce the ER Ca^{2+} content of intracellular stores. The effect of the transient over-expression of PS2-T122R was chosen as a reference to compare the different cell types; consistently, a reduction in the steady-state $[Ca^{2+}]_{ER}$ was observed, ranging from about 50% to 20%, with the following efficacy order: SH-SY5Y > wt MEFs ≥ DKO MEFs > HeLa cells. All these models were thus employed to untangle the likely common mechanism(s) underlying the PS2 effect.

The reduction in the $[Ca^{2+}]_{ER}$ induced by PS2-T122R was previously detected with ER Ca^{2+} refilling experiments in intact cells. However, in intact cells, ER Ca^{2+} uptake rates do not simply reflect the SERCA pump activity, as they are also affected by Ca^{2+} influx/extrusion processes across the PM and mitochondria Ca^{2+} buffering. To avoid these interferences, experiments were carried out in digitonin permeabilized cells with the free $[Ca^{2+}]$ of the bathing medium buffered at different values (0.1-2 μM). Under these conditions, in cells expressing PS2-T122R, Ca^{2+} uptake rates were reduced at each $[Ca^{2+}]$ tested. Similar results were also obtained in DKO MEFs expressing wt PS2; noteworthy, we also found about a 20% increase in ER Ca^{2+} uptake rates in permeabilized DKO MEFs, if compared to the wt clone. These variations in the uptake rates in DKO MEFs following the presence of absence of wt PS2 suggested a role for endogenous PS2, that might act as a physiological brake on ER Ca^{2+} uptake and SERCA pumps. We took advantage of the two available MEF clones to investigate this hypothesis through opposite approaches. In fact, while over-expression of wt PS2 in DKO MEFs reduced the SERCA uptake rate and $[Ca^{2+}]_{ER}$, in wt MEFs, knocking down the endogenous level of PS2 by siRNAs increased both ER Ca^{2+} pumping and steady-state levels, thus unmasking the inhibitory role played

by endogenous PS2. Along this line, in SH-SY5Y, over-expression of SERCA-2B together with PS2-T122R rescued both the rate of ER Ca^{2+} uptake and the steady-state $[Ca^{2+}]_{ER}$ at, or slightly above, the respective values observed in control, void-vector transfected cells.
Recently, it has been shown that wt PS1 and PS2 as well as a FAD-linked mutant (PS1-M146V) increase SERCA-2 activity (Green et al., 2008). Those data, however, were obtained by monitoring cytosolic Ca^{2+} clearance in intact *Xenopus* oocytes: under such conditions, other factors as the amplitude of capacitative Ca^{2+} influx, the activity of the PMCA and the contribution of mitochondrial Ca^{2+} uptake may mislead data interpretation. From our results obtained in permeabilized cells, we could conclude that PS2-T122R affects the maximal capacity of the pump rather than its K_m which appears to be set around 0.15-0.3 μM, a value not far from that reported for purified SERCA-2B (0.17 μM) (Lytton et al., 1992). Co-immunoprecipitation experiments strongly indicate a physical interaction between PS2-T122R and SERCA-2 in neuroblastoma cells, as also demonstrated in brain extract by Green and co-workers (Green et al., 2008). Nonetheless, over-expression of mutant PS2 did not alter the endogenous SERCA-2 protein level.
In conclusion, the FAD-linked PS2-T122R consistently and dramatically lowers the steady-state $[Ca^{2+}]_{ER}$ in all the cell models tested so far. The main mechanism responsible for this effect is likely a reduction in the maximal uptake rate of SERCA-2.

One of the future perspectives of this project will be studying Ca^{2+} dynamics in cellular sub-compartments of cortical neurons from model AD mice carrying a FAD-linked PS2 mutant as well as from wt animals. The approach of choice will be single cell live Ca^{2+} imaging by *cameleon* probes selectively targeted to intracellular organelles. Before getting started with neurons, however, it is necessary to set the proper experimental conditions of these probes in well known model cells, as SH-SY5Y cells are. This was the aim of the second part of this work.
A *cameleon* targeted to the ER lumen, the ER-D1 probe (Palmer et al., 2004; Rudolf et al., 2006), was transiently co-transfected with PS2-T122R or the void vector in SH-SY5Y cells and the experiments were performed following a protocol very similar to that used for ER-Aeq measurements in intact cells, i.e. ER Ca^{2+} stores were pre-emptied and the refilling process was then followed. The results were consistent with those obtained from ER-Aeq experiments: PS2-T122R expressing cells showed a significantly lower ER steady-state, expressed as the ratio $\Delta R/R_0$, when compared to control cells, proving that the ER-D1 *cameleon*, as ER Ca^{2+} sensor, can reliably detect the effect of mutant PS2 in our cell model.
A novel *cameleon* probe genetically targeted to the lumen of the Golgi apparatus, the Go-D1cpV *cameleon*, was recently created in our lab (Lissandron et al., submitted). This new sensor has also been tested in SH-SY5Y cells; experiments were carried out in PS2-T122R expressing and control cells, according to the same protocol used with the ER-D1 *cameleon*. Surprisingly, this time the results obtained were not as expected. In fact, previous experiments performed in SH-SY5Y cells with Go-Aeq demonstrated that PS2-

T122R expressing cells had significantly reduced steady-state $[Ca^{2+}]_{Go}$, compared to control cells (Zatti et al., 2006). Instead, the steady-state ratio measured at the Golgi level in PS2-T122R expressing cells was comparable to that reached in void vector transfected cells. The difference between the two probes in estimating Golgi Ca^{2+} levels was at first confounding because both Go-Aeq and Go-D1cpV have the same Golgi targeting sequence (see Matherials and Methods, p. 63). However, immunocytochemistry experiments showed that Go-D1cpV localized to the trans-Golgi cisternae, accordingly to the targeting sequence, whereas the Go-Aeq localized also to the cis Golgi sub-compartment (Lissandron et al., submitted).

This observation explains why with the two Golgi probes we obtained different results when considering the effect of PS2-T122R on the steady-state Ca^{2+} level of this complex organelle. In fact, it is known that the cis-Golgi compartment has characteristic in between the ER and the trans Golgi compartment. In particular, in the cis Golgi, Ca^{2+} uptake mainly relies on SERCA pumps (which should be impaired by PS2-T122R) whereas, in the trans-Golgi, Ca^{2+} uptake only depends on SPCA1 pumps (Missiaen et al., 2007), which appear to be unaffected by the mutant PS2.

Thus, an unexpected result was obtained by choosing a novel Ca^{2+} probe with a localization restricted to a sub-compartment of the Golgi apparatus. The Go-D1cpV *cameleon* helped us to better define the mechanism of action of PS2-T122R, showing that it selectively acts on SERCA-2 but not on SPCA-1 pumps.

Materials and Methods

Cell lines and transfection

SH-SY5Y and HeLa cells were grown in DMEM supplemented with 10% foetal calf serum (FCS) containing penicillin (100 U/ml) and streptomycin (100 µg/ml). Before transfection, cells were seeded on coverslips (13 or 24 mm diameter) and allowed to grow to 50% confluence. For perfusion experiments, SH-SY5Y cells were seeded on coverslips previously treated with laminin (10 µg/ml). SH-SY5Y and HeLa cells were transfected by means of Lipofectamine^{TM}2000 using 1,5 / 3 µg of DNA for 13 / 24 mm diameter coverslips respectively (1 / 2 µg PS2-cDNA or void vector (pcDNA3) plus 0.5 / 1 µg aequorin (Aeq) or *cameleon* cDNA). PS1/PS2-null (PS1$^{-/-}$, PS2$^{-/-}$) and wild-type (wt) mouse embryonic fibroblasts (MEFs), obtained as previously described (Herreman et al., 1999; Nyabi et al., 2002), were kindly provided by Dr. Bart De Strooper (Center for Human Genetics, KUL, VIB, Leuven, Belgium). Cells, grown in DMEM-F12 supplemented with 10% FCS and 100 U/ml penicillin/streptomycin, were transfected by Lipofectamine^{TM}2000 employing 2 µg of DNA (1,5 µg PS2-cDNA or void vector plus 0.5 µg Aeq cDNA). For perfusion experiments, DKO and wt MEFs were seeded on coverslips previously treated with poly-L-Lysin (50 µg/ml). For RNA interference experiments, the growth medium was substituted 1 hour before transfection with antibiotics-free medium; siRNAs mouse PS2 (target sequence: GAUAUACUCAUCUGCCAUG) and siGENOME RISC-Free Control siRNA; (Dharmacon Research, Lafayette, CO) were added to the transfection mixes to a final concentration of 20 nM.

Intracellular Ca^{2+} measurements were carried out 48 or 24 h after transfection by means of the Aeq technique, as previously described (Brini et al., 1995) and summarised below, or by single cell live Ca^{2+} imaging with the *cameleon* probes.

Ca^{2+} measurements

Aequorin

Cells seeded on 13 mm diameter coverslips and transfected with Aeq constructs were incubated at 37°C with coelenterazine (5 µM) for 1-2 h in a modified Krebs–Ringer buffer (mKRB, in mM: 140 NaCl, 2.8 KCl, 2 $MgCl_2$, 1 $CaCl_2$, 10 HEPES, 11 glucose, pH 7.4) and then transferred to the perfusion chamber. For reconstitution of ER-Aeq and Go-Aeq, luminal [Ca^{2+}] was reduced before coelenterazine addition by exposing the cells to CPA (20 µM) in mKRB without $CaCl_2$ (Ca^{2+}-free mKRB) and containing EGTA (600 µM). Upon 1h incubation at 4°C in the same medium, the cells were extensively washed with Ca^{2+}-free mKRB supplemented with EGTA (1 mM) and bovine serum albumin (BSA, 2%). All the luminescence measurements were carried out in mKRB at 37°C. For SH-

SY5Y and MEF cells, a high potassium medium (in mM: KCl 100, NaCl 43, $MgCl_2$ 1, HEPES 10, pH 7.4 at 37°C) was used. The experiments were terminated by cell permeabilization with digitonin (100 μM) in a hypotonic Ca^{2+}-rich solution (10 mM $CaCl_2$ in H_2O) to discharge the remaining unused Aeq pool. The light signal was collected as previously described (Brini et al., 1995).

For permeabilization, cells were exposed for 1-2 minutes to digitonin (20-100 μM) in an intracellular medium containing (in mM): KCl 130, NaCl 10, KH_2PO_4 1, succinic acid 2, $MgSO_4$ 1, HEPES 20, EGTA 0.05 pH 7, at 37°C. The cells were then washed with the same intracellular medium containing EGTA 50 μM for 2-5 minutes. The Ca^{2+}-buffer solution was prepared by adding to the intracellular medium: HEDTA, piruvic acid and $MgCl_2$ (1 mM each), EGTA or BAPTA (2 mM) and $CaCl_2$ at different concentrations (0.5-1.8 mM) and the pH was brought to 7 at 37°C. $ATPNa_2$ (0.2 mM) was added to this Ca^{2+}-buffered solution. The free [Ca^{2+}] (0.1-2 μM) was estimated by MaxChelator2.5 and checked by fluorimetric measurements with fura-2.

Cameleon

Cells expressing the fluorescent probe were analyzed using an inverted fluorescence microscope (Zeiss Axiovert 100) with an immersion oil objective (40 X, N.A. 1.30). Excitation light at the proper wavelength (425 nm) was produced by a monochromator (Polychrome V, TILL Photonics, Martinsried, Germany). The emitted light was collected through a beamsplitter (OES s.r.l., Padova) and a dichroic mirror 440 DCXR. The beamsplitter allows the collection of the two emitted wavelengths at the same time, thus preventing any artefact due to movement of the organelles. Filters and dichroic mirrors were purchased from Omega Optical (Brattleboro, VT) and Chroma Technology Corp. (Rockingham, VT). Images were acquired using a 12-bit cooled CCD camera (PCO SensiCam). The software used for image analysis were Roboscope (custom-made, Padova) and ImageJ (free download) for off-line data processing. For time-course experiments, the fluorescence intensity was determined over regions of interest covering the ER or the Golgi compartment. Exposure time varied from 300 to 800 ms, depending on the intensity of the fluorescent signal of the cells analyzed. The frequency of image capture was 0.05 Hz. Cells were mounted into an open-topped chamber at room temperature, and maintained in an extracellular high K^+ medium (see aequorin Ca^{2+} measurement). The refilling protocol was performed essentially as described (Pinton et al., 1998). Briefly, the cells, incubated in Ca^{2+}-free mKRB medium containing 0.6 mM EGTA, were treated with 1 μM ionomycin for at least 10 minutes and then ionomycin was removed by extensive washing with the same medium containing 2% BSA and EGTA (1 mM). The store refilling was then visualized by addition of 2 mM $CaCl_2$ to the EGTA-containing (50 μM) high K^+ solution.

Plasmids

pcDNA3 vector codifying for PS2-T122R mutant was created by site directed mutagenesis

of pcDNA3/PS2-wt (QuikChange Site-directed mutagenesis Kit, Stratagene, La Jolla, CA). The construct was checked by sequence analysis (ABI Prism Genetic Analyzer 310, Applied Biosystems, Monza, Italy).
The D1cpV *cameleon* (Palmer et al., 2006) is formed by an enhanced cyan fluorescent protein (ECFP) and a circularly permutated Venus, a yellow fluorescent protein variant (YFP), linked by modified calmodulin (CaM) and calmodulin-binding domain M13. The construct (kindly provided by Dr. R.Y. Tsien) was modified inserting at the N-terminal the targeting sequence of the trans-Golgi enzyme sialyl-transferase, after its isolation from the Go-Aeq construct (Pinton et al.,1998) (Lissandron et al., submitted).

Protein extracts preparation and Western blot analysis

The different cell types were harvested and treated as previously reported (Giacomello et al., 2005). Briefly, cells were washed twice with ice-cold phosphate-buffered saline (PBS) and harvested with RIPA buffer supplemented with proteases inhibitors cocktail (Complete Mini™, Roche). Samples were analyzed in SDS-PAGE gel and Western blotting immunodetection was carried out with the polyclonal antibody (Ab) anti-PS2 (324-335; Ab-2, Calbiochem, Merck, Darmstadt, Germany) and with the monoclonal mouse Ab anti-PS2 (MMS-359S, Covance Research Products Inc.). SERCA-2B detection was carried out with a polyclonal anti-SERCA-2 Ab (N-19, Santa Cruz Biotechnology, Inc.). Actin was detected by the monoclonal mouse Ab (A4700, Sigma-Aldrich). The proteins were visualised by the chemiluminescence reagent ECL (Amersham, GE Healthcare, UK Ltd Amersham PlaceLittle Chalfont Buckinghamshire HP7 9NA England).

Co-immunoprecipitation

The immunoprecipitation technique is based on the selective interaction between a protein of interest and an antibody recognizing an antigen on it. Upon the Ab-protein binding, the Ab heavy chain is then recognized by a specific protein (called protein A for rabbit Abs and protein G for mouse Abs), bound to an agarose bead. After centrifugation, the complex formed by the protein of interest (plus other potential interacting proteins), the Ab and the agarose-bound A/G protein precipitates, allowing the isolation of the desired protein together with its potential partners.
SH-SY5Y cells were trasfected with PS2-T122R or the void vector; 24 h after transfection the cells were harvested and protein extracts were prepared as described. Before the addition of the Ab anti PS2 (324-335; Ab-2, Calbiochem, Merck, Darmstadt, Germany) or SERCA-2 (monoclonal mouse anti SERCA-2, clone 2A7-A1, Sigma-Aldrich, Inc), the protein extracts were incubated with protein A-Agarose and normal rabbit AG (both from Santa Cruz Biotechnology, Inc) or protein G-Agarose (Santa Cruz Biotechnology, Inc) respectively, for 30 minutes at 4°C. This step was necessary to remove the proteins aspecifically binding to the agarose. After centrifugation at 2400 rpm for 5 minutes at 4°C, the surnatant was collected and the protein concentration quantified. 100 μg of each

protein sample were treated with the anti PS2 or anti SERCA-2 Ab, while 100 μg were incubated with Normal Rabbit IgG-AC (Agarose Coniugated) or Normal Mouse IgG-AC respectively (both Santa Cruz Biotechnology, Inc). This control sample allows to sort the proteins aspecifically binding to a random immunoglobulin produced in the same species as the Ab used from the proteins specifically interacting with the Ab. Samples were incubated for 2 h at 4°C under constant mixing, then the proper agarose-bound protein (protein A-Agarose for PS2 samples and the respective mock-treated samples; protein G-Agarose for SERCA-2 samples and the respective control samples) was added. 3 h later the samples were centrifuged for 5 minutes at 2400 rpm at 4°C; the agarose pellet with the protein complexes was washed with a solution containing NaCl (0.1 M) and a proteases inhibitors cocktail (Complete Mini™, Roche) for 4 times. After the last washing, the pellet was resuspended in a loading buffer 2X containing 10% β-mercaptoethanol, which helps releasing the immunoprecipitated proteins from the IgG-agarose complexes.

Chemicals and reagents

Antibiotics, sera, culture media, plasmids and Lipofectamine^{TM}2000 were purchased from Invitrogen (Carlsbad, CA, USA), while all other reagents were from Sigma Chemical Co. (St. Louis, Mo), unless otherwise stated.

Statistical analysis

Data were analyzed by Origin 7.5 SR5 (OriginLab Corporation). Averages are expressed as mean ± s.e.m. (n = number of independent experiments; ∗ = $p < 0.05$; ∗∗=$p<0.01$; ∗∗∗ = $p < 0.001$, unpaired Student's t test).

References

Albrecht S, Bogdanovic N, Ghetti B, Winblad B, LeBlanc AC (2009) Caspase-6 activation in familial alzheimer disease brains carrying amyloid precursor protein or presenilin i or presenilin II mutations. J Neuropathol Exp Neurol. 68(12):1282-1293

Albrecht S, Bourdeau M, Bennett D, Mufson EJ, Bhattacharjee M, LeBlanc AC (2007) Activation of caspase-6 in aging and mild cognitive impairment. Am J Pathol. 170(4):1200-1209

Alvarez A, Toro R, Caceres A, Maccioni RB (1999) Inhibition of tau phosphorylating protein kinase cdk5 prevents beta-amyloid-induced neuronal death. FEBS Lett. 459(3):421–426

Andersen OM, Reiche J, Schmidt V, Gotthardt M, Spoelgen R, Behlke J, von Arnim CA, Breiderhoff T, Jansen P, Wu X, Bales KR, Cappai R, Masters CL, Gliemann J, Mufson EJ, Hyman BT, Paul SM, Nykjaer A, Willnow TE (2005) Neuronal sorting protein-related receptor sorLA/LR11 regulates processing of the amyloid precursor protein. Proc Natl Acad Sci USA 102(38):13461–13466

Annaert W, De Strooper B (1999) Presenilins: molecular switches between proteolysis and signal transduction. Trends Neurosci. 22(10):439–443

Arispe N, Rojas E, Pollard HB (1993) Alzheimer disease amyloid beta protein forms calcium channels in bilayer membranes: blockade by tromethamine and aluminum. Proc. Natl. Acad. Sci. USA 90(2):567–571

Augustinack JC, Schneider A, Mandelkow EM, Hyman BT (2002) Specific tau phosphorylation sites correlate with severity of neuronal cytopathology in Alzheimer's disease. Acta Neuropathol. 103(1):26–35

Avidor T, Clementi E, Schwartz L, Atlas D (1994) Caffeine-induced transmitter release is mediated via ryanodine-sensitive channel. Neurosci. Lett. 165(1-2):133–136

Baird GS, Zacharias DA, Tsien RY (1999) Circular permutation and receptor insertion within green fluorescent proteins. Proc. Natl Acad. Sci. USA 96(20):11241–11246

Bentahir M, Nyabi O, Verhamme J, Tolia A, Horre K, Wiltfang J, Esselmann H, De Strooper B (2006) Presenilin clinical mutations can affect gamma-secretase activity by different mechanisms. J Neurochem. 96(3):732-742

Benzing WC, Ikonomovic MD, Brady DR, Mufson EJ, Armstrong DM (1993) Evidence that transmitter-containing dystrophic neurites precede paired helical filament and Alz-50 formation within senile plaques in the amygdala of nondemented elderly and patients with Alzheimer's disease. J Comp Neurol. 334(2):176–191

Berezovska O, Ramdya P, Skoch J, Wolfe MS, Bacskai BJ, Hyman BT (2003) Amyloid precursor protein associates with a nicastrin-dependent docking site on the presenilin 1-gamma-secretase complex in cells demonstrated by fluorescence lifetime imaging. J. Neurosci. 23(11):4560–4566

Bergman A, Hansson EM, Pursglove SE, Farmery MR, Lannfelt L, Lendahl U, Lundkvist J, Naslund J (2004) Pen-2 is sequestered in the endoplasmic reticulum and subjected to ubiquitylation and proteasome-mediated degradation in the absence of presenilin. J Biol Chem. 279(16):16744–16753

Bertram L, Hiltunen M, Parkinson M, Ingelsson M, Lange C, Ramasamy K, Mullin K, Menon R, Sampson AJ, Hsiao MY, Elliott KJ, Velicelebi G, Moscarillo T, Hyman BT, Wagner SL, Becker KD, Blacker D, Tanzi RE (2005) Family-based association between Alzheimer's disease and variants in UBQLN1. N Engl J Med. 352(9):884–894

Bezprozvanny I (2005) The inositol 1,4,5-trisphosphate receptors. Cell Calcium 38(3-4):261–272

Bezprozvanny I, Mattson MP (2008) Neuronal calcium mishandling and the pathogenesis of Alzheimer's disease. Trends Neurosci. 31(9):454-463

Bitan G, Kirkitadze MD, Lomakin A Vollers SS, Benedek GB, Teplow DB (2003) Amyloid beta-protein (Abeta) assembly: Abeta 40 and Abeta 42 oligomerize through distinct pathways. Proc Natl Acad Sci USA 100(1):330–335

Borchelt DR, Thinakaran G, Eckman CB, Lee MK, Davenport F, Ratovitsky T, Prada CM, Kim G, Seekins S, Yager D, Slunt HH, Wang R, Seeger M, Levey AI, Gandy SE, Copeland NG, Jenkins NA, Price DL, Younkin SG, Sisodia SS (1996) Familial Alzheimer's disease-linked presenilin 1 variants elevate Abeta1–42/1–40 ratio in vitro and in vivo. Neuron 17(5):1005–1013

Braak H, Braak E (1991) Neuropathological stageing of Alzheimer-related changes. Acta Neuropathol. 82(4):239–259

Brandl CJ, Green NM, Korczak B, MacLennan DH (1986) Two Ca2+ ATPase genes: homologies and mechanistic implications of deduced amino acid sequences. Cell 44(4):597–607

Brandman O, Liou J, Park WS, Meyer T (2007) STIM2 is a feedback regulator that stabilizes basal cytosolic and endoplasmic reticulum Ca2+ levels. Cell 131(7):1327–1339

Braunewell KH, Gundelfinger ED (1999) Intracellular neuronal calcium sensor proteins: a family of EF-hand calcium-binding proteins in search of a function. Cell Tissue Res. 295(1):1–12

Brini M, Marsault R, Bastianutto C, Alvarez J, Pozzan T, Rizzuto R (1995) Transfected aequorin in the measurement of cytosolic Ca^{2+} concentration ($[Ca^{2+}]_c$): a critical evaluation J. Biol. Chem. 270(17):9896-9903

Brini M, Marsault R, Bastianutto C, Pozzan T, Rizzuto R (1994) Nuclear targeting of aequorin. A new approach for measuring nuclear Ca2+ concentration in intact cells. Cell Calcium 16(4):259-268

Brini M, Murgia M, Pasti L, Picard D, Pozzan T, Rizzuto R (1993) Nuclear Ca2+ concentration measured with specifically targeted recombinant aequorin. EMBO J. 12(12):4813-4819

Brown MS, Ye J, Rawson RB, Goldstein JL (2000) Regulated intramembrane proteolysis: a control mechanism conserved from bacteria to humans. Cell 100(4): 391-398

Brunello L, Zampese E, Florean C, Pozzan T, Pizzo P, Fasolato C (2009) Presenilin-2 dampens intracellular Ca(2+) stores by increasing Ca(2+) leakage and reducing Ca(2+) uptake. J Cell Mol Med. 2009 Mar 27. [Epub ahead of print] PMID: 19382908

Busciglio J, Gabuzda DH, Matsudaira P, Yankner BA (1993) Generation of beta-amyloid in the secretory pathway in neuronal and nonneuronal cells. Proc Natl Acad Sci USA. 90(5):2092-2096

Butterfield DA, Castegna A, Lauderback CM, Drake J (2002) Evidence that amyloid beta-peptide-induced lipid peroxidation and its sequelae in Alzheimer's disease brain contribute to neuronal death. Neurobiol Aging 23(5):655-664

Button D, Brownstein M (1993) Aequorin-expressing mammalian cell lines used to report Ca2+ mobilization. Cell Calcium. 14(9):663-671

Buxbaum JD, Choi EK, Luo Y, Lilliehook C, Crowley AC, Merriam DE, Wasco W (1998) Calsenilin: a calcium-binding protein that interacts with the presenilins and regulates the levels of a presenilin fragment. Nat Med. 4(10):1177-1181

Buxbaum JD, Ruefli AA, Parker CA, Cypess AM, Greengard P (1994) Calcium regulates processing of the Alzheimer amyloid protein precursor in a protein kinase C-independent manner. Proc. Natl. Acad. Sci. USA 91(10):4489–4493

Capell A, Grunberg J, Pesold B, Diehlmann A, Citron M, Nixon R, Beyreuther K, Selkoe DJ, Haass C (1998) The proteolytic fragments of the Alzheimer's disease-associated presenilin-1 form heterodimers and occur as a 100–150-kDa molecular mass complex. J Biol Chem. 273(6):3205–3211

Cedazo-Minguez A, Cowburn RF (2001) Apolipoprotein E: a major piece in the Alzheimer's disease puzzle. J. Cell. Mol. Med. 5(3):254–266

Cervantes S, Gonzalez-Duarte R, Marfany G (2001) Homodimerization of presenilin N-terminal fragments is affected by mutations linked to Alzheimer's disease. FEBS Lett. 505(1):81–86

Chalfie M, Tu Y, Euskirchen G, Ward WW, Prasher DC (1994) Green fluorescent protein as a marker for gene expression. Science 263(5148):802–805

Chan SL, Mayne M, Holden CP, Geiger JD, Mattson MP (2000) Presenilin-1 mutations increase levels of ryanodine receptors and calcium release in PC12 cells and cortical neurons. J Biol Chem. 275(24):18195-18200

Chandra S, Kable EP, Morrison GH, Webb WW (1991) Calcium sequestration in the Golgi apparatus of cultured mammalian cells revealed by laser scanning confocal microscopy and ion microscopy. J. Cell. Sci. 100(Pt 4):747–752

Chen F, Hasegawa H, Schmitt-Ulms G, Kawarai T, Bohm C, Katayama T, Gu Y, Sanjo N, Glista M, Rogaeva E, Wakutani Y, Pardossi-Piquard R, Ruan X, Tandon A, Checler F, Marambaud P, Hansen K, Westaway D, St. George-Hyslop P, Fraser P (2006) TMP21 is a presenilin complex component that modulates gamma-secretase but not epsilon-secretase activity. Nature 440(7088):1208-1212

Choi EK, Zaidi NF, Miller JS, Crowley AC, Merriam DE, Lilliehook C, Buxbaum JD, Wasco W (2001) Calsenilin is a substrate for caspase-3 that preferentially interacts with the familial Alzheimer's disease-associated C-terminal fragment of presenilin 2. J Biol Chem. 276(22):19197–19204

Chyung JH, Raper DM, Selkoe DJ (2005) Gamma-secretase exists on the plasma membrane as an intact complex that accepts substrates and effects intramembrane cleavage. J Biol Chem 280(6):4383-4392

Clapham DE (2003) TRP channels as cellular sensors. Nature 426(6966):517–524

Cole SL, Vassar R (2008) The role of amyloid precursor protein processing by BACE1, the beta-secretase, in Alzheimer disease pathophysiology. J Biol Chem. 283(44):29621-29625

Cowburn RF, Popescu BO, Ankarcrona M, Dehvari N, Cedazo-Minguez A (2007) Presenilin-mediated signal transduction Physiol Behav. 92(1-2):93-97

Csordás G, Thomas AP, Hajnóczky G (1999) Quasi-synaptic calcium signal transmission between endoplasmic reticulum and mitochondria. EMBO J. 18(1):96–108

De Felice FG, Velasco PT, Lambert MP, Viola K, Fernandez SJ, Ferreira ST, Klein WL (2007) Abeta oligomers induce neuronal oxidative stress through an N-methyl-D-aspartate receptor-dependent mechanism that is blocked by the Alzheimer drug memantine. J Biol Chem. 282(15):11590-11601

De Felice FG, Wu D, Lambert MP, Fernandez SJ, Velasco PT, Lacor PN, Bigio EH, Jerecic J, Acton PJ, Shughrue PJ, Chen-Dodson E, Kinney GG, Klein WL (2008) Alzheimer's disease-type neuronal tau hyperphosphorylation induced by A-beta oligomers. Neurobiol Aging 29(9):1334-1347

Demuro A, Mina E, Kayed R, Milton SC, Parker I, Glabe CG (2005) Calcium dysregulation and membrane disruption as a ubiquitous neurotoxic mechanism of soluble amyloid oligomers. J. Biol. Chem. 280(17):17294–17300

De Strooper B (2003) Aph-1, Pen-2, and Nicastrin with Presenilin generate an active gamma-secretase complex. Neuron 38(1):9–12

De Strooper B (2007) Loss-of-function presenilin mutations in Alzheimer disease. Talking Point on the role of presenilin mutations in Alzheimer disease. EMBO Rep. 8(2):141-6

De Strooper B, Annaert W (2000) Proteolytic processing and cell biological functions of the amyloid precursor protein. J Cell Sci. 113(Pt 11):1857–1870

De Strooper B, Saftig P, Craessaerts K, Vanderstichele H, Guhde G, Annaert W, Von Figura K, Van Leuven F (1998) Deficiency of presenilin-1 inhibits the normal cleavage of amyloid precursor protein. Nature 391(6665):387–390

Dineley KT, Hogan D, Zhang WR, Taglialatela G (2007) Acute inhibition of calcineurin restores associative learning and memory in Tg2576 APP transgenic mice. Neurobiol Learn Mem. 88(2):217–224

Dreses-Werringloer U, Lambert JC, Vingtdeux V, Zhao H, Vais H, Siebert A, Jain A, Koppel J, Rovelet-Lecrux A, Hannequin D, Pasquier F, Galimberti D, Scarpini E, Mann D, Lendon C, Campion D, Amouyel P, Davies P, Foskett JK, Campagne F, Marambaud P (2008) A polymorphism in CALHM1 influences Ca2+ homeostasis, Abeta levels, and Alzheimer's disease risk. Cell 133(7):1149-61

Dumanchin C, Tournier I, Martin C, Didic M, Belliard S, Carlander B, Rouhart F, Duyckaerts C, Pellissier JF, Latouche JB, Hannequin D, Frebourg T, Tosi M, Campion D (2006) Biological effects of four PSEN1 gene mutations causing Alzheimer disease with spastic paraparesis and cotton wool plaques. Hum Mutat. 27(10):1063–1071

Edbauer D, Winkler E, Regula JT, Pesold B, Steiner H, Haass C (2003) Reconstitution of gamma-secretase activity. Nat. Cell Biol. 5(5):486-488

Emmanouilidou E, Teschemacher AG, Pouli AE, Nicholls LI, Seward EP, Rutter GA (1999) Imaging Ca2+ concentration changes at the secretory vesicle surface with a recombinant targeted cameleon. Curr. Biol. 9(16):915–918

Etcheberrigaray R, Fiedler JL, Pollard HB, Rojas E (1991) Endoplasmic reticulum as a source of Ca2+ in neurotransmitter secretion. Ann. New York Acad. Sci. 635:90–99

Etcheberrigaray R, Hirashima N, Nee L, Prince J, Govoni S, Racchi M, Tanzi RE, Alkon DL (1998) Calcium responses in fibroblasts from asymptomatic members of Alzheimer's disease families. Neurobiol. Dis. 5(1):37–45

Fedrizzi L, Lim D, Carafoli E, Brini M (2008) Interplay of the Ca2+-binding protein DREAM with presenilin in neuronal Ca2+ signaling. J Biol Chem. 283(41):27494-503

Felix R (2005) Molecular regulation of voltage-gated Ca2+ channels. J. Recept. Signal Transduct. Res. 25(2):57–71

Feng L, Yan H, Wu Z, Yan N, Wang Z, Jeffrey PD, Shi Y (2007) Structure of a site-2 protease family intramembrane metalloprotease. Science 318(5856): 1608-1612

Flourakis M, Van Coppenolle F, Lehen'kyi V, Beck B, Skryma R, Prevarskaya N (2006) Passive calcium leak via translocon is a first step for iPLA2-pathway regulated store operated channels activation. FASEB J. 20(8):1215-7

Foskett JK, White C, Cheung KH, Mak DO (2007) Inositol trisphosphate receptor Ca2+ release channels. Physiol. Rev. 87(2):593–658

Fox NC, Cousens S, Scahill R, Harvey RJ, Rossor MN (2000) Using serial registered brain magnetic resonance imaging to measure disease progression in Alzheimer disease: power calculations and estimates of sample size to detect treatment effects. Arch Neurol 57(3):339–344

Gahtan E, Overmier JB (1999) Inflammatory pathogenesis in Alzheimer's disease: biological mechanisms and cognitive sequeli. Neurosci Biobehav Rev. 23(5):615–633

Garcia-Alloza M, Robbins EM, Zhang-Nunes SX, Purcell SM, Betensky RA, Raju S, Prada C, Greenberg SM, Bacskai BJ, Frosch MP (2006) Characterization of amyloid deposition in the APPswe/PS1dE9 mouse model of Alzheimer disease. Neurobiol Dis. 24(3):516-524

Georgakopoulos A, Marambaud P, Efthimiopoulos S, Shioi J, Cui W, Li HC, Schutte M, Gordon R, Holstein GR, Martinelli G, Mehta P, Friedrich Jr. VL, Robakis NK (1999) Presenilin-1 forms complexes with the cadherin/catenin cell-cell adhesion system and is recruited to intercellular and synaptic contacts. Mol. Cell. 4(6):893–902

Gervais FG, Xu D, Robertson GS, Vaillancourt JP, Zhu Y, Huang J, LeBlanc A, Smith D, Rigby M, Shearman MS, Clarke EE, Zheng H, Van Der Ploeg LH, Ruffolo SC, Thornberry NA, Xanthoudakis S, Zamboni RJ, Roy S, Nicholson DW (1999) Involvement of caspases in proteolytic cleavage of Alzheimer's amyloid-beta precursor protein and amyloidogenic A beta peptide formation. Cell 97(3):395-406.

Geula C, Bu J, Nagykery N, Scinto LFM, Chan J, Joseph J, Parker R, Wu C-K (2003) Loss of calbindin-D28K from aging human cholinergic basal forebrain: relation to neuronal loss. J Comp Neurol. 455(2):249–259

Giacomello M, Barbiero L, Zatti G, Squitti R, Binetti G, Pozzan T, Fasolato C, Ghidoni R, Pizzo P (2005) Reduction of Ca^{2+} stores and capacitative Ca^{2+} entry is associated with the familial Alzheimer's disease presenilin-2 T122R mutation and anticipates the onset of dementia Neurobiol. Dis. 18(3):638-648

Giacomello M, Drago I, Pizzo P, Pozzan T (2007) Mitochondrial Ca2+ as a key regulator of cell life and death. Cell Death Differ. 14(7):1267–1274

Gomez-Ramos A, Diaz-Hernandez M, Cuadros R, Hernandez R, Avila J (2006) Extracellular tau is toxic to neuronal cells. FEBS Lett. 580(20):4842–4850

Goutte C, Tsunozaki M, Hale VA, Priess JR (2002) APH-1 is a multipass membrane protein essential for the Notch signaling pathway in Caenorhabditis elegans embryos. Proc Natl Acad Sci USA 99(2):775–779

Grathwohl SA, Kälin RE, Bolmont T, Prokop S, Winkelmann G, Kaeser SA, Odenthal J, Radde R, Eldh T, Gandy S, Aguzzi A, Staufenbiel M, Mathews PM, Wolburg H, Heppner FL, Jucker M (2009) Formation and maintenance of Alzheimer's disease beta-amyloid plaques in the absence of microglia. Nat Neurosci. 12(11):1361-1363

Green KN, Demuro A, Akbari Y, Hitt BD, Smith IF, Parker I, LaFerla FM (2008) SERCA pump activity is physiologically regulated by presenilin and regulates amyloid beta production. J. Cell Biol. 181(7):1107–1116

Green KN, LaFerla FM (2008) Linking calcium to Abeta and Alzheimer's disease. Neuron 59(2):190-194

Gunteski-Hamblin AM, Greeb JA, Shull GE (1988) A novel Ca2+ pump expressed in brain, kidney, and stomach is encoded by an alternative transcript of the slow-twitch muscle sarcoplasmic reticulum Ca-ATPase gene. Identification of cDNAs encoding Ca2+ and other cation-transporting ATPases using an oligonucleotide probe derived from the ATP-binding site. J Biol Chem. 263(29):15032–15040

Guo H, Albrecht S, Bourdeau M, Petzke T, Bergeron C, LeBlanc AC (2004) Active caspase-6 and caspase-6 cleaved tau in neuropil threads, neuritic plaques and neurofibrillary tangles of Alzheimer's disease. Am J Pathol. 165(2):523-531

Guo Q, Furukawa K, Sopher BL, Pham DG, Xie J, Robinson N, Martin GM, Mattson MP (1996) Alzheimer's PS-1 mutation perturbs calcium homeostasis and sensitizes PC12 cells to death induced by amyloid beta-peptide. Neuroreport 8(1):379-383

Guo Q, Sopher BL, Furukawa K, Pham DG, Robinson N, Martin GM, Mattson MP (1997) Alzheimer's presenilin mutation sensitizes neural cells to apoptosis induced by trophic factor withdrawal and amyloid beta-peptide: involvement of calcium and oxyradicals. J Neurosci. 17(11):4212-4222

Haass C (2004) Take five--BACE and the gamma-secretase quartet conduct Alzheimer's amyloid beta-peptide generation. EMBO J. 23(3), 483-488

Haass C, Schlossmacher MG, Hung AY, Vigo-Pelfrey C, Mellon A, Ostaszewski BL, Lieberburg I, Koo EH, Schenk D, Teplow DB, Selkoe DJ (1992) Amyloid beta-peptide is produced by cultured cells during normal metabolism. Nature 359(6393):322-325

Haass C, Selkoe DJ (2007) Soluble protein oligomers in neurodegeneration: lessons from the Alzheimer's amyloid beta-peptide. Nat. Rev. Mol. Cell Biol. 8(2):101-112

Haass C, Steiner H (2002) Alzheimer disease gamma-secretase: a complex story of GxGD-type presenilin proteases. Trends Cell Biol. 12(12):556-562

Hamilton SL (2005) Ryanodine receptors. Cell Calcium 38(3-4):253–260

Hansson EM, Stromberg K, Bergstedt S, Yu G, Naslund J, Lundkvist J, Lendahl U (2005) Aph-1 interacts at the cell surface with proteins in the active gamma-secretase complex and membrane-tethered Notch. J Neurochem. 92(5):1010-1020

Hardy JA, Higgins GA (1992) Alzheimer's disease: the amyloid cascade hypothesis. Science 256(5054):184–185

Hayrapetyan V, Rybalchenko V, Rybalchenko N, Koulen P (2008) The N-terminus of presenilin-2 increases single channel activity of brain ryanodine receptors through direct protein-protein interaction. Cell Calcium 44(5):507-518

Henricson A, Kall L, Sonnhammer EL (2005) A novel transmembrane topology of presenilin based on reconciling experimental and computational evidence. FEBS J. 272(11):2727-2733

Heritage D, Wonderlin WF (2001) Translocon pores in the endoplasmic reticulum are permeable to a neutral, polar molecule. J. Biol. Chem. 276(25):22655–22662

Herreman A, Hartmann D, Annaert W, Saftig P, Craessaerts K, Serneels L, Umans L, Schrijvers V, Checler F, Vanderstichele H, Baekelandt V, Dressel R, Cupers P, Huylebroeck D, Zwijsen A, Van Leuven F, De Strooper B (1999) Presenilin 2 deficiency causes a mild pulmonary phenotype and no changes in amyloid precursor protein processing but enhances the embryonic lethal phenotype of presenilin 1 deficiency. Proc. Natl. Acad. Sci. USA 96(21):11872-11877

Herreman A, Serneels L, Annaert W, Collen D, Schoonjans L, De Strooper B (2000) Total inactivation of gamma-secretase activity in presenilin-deficient embryonic stem cells. Nat Cell Biol 2(7):461–462

Hsieh H, Boehm J, Sato C, Iwatsubo T, Tomita T, Sisodia S, Malinow R (2006) AMPAR removal underlies Abeta-induced synaptic depression and dendritic spine loss. Neuron 52(5):831–843

Huang GN, Zeng W, Kim JY, Yuan JP, Han L, Muallem S, Worley PF (2006) STIM1 carboxyl-terminus activates native SOC I(crac) and TPRC1 channels. Nat. Cell Biol. 8(9):1003–1010

Huang Y (2006) Apolipoprotein E and Alzheimer disease. Neurology 66(2 Suppl 1):S79–S85

Hutton M, Lendon CL, Rizzu P, Baker M, Froelich S, Houlden H, Pickering-Brown S, Chakraverty S, Isaacs A, Grover A, Hackett J, Adamson J, Lincoln S, Dickson D, Davies P, Petersen RC, Stevens M, de Graaff E, Wauters E, van Baren J, Hillebrand M, Joosse M, Kwon JM, Nowotny P, Heutink P et al. (1998) Association of missense and 5'-splice-site mutations in tau with the inherited dementia FTDP-17. Nature 393(6686), 702-705

Ichimiya Y, Emson PC, Mountjoy CQ, Lawson DE, Heizmann CW (1988) Loss of calbindin-28 K immunoreactive neurones from the cortex in Alzheimer-type dementia. Brain Res. 475(1):156–159

Iqbal K, Alonso Adel C, Grundke-Iqbal I (2008) Cytosolic abnormally hyperphosphorylated tau but not paired helical filaments sequester normal MAPs and inhibit microtubule assembly. J Alzheimer's Dis. 14(4):365–370

Iritani S, Niizato K, Emson PC (2001) Relationship of calbindin D28K-immunoreactive cells and neuropathological changes in the hippocampal formation of Alzheimer's disease. Neuropathology 21(3):162–167

Isshiki M, Ying YS, Fujita T, Anderson RG (2002) A molecular sensor detects signal transduction from caveolae in living cells. J. Biol. Chem. 277(45):43389–43398

Ito E, Oka K, Etcheberrigaray R, Nelson TJ, McPhie DL, Tofel-Grehl B, Gibson GE, Alkon DL (1994) Internal Ca2+ mobilization is altered in fibroblasts from patients with Alzheimer disease. Proc Natl Acad Sci USA 91(2):534–538

Iwatsubo T, Odaka A, Suzuki N, Mizusawa H, Nukina N, Ihara Y (1994) Visualization of A beta 42(43) and A beta 40 in senile plaques with end-specific A beta monoclonals: evidence that an initially deposited species is A beta 42(43). Neuron 13(1): 45–53

Jacobsen JS, Wu C-C, Redwine JM, Comery TA, Arias R, Bowlby M, Martone M, Morrison JH, Pangalos MN, Reinhart PH, Bloom FE (2006) Early-onset behavioral and synaptic deficits in a mouse model of Alzheimer's disease. Proc Natl Acad Sci USA 103(13):5161–5166

Jaconi M, Bony C, Richards SM, Terzic A, Arnaudeau S, Vassort G, Pucéat M (2000) Inositol 1,4,5-trisphosphate directs Ca^{2+} flow between mitochondria and the endoplasmic/sarcoplasmic reticulum: a role in regulating cardiac autonomic Ca^{2+} spiking. Mol Biol Cell. 11(5):1845–1858

Jarrett JT, Lansbury PT Jr (1993) Seeding "one-dimensional crystallization" of amyloid: a pathogenic mechanism in Alzheimer's disease and scrapie? Cell 73(6):1055–1058

Jiang Q, Lee CY, Mandrekar S, Wilkinson B, Cramer P, Zelcer N, Mann K, Lamb B, Willson TM, Collins JL, Richardson JC, Smith JD, Comery TA, Riddell D, Holtzman DM, Tontonoz P, Landreth GE (2008) ApoE promotes the proteolytic degradation of Abeta. Neuron 58(5):681-693

Jin JK, Choi JK, Wasco W, Buxbaum JD, Kozlowski PB, Carp RI, Kim YS, Choi EK (2005) Expression of calsenilin in neurons and astrocytes in the Alzheimer's disease brain. Neuroreport. 16(5):451-5

Jo DG, Jang J, Kim BJ, Lundkvist J, Jung YK (2005) Overexpression of calsenilin enhances gamma-secretase activity. Neurosci Lett. 378(1):59–64

Kaether C, Haass C, Steiner H (2006a) Assembly, trafficking and function of gamma-secretase. Neurodegener. Dis. 3(4-5):275-83

Kaether C, Schmitt S, Willem M, Haass C (2006b) APP and Notch intracellular domains are generated after transport of their precursors to the cell surface. Traffic 7(4):408-15

Kakuda N, Funamoto S, Yagishita S, Takami M, Osawa S, Dohmae N, Ihara Y (2006) Equimolar production of amyloid beta-protein and amyloid precursor protein intracellular domain from beta-carboxyl-terminal fragment by gamma-secretase. J Biol Chem 281:14776-14786

Kasri NN, Kocks SL, Verbert L, Hébert SS, Callewaert G, Parys JB, Missiaen L, De Smedt H (2006) Up-regulation of inositol 1,4,5-trisphosphate receptor type 1 is responsible for a decreased endoplasmic-reticulum Ca2+ content in presenilin double knock-out cells. Cell Calcium 40(1):41-51

Keller JN, Guo Q, Holtsberg FW, Bruce-Keller AJ, Mattson MP (1998) Increased sensitivity to mitochondrial toxin-induced apoptosis in neural cells expressing mutant presenilin-1 is linked to perturbed calcium homeostasis and enhanced oxyradical production. J Neurosci. 18(12):4439-4450

Kendall JM, Badminton MN, Dormer RL, Campbell AK (1994) Changes in free calcium in the endoplasmic reticulum of living cells detected using targeted aequorin. Anal Biochem. 221(1):173-181

Kendall JM, Dormer RL, Campbell AK (1992) Targeting aequorin to the endoplasmic reticulum of living cells. Biochem Biophys Res Commun. 189(2):1008-1016

Khachaturian ZS (1987) Hypothesis on the regulation of cytosol calcium concentration and the aging brain. Neurobiol. Aging 8(4):345–346

Khachaturian ZS (1994) Calcium hypothesis of Alzheimer's disease and brain aging. Ann N Y Acad Sci. 747:1-11

Kidd M (1963) Paired helical filaments in electron microscopy of Alzheimer’s disease. Nature 197, 192-193

Kim SH, Yin YI, Li YM, Sisodia SS (2004) Evidence that assembly of an active gamma-secretase complex occurs in the early compartments of the secretory pathway. J Biol Chem. 279(47):48615-48619

Kimberly WT, Xia W, Rahmati T, Wolfe MS, Selkoe DJ (2000) The transmembrane aspartates in presenilin 1 and 2 are obligatory for gamma-secretase activity and amyloid beta-protein generation. J Biol Chem. 275(5):3173–3178

Kölsch H, Jessen F, Wiltfang J, Lewczuk P, Dichgans M, Teipel SJ, Kornhuber J, Frölich L, Heuser I, Peters O, Wiese B, Kaduszkiewicz H, van den Bussche H, Hüll M, Kurz A, Rüther E, Henn FA, Maier W (2009) Association of SORL1 gene variants with Alzheimer's disease. Brain Res. 1264:1-6

Kovacs DM, Fausett HJ, Page KJ, Kim TW, Moir RD, Merriam DE, Hollister RD, Hallmark OG, Mancini R, Felsenstein KM, Hyman BT, Tanzi RE, Wasco W (1996) Alzheimer-associated presenilins 1 and 2: neuronal expression in brain and localization to intracellular membranes in mammalian cells. Nat Med. 2(2):224–229

Kuchibhotla KV, Goldman ST, Lattarulo CR, Wu H-Y, Hyman BT, Bacskai BJ (2008) Aβ plaques lead to aberrant regulation of calcium homeostasis in vivo resulting in structural and functional disruption of neuronal networks. Neuron 59(2):214–225

Kumar-Singh S, Theuns J, Van Broeck B, Pirici D, Vennekens K, Corsmit E, Cruts M, Dermaut B, Wang R, Van Broeckhoven C (2006) Mean age-of onset of familial Alzheimer disease caused by presenilin mutations correlates with both increased Abeta42 and decreased Abeta40. Hum Mutat. 27(7):686-695

Lacor PN, Buniel MC, Furlow PW, Clemente AS, Velasco PT, Wood M, Viola KL, Klein WL (2007) Abeta oligomer-induced aberrations in synapse composition, shape, and density provide a molecular basis for loss of connectivity in Alzheimer’s disease. J Neurosci. 27(4):796–807

Lai MT, Chen E, Crouthamel MC, DiMuzio-Mower J, Xu M, Huang Q, Price E, Register RB, Shi XP, Donoviel DB, Bernstein A, Hazuda D, Gardell SJ, Li YM (2003) Presenilin-1 and presenilin-2 exhibit distinct yet overlapping gamma-secretase activities. J Biol Chem. 278(25):22475-22481

LaFerla FM (2002) Calcium dyshomeostasis and intracellular signalling in Alzheimer's disease. Nat Rev Neurosci. 3(11):862-72

Lambert MP, Barlow AK, Chromy BA, Edwards C, Freed R, Liosatos M, Morgan TE, Rozovsky I, Trommer B, Viola KL, Wals P, Zhang C, Finch CE, Krafft GA, Klein WL (1998) Diffusible, nonfibrillar ligands derived from Abeta1-42 are potent central nervous system neurotoxins. Proc Natl Acad Sci USA 95(11):6448-6453

Laurén J, Gimbel DA, Nygaard HB, Gilbert JW, Strittmatter SM (2009) Cellular prion protein mediates impairement of synaptic plasticity by amyloid-β oligomers. Nature 457(7233):1128–1132

LaVoie MJ, Fraering PC, Ostaszewski BL, Ye W, Kimberly WT, Wolfe MS, Selkoe DJ (2003) Assembly of the gamma-secretase complex involves early formation of an intermediate subcomplex of Aph-1 and nicastrin. J Biol Chem. 278(39):37213–37222

Lazarov VK, Fraering PC, Ye W, Wolfe MS, Selkoe DJ, Li H (2006) Electron microscopic structure of purified, active gamma-secretase reveals an aqueous intramembrane chamber and two pores. Proc Natl Acad Sci USA 103(18):6889-6894

Le T, Crook R, Hardy J, Dickson D (2001) Cotton wool plaques in non-familial late-onset Alzheimer's disease. J Neuropathol Exp Neurol. 60(11):1051–1061

LeBlanc A (1995) Increased production of 4 kDa amyloid beta peptide in serum deprived human primary neuron cultures: Possible involvement of apoptosis. J Neurosci. 15(12):7837-7846

Lee G, Pollard HB, Arispe N (2002) Annexin 5 and apolipoprotein E2 protect against Alzheimer's amyloid-beta-peptide cytotoxicity by competitive inhibition at a common phosphatidylserine interaction site. Peptides 23(7):1249–1263

Lee JH, Barral S, Reitz C (2008a) The neuronal sortilin-related receptor gene SORL1 and late-onset Alzheimer's disease. Curr Neurol Neurosci Rep. 8(5):384-91

Lee JH, Cheng R, Honig LS, Vonsattel JP, Clark L, Mayeux R (2008b) Association between genetic variants in SORL1 and autopsy-confirmed Alzheimer disease. Neurology 70(11):887–889

Lee SF, Shah S, Li H, Yu C, Han W, Yu G (2002) Mammalian APH-1 interacts with presenilin and nicastrin and is required for intramembrane proteolysis of amyloid-beta precursor protein and Notch. J Biol Chem. 277(47):45013–45019

Lee SY, Hwang DY, Kim YK, Lee JW, Shin IC, Oh KW, Lee MK, Lim JS, Yoon DY, Hwang SJ, Hong JT (2006) PS2 mutation increases neuronal cell vulnerability to neurotoxicants through activation of caspase-3 by enhancing of ryanodine receptor-mediated calcium release. FASEB J. 20(1):151-153

Leimer U, Lun K, Romig H, Walter J, Grunberg J, Brand M, Haass C (1999) Zebrafish *(Danio rerio)* presenilin promotes aberrant amyloid beta-peptide production and requires a critical aspartate residue for its function in amyloidogenesis. Biochemistry 38(41):13602-13609

Leissring MA, Murphy MP, Mead TR, Akbari Y, Sugarman MC, Jannatipour M, Anliker B, Muller U, Saftig P, De Strooper B, Wolfe MS, Golde TE, LaFerla FM (2002) A physiological signalling role for the γ-secretase derived intracellular fragment of APP. Proc Natl Acad Sci USA 99(7):4697–4702

Leissring MA, Yamasaki TR, Wasco W, Buxbaum JD, Parker I, LaFerla FM (2000) Calsenilin reverses presenilin-mediated enhancement of calcium signaling. Proc Natl Acad Sci USA 97(15):8590–8593

Lessard CB, Lussier MP, Cayouette S, Bourque G, Boulay G (2005) The overexpression of presenilin2 and Alzheimer's-disease-linked presenilin2 variants influences TRPC6-enhanced Ca2+ entry into HEK293 cells. Cell Signal. 17(4):437-445

Levy-Lahad F, Wasco W, Poorkaj P, Romano DM, Oshima J, Pettingell WH, Yu C-E, Jondro PD, Schmidt SD, Wang K, Crowley AC, Fu Y-H, Guenette SY, Galas O, Nemens F, Wijsman PM, Bird TD, Schellenberg GD, Tanzi RE (1995) Candidate gene for the chromosome 1 familial Alzheimer's disease locus. Science 269(5226):973-977

Lewis RS (2007) The molecular choreography of a store-operated calcium channel. Nature 446(7133):284–287

Li YX, Keizer J, Stojilković SS, Rinzel J (1995) Ca2+ excitability of the ER membrane: an explanation for IP3-induced Ca2+ oscillations. Am. J. Physiol. 269(5 Pt 1):C1079–1092

Lilliehook C, Chan S, Choi EK, Zaidi NF, Wasco W, Mattson MP, Buxbaum JD (2002) Calsenilin enhances apoptosis by altering endoplasmic reticulum calcium signaling. Mol Cell Neurosci. 19(4):552–559

Lin H, Bhatia R, Lal R (2001) Amyloid beta protein forms ion channels: implications for Alzheimer's disease pathophysiology. FASEB J 15(13):2433–2444

Liou J, Fivaz M, Inoue T, Meyer T (2007) Live-cell imaging reveals sequential oligomerization and local plasma membrane targeting of stromal interaction molecule 1 after Ca2+ store depletion. Proc Natl Acad Sci USA 104(22):9301–9306

Lissandron V, Podini P, Pizzo P, Pozzan T (2009) Unique characteristics of Ca2+ homeostasis of the trans-Golgi compartment. J Cell Biol., submitted

Lomax RB, Camello C, Van Coppenolle F, Petersen OH, Tepikin AV (2002) Basal and physiological Ca(2+) leak from the endoplasmic reticulum of pancreatic acinar cells. Second messenger-activated channels and translocons. J. Biol. Chem. 277(29):26479–26485

Lucas JJ, Hernandez F, Gomez-Ramos P, Moran MA, Hen R, Avila J (2001) Decreased nuclear beta-catenin, tau hyperphosphorylation and neurodegeneration in GSK-3beta conditional transgenic mice. EMBO J 20(1–2):27–39

Luik RM, Wang B, Prakriya M, Wu MM, Lewis RS (2008) Oligomerization of STIM1 couples ER calcium depletion to CRAC channel activation. Nature 454(7203):538–542

Lytton J, MacLennan DH (1988) Molecular cloning of cDNAs from human kidney coding for two alternatively spliced products of the cardiac Ca2+-ATPase gene. J Biol Chem. 263(29):15024–15031

Lytton J, Westlin M, Burk SE, Shull GE, MacLennan DH (1992) Functional comparisons between isoforms of the sarcoplasmic or endoplasmic reticulum family of calcium pumps J. Biol. Chem. 267(20):14483-14489

Mandelkow E, von Bergen M, Biernat J, Mandelkow EM (2007) Structural principles of tau and the paired helical filaments of Alzheimer's disease. Brain Pathol 17(1):83–90

Marjaux E, Hartmann D, De Strooper B (2004) Presenilins in memory, Alzheimer's disease, and therapy. Neuron 42(2):189–192

Mark RJ, Pang Z, Geddes JW, Uchida K, Mattson MP (1997) Amyloid beta-peptide impairs glucose transport in hippocampal and cortical neurons: involvement of membrane lipid peroxidation. J. Neurosci. 17(3):1046–1054

Massey LK, Mah AL, Ford DL, Miller J, Liang J, Doong H, Monteiro MJ (2004) Overexpression of ubiquilin decreases ubiquitination and degradation of presenilin proteins. J Alzheimers Dis. 6(1):79–92

Massey LK, Mah AL, Monteiro MJ (2005) Ubiquilin regulates presenilin endoproteolysis and modulates gamma-secretase components, Pen-2 and nicastrin. Biochem J. 391(Pt 3):513–525

Mattson MP (2004) Pathways towards and away from Alzheimer's disease. Nature 430(7000):631–639

Mattson MP, Cheng B, Davis D, Bryant K, Lieberburg I, Rydel RE (1992) beta-Amyloid peptides destabilize calcium homeostasis and render human cortical neurons vulnerable to excitotoxicity. J. Neurosci. 12(2):376–389

Mattson MP, Engle MG, Rychlik B (1991) Effects of elevated intracellular calcium levels on the cytoskeleton and tau in cultured human cortical neurons. Mol. Chem. Neuropathol. 15(2):117–142

Mattson MP, Guo Q, Furukawa K, Pedersen WA (1998) Presenilins, the endoplasmic reticulum, and neuronal apoptosis in Alzheimer's disease. J Neurochem. 70(1):1-14

Mattson MP, LaFerla FM, Chan SL, Leissring MA, Shepel PN, Geiger JD (2000) Calcium signaling in the ER: its role in neuronal plasticity and neurodegenerative disorders. Trends Neurosci. 23(5):222-229

Mattson MP, Magnus T (2006) Ageing and neuronal vulnerability. Nat. Rev. Neurosci. 7(4):278–294

McLean CA, Cherny RA, Fraser FW, Fuller SJ, Smith MJ, Beyreuther K, Bush AI, Masters CL (1999) Soluble pool of Abeta amyloid as a determinant of severity of neurodegeneration in Alzheimer's disease. Ann Neurol. 46(6):860–866

Mikoshiba K (2007) IP3 receptor/Ca2+ channel: from discovery to new signaling concepts. J. Neurochem. 102(5):1426–1446

Missiaen L, Dode L, Vanoevelen J, Raeymaekers L, Wuytack F (2007) Calcium in the Golgi apparatus. Cell Calcium 41(5):405-416

Mitchell KJ, Pinton P, Varadi A, Tacchetti C, Ainscow EK, Pozzan T, Rizzuto R, Rutter GA (2001) Dense core secretory vesicles revealed as a dynamic Ca(2+) store in neuroendocrine cells with a vesicle-associated membrane protein aequorin chimaera. J Cell Biol. 155(1):41-51

Miyawaki A, Griesbeck O, Heim R, Tsien RY (1999) Dynamic and quantitative Ca2+ measurements using improved cameleons. Proc. Natl Acad. Sci. USA 96(5):2135–2140

Miyawaki A, Llopis J, Heim R, McCaffery JM, Adams JA, Ikura M, Tsien RY (1997) Fluorescent indicators for Ca2+ based on green fluorescent proteins and calmodulin. Nature 388(6645):882–887

Moerman AM, Barger SW (1999) Inhibition of AMPA responses by mutated presenilin 1. J Neurosci Res. 57(6):962-967

Moller JV, Nissen P, Sorensen TL, le Maire M (2005) Transport mechanism of the sarcoplasmic reticulum Ca2+-ATPase pump. Curr Opin Struct Biol. 15(4):387–393

Moreno H, Yu E, Pigino G, Hernandez AI, Kim N, Moreira JE, Sugimori M, Llinás RR (2009) Synaptic transmission block by presynaptic injection of oligomeric amyloid beta. Proc Natl Acad Sci USA 106(14):5901-5906

Morise H, Shimomura O, Johnson FH, Winant J (1974) Intermolecular energy transfer in the bioluminescent system of *Aequorea*. Biochemistry 13(12):2656–2662

Nagai T, Sawano A, Park ES, Miyawaki A (2001) Circularly permuted green fluorescent proteins engineered to sense Ca2+. Proc. Natl Acad. Sci. USA 98(6):3197–3202

Nagele RG, D'Andrea MR, Lee H, Venkataraman V, Wang HY (2003) Astrocytes accumulate A beta 42 and give rise to astrocytic amyloid plaques in Alzheimer disease brains. Brain Res. 971(2):197–209

Neher E, Sakaba T (2008) Multiple roles of calcium ions in the regulation of neurotransmitter release. Neuron 59(6):861–872

Nelson O, Tu H, Lei T, Bentahir M, de Strooper B, Bezprozvanny I (2007) Familial Alzheimer disease-

linked mutations specifically disrupt Ca2+ leak function of presenilin 1. J Clin Invest. 117(5):1230-1239

Nixon RA (2007) Autophagy, amyloidogenesis and Alzheimer's disease. J Cell Sci. 120(Pt23):4081–4091

Nizzari M, Venezia V, Repetto E, Caorsi V, Magrassi R, Gagliani MC, Carlo P, Florio T, Schettini G, Tacchetti C, Russo T, Diaspro A, Russo C (2007) Amyloid precursor protein and Presenilin1 interact with the adaptor GRB2 and modulate ERK 1,2 signaling. J Biol Chem. 282(18):13833-13844

Nyabi O, Pype S, Mercken M, Herreman A, Saftig P, Craessaerts K, Serneels L, Annaert W, De Strooper B (2002) No endogenous A beta production in presenilin-deficient fibroblasts Nat. Cell Biol. 4(7):E164; author reply E5-6

Offe K, Dodson SE, Shoemaker JT, Fritz JJ, Gearing M, Levey AI, Lah JJ (2006) The lipoprotein receptor LR11 regulates amyloid β production and amyloid precursor protein traffic in endosomal compartments. J Neurosci. 26(5):1596–1603

Okochi M, Steiner H, Fukumori A, Tanii H, Tomita T, Tanaka T, Iwatsubo T, Kudo T, Takeda M, Haass C (2002) Presenilins mediate a dual intramembranous gamma-secretase cleavage of Notch-1. EMBO J 21(20):5408-5416

Pack-Chung E, Meyers MB, Pettingell WP, Moir RD, Brownawell AM, Cheng I, Tanzi RE, Kim TW (2000) Presenilin 2 interacts with sorcin, a modulator of the ryanodine receptor. J. Biol. Chem. 275(19)14,440–14,445

Pak K, Chan SL, Mattson MP (2003) Presenilin-1 mutation sensitizes oligodendrocytes to glutamate and amyloid toxicities, and exacerbates white matter damage and memory impairment in mice. Neuromolecular Med. 3(1):53-64

Palmer AE, Giacomello M, Kortemme T, Hires SA, Lev-Ram V, Baker D, Tsien RY (2006) Ca2+ indicators based on computationally redesigned calmodulin-peptide pairs. Chem Biol. 13(5):521-530

Palmer AE, Jin C, Reed JC, Tsien RY (2004) Bcl-2-mediated alterations in endoplasmic reticulum Ca2+ analyzed with an improved genetically encoded fluorescent sensor. Proc Natl Acad Sci USA 101(50):17404-17409

Palop JJ, Jones B, Kekonius L, Chin J, Yu G-Q, Raber L, Masliah E, Mucke L (2003) Neuronal depletion of calcium-dependent proteins in the dentate gyrus is tightly linked to Alzheimer's disease-related cognitive deficits. Proc Natl Acad Sci USA 100(16):9572–9577

Paresce D, Chung H, Maxfield F (1997) Slow degradation of aggregates of the Alzheimer's disease amyloid beta-protein by microglial cells. J Biol Chem. 272(46):29390–29397

Periasamy M, Kalyanasundaram A (2007) SERCA pump isoforms: their role in calcium transport and disease. Muscle Nerve 35(4):430–442

Persechini A, Lynch JA, Romoser VA (1997) Novel fluorescent indicator proteins for monitoring free intracellular Ca2+. Cell Calcium 22(3):209–216

Pickford F, Masliah E, Britschgi M, Lucin K, Narasimhan R, Jaeger PA, Small S, Spencer B, Rockenstein E, Levine B, Wyss-Coray T (2008) The autophagy-related protein beclin 1 shows reduced expression in early Alzheimer disease and regulates amyloid beta accumulation in mice. J Clin Invest. 118(6):2190-2199

Pierrot N, Ghisdal P, Caumont AS, Octave JN (2004) Intraneuronal amyloid-beta1–42 production triggered by sustained increase of cytosolic calcium concentration induces neuronal death. J Neurochem. 88(5):1140–1150

Pinton P, Pozzan T, Rizzuto R (1998) The Golgi apparatus is an inositol 1,4,5-trisphosphate-sensitive Ca2+ store, with functional properties distinct from those of the endoplasmic reticulum. EMBO J. 17(18):5298–

5308

Podlisny MB, Citron M, Amarante P, Sherrington R, Xia W, Zhang J, Diehl T, Levesque G, Fraser P, Haass C, Koo EH, Seubert P, St George-Hyslop P, Teplow DB, Selkoe DJ (1997) Presenilin proteins undergo heterogeneous endoproteolysis between Thr291 and Ala299 and occur as stable N- and C-terminal fragments in normal and Alzheimer brain tissue. Neurobiol Dis. 3(4):325–337

Prasher D, McCann RO, Cormier MJ (1985) Cloning and expression of the cDNA coding for aequorin, a bioluminescent calcium-binding protein. Biochem. Biophys. Res. Commun. 126(3):1259–1268

Price JL, Morris JC (1999) Tangles and plaques in nondemented aging and "preclinical" Alzheimer's disease. Ann Neurol. 45(3):358–368

Prokop S, Haass C, Steiner H (2005) Length and overall sequence of the PEN-2 C-terminal domain determines its function in the stabilization of presenilin fragments. J Neurochem. 94(1):57–62

Puzianowska-Kuznicka M, Kuznicki J (2009) The ER and ageing II: calcium homeostasis. Ageing Res Rev. 8(3):160-172

Qi-Takahara Y, Morishima-Kawashima M, Tanimura Y, Dolios G, Hirotani N, Horikoshi Y, Kametani F, Maeda M, Saido TC, Wang R, Ihara Y (2005) Longer forms of amyloid beta protein: implications for the mechanism of intramembrane cleavage by gamma-secretase. J Neurosci. 25(2):436–445

Querfurth HW, Selkoe DJ (1994) Calcium ionophore increases amyloid beta peptide production by cultured cells. Biochemistry 33(15):4550–4561

Reyes M, Stanton PK (1996) Induction of hippocampal long-term depression requires release of Ca2+ from separate presynaptic and postsynaptic intracellular stores. J. Neurosci. 16(19):5951–5960

Rizzuto R, Bastianutto C, Brini M, Murgia M, Pozzan T (1994a) Mitochondrial Ca2+ homeostasis in intact cells. J Cell Biol. 126(5):1183-1194

Rizzuto R, Brini M, Bastianutto C, Marsault R, Pozzan T (1995) Photoprotein-mediated measurement of calcium ion concentration in mitochondria of living cells. Methods Enzymol. 260:417-428

Rizzuto R, Brini M, Murgia M, Pozzan T (1993) Microdomains with high Ca2+ close to IP3-sensitive channels that are sensed by neighboring mitochondria. Science 262(5134):744-747

Rizzuto R, Brini M, Pozzan T (1994b) Targeting recombinant aequorin to specific intracellular organelles. Methods Cell Biol. 40:339–358

Rizzuto R, Pinton P, Carrington W, Fay FS, Fogarty KE, Lifshitz LM, Tuft RA, Pozzan T (1998) Close contacts with the endoplasmic reticulum as determinants of mitochondrial calcium responses. Science 280(5370):1763–1766

Rizzuto R, Simpson AW, Brini M, Pozzan T (1992) Rapid changes of mitochondrial Ca2+ revealed by specifically targeted recombinant aequorin. Nature 358(6384):325-327

Rogaev FI, Sherrington R, Rogaeva EA, Levesque G, Ikeda M, Liang Y, Chi H, Lin C, Holman K, Tsuda T, et al. (1995) Familial Alzheimer's disease in kindreds with missense mutations in a gene on chromosome 1 related to the Alzheimer's disease type 3 gene. Nature 376(6543):775-778

Rogaeva E, Meng Y, Lee JH, Gu Y, Kawarai T, Zou F, Katayama T, Baldwin CT, Cheng R, Hasegawa H, Chen F, Shibata N, Lunetta KL, Pardossi-Piquard R, Bohm C, Wakutani Y, Cupples LA, Cuenco KT, Green RC, Pinessi L, Rainero I, Sorbi S, Bruni A, Duara R, Friedland RP, Inzelberg R, Hampe W, Bujo H, Song YQ, Andersen OM, Willnow TE, Graff-Radford N, Petersen RC, Dickson D, Der SD, Fraser PE, Schmitt-Ulms G, Younkin S, Mayeux R, Farrer LA, St George-Hyslop P (2007) The neuronal sortilin-related receptor SORL1 is genetically associated with Alzheimer disease. Nat Genet. 39(2):168-177

Romoser VA, Hinkle PM, Persechini A (1997) Detection in living cells of Ca2+-dependent changes in the fluorescence emission of an indicator composed of two green fluorescent protein variants linked by a calmodulin binding sequence. A new class of fluorescent indicators. J. Biol. Chem. 272(20):13270–13274

Rossi D, Barone V, Giacomello E, Cusimano V, Sorrentino V (2008) The sarcoplasmic reticulum: an organized patchwork of specialized domains. Traffic 9(7):1044–1049

Roy A, Wonderlin WF (2003) The permeability of the endoplasmic reticulum is dynamically coupled to protein synthesis. J. Biol. Chem. 278(7):4397–4403

Ruan L, Kang Z, Pei G, Le Y (2009) Amyloid deposition and inflammation in APPswe/PS1dE9 mouse model of Alzheimer's disease. Curr Alzheimer Res. 6(6):531-540

Rudolf R, Magalhães PJ, Pozzan T (2006) Direct in vivo monitoring of sarcoplasmic reticulum Ca2+ and cytosolic cAMP dynamics in mouse skeletal muscle. J Cell Biol. 173(2):187-193

Rudolf R, Mongillo M, Rizzuto R, Pozzan T (2003) Looking forward to seeing calcium. Nat Rev Mol Cell Biol. 4(7):579-586

Russo C, Dolcini V, Salis S, Venezia V, Zambrano N, Russo T, Schettini G (2002) Signal transduction through tyrosine-phosphorylated C-terminal fragments of amyloid precursor protein via an enhanced interaction with Shc/Grb2 adaptor proteins in reactive astrocytes of Alzheimer's disease brain. J. Biol. Chem. 277(38):35282–35288

Rybalchenko V, Hwang SY, Rybalchenko N, Koulen P (2008) The cytosolic N-terminus of presenilin-1 potentiates mouse ryanodine receptor single channel activity. Int. J. Biochem. Cell Biol. 40(1):84–97

Sato T, Diehl TS, Narayanan S, Funamoto S, Ihara Y, De Strooper B, Steiner H, Haass C, Wolfe MS (2007) Active gamma-secretase complexes contain only one of each component. J. Biol. Chem. 282(47):33985-33993

Scherzer CR, Offe K, Gearing M, Rees HD, Fang G, Heilman CJ, Schaller C, Bujo H, Levey AI, Lah JJ (2004) Loss of apolipoprotein E receptor LR11 in Alzheimer disease. Arch. Neurol. 61(8):1200–1205

Schroeter EH, Ilagan MX, Brunkan AL, Hecimovic S, Li YM, Xu M, Lewis HD, Saxena MT, De Strooper B, Coonrod A, Tomita T, Iwatsubo T, Moore CL, Goate A, Wolfe MS, Shearman M, Kopan R (2003) A presenilin dimer at the core of the gamma-secretase enzyme: insights from parallel analysis of Notch 1 and APP proteolysis. Proc Natl Acad Sci. USA 100(22):13075-13080

Selkoe DJ (2002) Alzheimer’s disease is a synaptic failure. Science 298(5594):789–791

Selkoe D, Kopan R (2003) Notch and Presenilin: regulated intramembrane proteolysis links development and degeneration. Annu. Rev. Neurosci. 26:565–597

Selkoe DJ, Wolfe MS (2007) Presenilin: running with scissors in the membrane. Cell131(2):215-221

Shah S, Lee SF, Tabuchi K, Hao YH, Yu C, LaPlant Q, Ball H, Dann CE III, Sudhof T, Yu G (2005) Nicastrin functions as a gamma-secretase-substrate receptor. Cell 122(3):435–447

Shankar GM, Li S, Mehta TH, Garcia-Munoz A, Shepardson NE, Smith I, Brett FM, Farrell MA, Rowan MJ, Lemere CA, Regan CM, Walsh DM, Sabatini BL, Selkoe DJ (2008) Amyloid-beta protein dimers isolated directly from Alzheimer's brains impair synaptic plasticity and memory. Nat Med. 14(8):837-842

Sheng JG, Mrak RE, GriYn WS (1997) Neuritic plaque evolution in Alzheimer’s disease is accompanied by transition of activated microglia from primed to enlarged to phagocytic forms. Acta Neuropathol. 94(1):1–5

Shepherd C, McCann H, Halliday GM (2009) Variations in the neuropathology of familial Alzheimer’s disease. Acta Neuropathol. 118(1):37-52

Sheu YA, Kricka LJ, Pritchett DB (1993) Measurement of intracellular calcium using bioluminescent aequorin expressed in human cells. Anal Biochem. 209(2):343-347

Shimomura O, Johnson FH, Saiga Y (1962) Extraction, purification and properties of aequorin, a bioluminescent protein from the luminous hydromedusan, *Aequorea*. J. Cell. Comp. Physiol. 59:223–239

Shirotani K, Edbauer D, Prokop S, Haass C, Steiner H (2004) Identification of distinct gamma-secretase complexes with different APH-1 variants. J Biol Chem. 279(40):41340-41345

Shirwany NA, Payette D, Xie J, Guo Q (2007) The amyloid beta ion channel hypothesis of Alzheimer's disease. Neuropsychiatric Dis Treatment 3(5):597–612

Shoji M, Golde TE, Ghiso J, Cheung TT, Estus S, Shaffer LM, Cai XD, McKay DM, Tintner R, Frangione B, Younkin SG (1992) Production of the Alzheimer amyloid beta protein by normal proteolytic processing. Science 258(5079):126-129

Small SA, Kent K, Pierce A, Leung C, Kang MS, Okada H, Honig L, Vonsattel JP, Kim TW (2005) Model-guided microarray implicates the retromer complex in Alzheimer's disease. Ann Neurol. 58(6):909–919

Smith IF, Hitt B, Green KN, Oddo S, LaFerla FM (2005) Enhanced caffeine-induced Ca2+ release in the 3xTg-AD mouse model of Alzheimer's disease. J Neurochem. 94(6):1711-1718

Song W, Nadeau P, Yuan M, Yang X, Shen J, Yankner BA (1999) Proteolytic release and nuclear translocation of Notch-1 are induced by presenilin-1 and impaired by pathogenic presenilin-1 mutations. Proc Natl Acad Sci USA 96(12):6959–6963

Spasic D, Annaert W (2008) Building gamma-secretase: the bits and pieces. J Cell Sci. 121(Pt 4):413-420

Spasic D, Raemaekers T, Dillen K, Declerck I, Baert V, Serneels L, Fullekrug J, Annaert W (2007) Rer1p competes with APH-1 for binding to nicastrin and regulates gamma-secretase complex assembly in the early secretory pathway. J. Cell Biol. 176(5):629-640

Stadelmann C, Deckwerth TL, Srinivasan A, Bancher C, Bruck W, Jellinger K, Lassmann H (1999) Activation of caspase-3 in single neurons and autophagic granules of granulovacuolar degeneration in Alzheimer's disease. Evidence for apoptotic cell death. Am J Pathol. 155(5):1459–1466

Stathopulos PB, Zheng L, Li G-Y, Plevin MJ, Ikura M (2008) Structural and mechanistic insights into STIM1-mediated initiation of store-operated calcium entry. Cell 135(1):110–122

Steiner H, Capell A, Pesold B, Citron M, Kloetzel PM, Selkoe DJ, Romig H, Mendla K, Haass C (1998) Expression of Alzheimer's disease associated presenilin-1 is controlled by proteolytic degradation and complex formation. J Biol Chem. 273(48):32322–32331

Steiner H, Fluhrer R, Haass C (2008) Intramembrane proteolysis by gamma-secretase. J Biol Chem. 283(44):29627-31

Stoothoff WH, Johnson GV (2005) Tau phosphorylation: physiological and pathological consequences. Biochem Biophys Acta 1739(2–3):280–297

Struhl G, Adachi A (200) Requirements for presenilin dependent cleavage of notch and other transmembrane proteins. Mol Cell. 6(3): 625–636

Stutzmann GE, Caccamo A, LaFerla FM, Parker I (2004) Dysregulated IP3 signaling in cortical neurons of knock-in mice expressing an Alzheimer's-linked mutation in presenilin1 results in exaggerated Ca2+ signals and altered membrane excitability. J Neurosci. 24(2):508-513

Stutzmann GE, Smith I, Caccamo A, Oddo S, LaFerla FM, Parker I (2006) Enhanced ryanodine receptor recruitment contributes to Ca2+ disruptions in young, adult, and aged Alzheimer's disease mice. J Neurosci.

26(19):5180-5189

Stutzmann GE, Smith I, Caccamo A, Oddo S, Parker I, LaFerla F (2007) Enhanced ryanodine-mediated calcium release in mutant PS1-expressing Alzheimer's mouse models. Ann. N Y Acad. Sci. 1097:265–277

Su JH, Deng G, Cotman CW (1997) Bax protein expression is increased in Alzheimer's brain: correlations with DNA damage, Bcl-2 expression, and brain pathology. J Neuropathol Exp Neurol. 56(1):86–93

Suzuki N, Cheung TT, Cai XD, Odaka A, Otvos L, Eckman C, Golde TE, Younkin SG (1994) An increased percentage of long amyloid beta protein secreted by familial amyloid beta protein precursor (beta APP717) mutants. Science 264(5163):1336–1340

Takao M, Ghetti B, Hayakawa I, Ikeda E, Fukuuchi Y, Miravalle L, Piccardo P, Murrell JR, Glazier BS, Koto A (2002) A novel mutation (G217D) in the Presenilin 1 gene (PSEN1) in a Japanese family: presenile dementia and parkinsonism are associated with cotton wool plaques in the cortex and striatum. Acta Neuropathol. 104(2):155–170

Takasugi N, Tomita T, Hayashi I, Tsuruoka M, Niimura M, Takahashi Y, Thinakaran G, Iwatsubo T (2003) The role of presenilin cofactors in the gamma-secretase complex. Nature 422(6930):438–441

Takeda T, Asahi M, Yamaguchi O, Hikoso S, Nakayama H, Kusakari Y, Kawai M, Hongo K, Higuchi Y, Kashiwase K, Watanabe T, Taniike M, Nakai A, Nishida K, Kurihara S, Donoviel DB, Bernstein A, Tomita T, Iwatsubo T, Hori M, Otsu K (2005) Presenilin 2 regulates the systolic function of heart by modulating Ca2+ signaling. FASEB J. 19(14):2069-2071

Targos B, Baranska J, Pomorski P (2005) Store-operated calcium entry in physiology and pathology of mammalian cells. Acta Biochim. Pol. 52(2):379–409

Tesco G, Koh YH, Tanzi RE (2003) Caspase activation increases beta-amyloid generation independently of caspase cleavage of the beta-amyloid precursor protein (APP). J Biol Chem. 278(46):46074-46080

Thibault O, Gant JC, Landfield PW (2007) Expansion of the calcium hypothesis of brain aging and Alzheimer's disease: minding the store. Aging Cell 6(3):307–317

Thinakaran G, Borchelt DR, Lee MK, Slunt HH, Spitzer L, Kim G, Ratovitsky T, Davenport F, Nordstedt C, Seeger M, Hardy J, Levey AI, Gandy SE, Jenkins NA, Copeland NG, Price DL, Sisodia SS (1996) Endoproteolysis of presenilin 1 and accumulation of processed derivatives in vivo. Neuron 17(1):181-190

Thinakaran G, Harris CL, Ratovitski T, Davenport F, Slunt HH, Price DL, Borchelt DR, Sisodia SS (1997) Evidence that levels of presenilins (PS1 and PS2) are coordinately regulated by competition for limiting cellular factors. J Biol Chem. 272(45):28415–28422

Thinakaran G, Sisodia SS (2006) Presenilins and Alzheimer disease: the calcium conspiracy. Nat Neurosci. 9(11):1354-5

Tian G, Ghanekar SV, Aharony D, Shenvi AB, Jacobs RT, Liu X, Greenberg BD (2003) The mechanism of gamma-secretase: multiple inhibitor binding sites for transition state analogs and small molecule inhibitors. J. Biol. Chem. 278(31):28968–28975

Tolar M, Keller JN, Chan S, Mattson MP, Marques MA, Crutcher KA (1999) Truncated apolipoprotein E (ApoE) causes increased intracellular calcium and may mediate ApoE neurotoxicity. J. Neurosci. 19(16):7100–7110

Tolia A, Chavez-Gutierrez L, De Strooper B (2006) Contribution of presenilin transmembrane domains 6 and 7 to a water-containing cavity in the gamma-secretase complex. J. Biol. Chem. 281(37):27633-27642

Traaseth NJ, Ha KN, Verardi R, Shi L, Buffy JJ, Masterson LR, Veglia G (2008) Structural and dynamic basis of phospholamban and sarcolipin inhibition of Ca2+-ATPase. Biochemistry 47(1)3–13

Trebak M, Vazquez G, Bird GS, Putney Jr. JW (2003) The TRPC3/6/7 subfamily of cation channels. Cell Calcium 33(5-6):451–461

Truong K, Sawano A, Mizuno H, Hama H, Tong KI, Mal TK, Miyawaki A, Ikura M (2001) FRET-based *in vivo* Ca2+ imaging by a new calmodulin–GFP fusion molecule. Nature Struct. Biol. 8(12):1069–1073

Tsien RY (1980) New calcium indicators and buffers with high selectivity against magnesium and protons: design, synthesis, and properties of prototype structures. Biochemistry 19(11):2396–2404

Tsien RY (1981) A non-disruptive technique for loading calcium buffers and indicators into cells. Nature 290(5806):527–528

Tu H, Nelson O, Bezprozvanny A, Wang Z, Lee SF, Hao YH, Serneels L, De Strooper B, Yu G, Bezprozvanny I (2006) Presenilins form ER Ca2+ leak channels, a function disrupted by familial Alzheimer's disease-linked mutations. Cell 126(5):981–993

Uchihara T, Nakamura A, Nakayama H, Arima K, Ishizuka N, Mori H, Mizushima S (2003) Triple immunofluorolabeling with two rabbit polyclonal antibodies and a mouse monoclonal antibody allowing three-dimensional analysis of cotton wool plaques in Alzheimer disease. J Histochem Cytochem. 51(9):1201–1206

Van Baelen K, Dode L, Vanoevelen J, Callewaert G, De Smedt H, Missiaen L, Parys JB, Raeymaekers L, Wuytack F (2004) The Ca2+/Mn2+ pumps in the Golgi apparatus. Biochim Biophys Acta 1742(1-3):103-12

Van Broeck B, Van Broeckhoven C, Kumar-Singh S (2007) Current insights into molecular mechanisms of Alzheimer disease and their implications for therapeutic approaches. Neurodegener Dis. 4(5):349-65

Vanoevelen J, Raeymaekers L, Parys JB, De Smedt H, Van Baelen K, Callewaert G, Wuytack F, Missiaen L (2004) Inositol trisphosphate producing agonists do not mobilize the thapsigargin-insensitive part of the endoplasmic-reticulum and Golgi Ca2+ store. Cell Calcium 35(2):115-121

Vecellio M, Schwaller B, Meyer M, Hunziker W, Celio MR (2000) Alterations in Purkinje cell spines of calbindin D-28 k and parvalbumin knock-out mice. Eur. J. Neurosci. 12(3):945–954

Verboomen H, Wuytack F, De Smedt H, Himpens B, Casteels R (1992) Functional difference between SERCA2a and SERCA2b Ca2+ pumps and their modulation by phospholamban. Biochem J. 286(Pt 2):591–595

Verdile G, Gandy SE, Martins RN (2007) The role of presenilin and its interacting proteins in the biogenesis of Alzheimer's beta amyloid. Neurochem Res. 32(4-5):609-623

Verdile G, Groth D, Mathews PM, St George-Hyslop P, Fraser PE, Ramabhadran TV, Kwok JB, Schofield PR, Carter T, Gandy S, Martins RN (2004) Baculoviruses expressing the human familial Alzheimer's disease presenilin 1 mutation lacking exon 9 increase levels of an amyloid beta-like protein in Sf9 cells. Mol Psychiatry 9(6):594-602

Walsh DM, Klyubin I, Fadeeva JV, Cullen WK, Anwyl R, Wolfe MS, Rowan MJ, Selkoe DJ (2002) Naturally secreted oligomers of amyloid beta protein potently inhibit hippocampal long-term potentiation in vivo. Nature 416(6880):535–539

Walsh DM, Lomakin A, Benedek GB, Condron MM, Teplow DB (1997) Amyloid beta-protein fibrillogenesis. Detection of a protofibrillar intermediate. J Biol Chem. 272(35):22364–22372

Wang XS, Gruenstein E (1997) Rapid elevation of neuronal cytosolic calcium by apolipoprotein E peptide. J. Cell. Physiol. 173(1):73–83

Wei W, Nguyen LN, Kessels HW, Hagiwara H, Sisodia S, Malinow R (2009) Amyloid beta from axons and dendrites reduces local spine number and plasticity. Nat Neurosci. 2009 Dec 27 [Epub ahead of print]

PMID: 20037574

Weidemann A, Eggert S, Reinhard FB, Vogel M, Paliga K, Baier G, Masters CL, Beyreuther K, Evin G (2002) A novel epsilon-cleavage within the transmembrane domain of the Alzheimer amyloid precursor protein demonstrates homology with Notch processing. Biochemistry 41(8):2825-2835

Wippold FJ 2nd, Cairns N, Vo K, Holtzman DM, Morris JC (2007) Neuropathology for the neuroradiologist: plaques and tangles. AJNR Am J Neuroradiol. 29(1):18-22

Wolfe MS, Kopan R (2004) Intramembrane proteolysis: theme and variations. Science 305(5687), 1119-1123

Wolfe MS, Xia W, Ostaszewski BL, Diehl TS, Kimberly WT, Selkoe DJ (1999) Two transmembrane aspartates in presenilin-1 required for presenilin endoproteolysis and gamma-secretase activity. Nature 398(6727):513–517

Wuytack F, Papp B, Verboomen H, Raeymaekers L, Dode L, Bobe R, Enouf J, Bokkala S, Authi KS, Casteels R (1994) A sarco/endoplasmic reticulum Ca2+-ATPase 3-type Ca2+ pump is expressed in platelets, in lymphoid cells, and in mast cells. J Biol Chem. 269(2):1410–1416

Wyss-Coray T (2006) Inflammation in Alzheimer's disease: driving force, bystander or beneficial response. Nat Med. 12(9):1005–1015

Yang DS, Tandon A, Chen F, Yu G, Yu H, Arawaka S, Hasegawa H, Duthie M, Schmidt SD, Ramabhadran TV, Nixon RA, Mathews PM, Gandy SE, Mount HT, St. George-Hyslop P, Fraser PE (2002) Mature glycosylation and trafficking of nicastrin modulate its binding to presenilins. J Biol Chem. 277(31):28135–28142

Yoshiike Y, Kayed R, Milton SC, Takashima A, Glabe CG (2007) Pore-forming proteins share structural and functional homology with amyloid oligomers. Neuromolecular Med. 9(3):270–275

Yu G, Nishimura M, Arawaka S, Levitan D, Zhang L, Tandon A, Song YQ, Rogaeva E, Chen F, Kawarai T, Supala A, Levesque L, Yu H, Yang DS, Holmes E, Milman P, Liang Y, Zhang DM, Xu DH, Sato C, Rogaev E, Smith M, Janus C, Zhang Y, Aebersold R, Farrer LS, Sorbi S, Bruni A, Fraser P, St. George-Hyslop P (2000) Nicastrin modulates presenilin-mediated notch/glp-1 signal transduction and betaAPP processing. Nature 407(6800):48–54

Zampese E, Brunello L, Fasolato C, Pizzo P (2009) Ca2+ dysregulation mediated by presenilins in Familial Alzheimer's Disease: Causing or modulating factor? Curr Trends Neurol., in press

Zatti G, Burgo A, Giacomello M, Barbiero L, Ghidoni R, Sinigaglia G, Florean C, Bagnoli S, Binetti G, Sorbi S, Pizzo P, Fasolato C (2006) Presenilin mutations linked to familial Alzheimer's disease reduce endoplasmic reticulum and Golgi apparatus calcium levels. Cell Calcium 39(6):539-550

Zatti G, Ghidoni R, Barbiero L, Binetti G, Pozzan T, Fasolato C, Pizzo P (2004) The presenilin 2 M239I mutation associated with familial Alzheimer's disease reduces Ca2+ release from intracellular stores. Neurobiol Dis. 15(2):269-278

Zhang C, Wu B, Beglopoulos V, Wines-Samuelson M, Zhang D, Dragatsis I, Südhof TC, Shen J (2009) Presenilins are essential for regulating neurotransmitter release. Nature 460(7255):632–636

Zhang J, Campbell RE, Ting AY, Tsien RY (2002) Creating new fluorescent probes for cell biology. Nat Rev Mol Cell Biol. 3(12):906-918

Zhang T, Tran S, Clouser C, Pignoni F (2005) Nicastrin controls aspects of photoreceptor neuron specification and differentiation in the Drosophila eye. Dev Dyn. 234(3):590–601

Zhao G, Mao G, Tan J, Dong Y, Cui MZ, Kim SH, Xu X (2004) Identification of a new presenilin-dependent zeta cleavage site within the transmembrane domain of amyloid precursor protein. J Biol Chem. 279(49):50647–50650

Ringraziamenti

Vorrei ringraziare il Prof. Tullio Pozzan per avermi dato l'opportunità di lavorare nel suo laboratorio, è stata un'esperienza importante di cui farò tesoro.
Un profondo ringraziamento alle Dott.sse Cristina Fasolato e Paola Pizzo, non semplicemente per tutto quello che mi hanno insegnato (e non è poco), ma soprattutto per la pazienza e la disponibilità che mi hanno sempre dimostrato, anche nei momenti più difficili.
Un grazie collettivo (ma non per questo meno sentito) a tutte le persone che hanno condiviso con me, per breve o per lungo tempo, la vita di laboratorio, in tutti i suoi aspetti. Un pensiero affettuoso va a Silvia, Laura, Valentina e Angela, le studentesse che mi hanno seguita (o era il contrario?!) in questi tre anni: non so se sono stata più paziente io con loro, o loro con la sottoscritta! :O) Ringrazio gli immigrati ferraresi, Erika, Roberta e Diego, per essere stati graditi e gradevolissimi ospiti e per aver portato un po' di buon senso in una gabbia di matti! ;O)
Infine (ma gli ultimi nomi sono spesso quelli fondamentali…), un grazie speciale ai miei Cari Leoni, Ilaria ed Enrico, perché senza di loro non sarei arrivata a scrivere queste righe. Period. :O)